



**CONTRIBUTION OF BIOGENIC EMISSIONS TO THE FORMATION OF
OZONE AND PARTICULATE MATTER:
MODELING STUDIES IN THE NASHVILLE, TENNESSEE AND NORTHEAST
DOMAINS**

**Phase 2 Report
CRC Project A-23**

Prepared for

Mr. Brent K. Bailey
Coordinating Research Council, Inc.
3650 Mansell Road, Suite 140
Alpharetta, GA 30022

Prepared by

Betty K. Pun, Shiang-Yuh Wu, and Christian Seigneur
Atmospheric & Environmental Research, Inc.
2682 Bishop Drive, Suite 120
San Ramon, CA 94583

Document Number CP051-01-1

September 2001

ACKNOWLEDGEMENTS

This work was co-sponsored by the American Chemistry Council under Agreement No. 0105. We would like to thank Professor John Seinfeld, Caltech; Professor Robert Griffin, Duke University; and Professor Spyros Pandis, CMU for the use of their chemical mechanism and organic aerosol modules in this project. EPRI and CARB sponsored the development of a new SOA module developed in house in collaboration with Professor Seinfeld. We thank EPRI for the authorization to use the Models-3/CMAQ input files of the Nashville simulation. Thanks are also due to Mr. Ralph Morris, Environ, for providing the CRC project files of the NARSTO/Northeast simulation.

In the spirit of scientific collaboration, many collaborators shared their files and data used in this project. Elizabeth Bailey, TVA, provided the biogenic emission files for the Nashville, TN simulation. We obtained PM and PM precursor emissions from the National Emissions Trends database with the help of Tom McMullen, EPA. Tom Braverman and Tom Pierce, EPA, provided seasonal and diurnal factors for emission sources. Professor Helen Hsu, Harvard University and Dr. Praveen Amar, NESCAUM, shared PM data that were used in developing boundary conditions and model evaluation. Professor Tim Stark, West Chester University, and Professor Paul Shepson, Purdue University, shared their isoprene data that were compared against model predictions for the Nashville simulation.

LEGAL NOTICE

This report was prepared by Atmospheric and Environmental Research, Inc. (AER) as an account of work sponsored by the Coordinating Research Council (CRC). Neither the CRC, members of the CRC, AER, nor any person acting on their behalf: (1) makes any warranty, express or implied, with respect to the use of any information, apparatus, method, or process disclosed in this report, or (2) assumes any liabilities with respect to the use, inability to use, or damages resulting from the use or inability to use, any information, apparatus, method, or process disclosed in this report.

TABLE OF CONTENTS

Executive Summary	E-1
E.1 Contribution of Biogenic Emissions to O ₃	E-2
E.2 Attainability of the 8-hour NAAQS.....	E-3
E.3 Contribution of Biogenic/Natural Emissions to PM _{2.5}	E-4
E.4 Uncertainties in the Modeling of SOA Formation.....	E-4
1. Introduction.....	1-1
2. Implementation of New Secondary Organic Aerosol Modules into MODELS-3/CMAQ	2-1
2.1 Odum/Griffin et al. Module.....	2-2
2.1.1 Gas-phase chemistry.....	2-2
2.1.2 Gas/particle partition	2-3
2.2 CMU/STI Module.....	2-6
2.2.1 Gas-phase chemistry.....	2-6
2.2.2 Gas/particle partition	2-7
2.3 MADRID 2 with the AER/EPRI/Caltech SOA Module.....	2-10
2.3.1 Gas-phase chemistry.....	2-10
2.3.2 Gas/particle partition	2-10
2.3.3 Sectional PM model.....	2-14
2.4 Dry Deposition.....	2-14
3. Base Case Simulation in the Nashville, TN Domain.....	3-1
3.1 Technical Approach	3-1
3.1.1 Compilation of Models-3.....	3-1
3.1.2 Meteorological files.....	3-2
3.1.3 Time-independent files	3-3
3.1.4 Initial conditions and boundary conditions.....	3-3
3.1.5 Emissions	3-6

TABLE OF CONTENTS (continued)

3.2	Simulation Results	3-11
3.2.1	Simulation time	3-11
3.2.2	O ₃ concentrations	3-11
3.2.3	Biogenic compounds	3-17
3.2.4	Condensable gases.....	3-19
3.2.5	PM	3-21
3.3	Detailed Comparison of Results from Three SOA Modules.....	3-33
3.3.1	Spatial distribution of SOA.....	3-33
3.3.2	Production of condensable compounds	3-37
3.3.3	Origins of SOA.....	3-40
3.3.4	Different implementations of absorption.....	3-41
3.3.5	Formation of SOA by dissolution	3-47
4.	Contribution of Biogenic Emissions to O ₃ and PM _{2.5} in the Nashville Domain..	4-1
4.1	Description of the Sensitivity Studies	4-1
4.1.1	Modeling scenarios.....	4-1
4.1.2	Treatment of the boundary conditions.....	4-2
4.2	Results	4-5
4.2.1	O ₃	4-5
4.2.2	PM	4-13
5.	Sensitivity of Modeled PM Contribution in Nashville to Terpene Speciation	5-1
5.1	Alternative Terpene Speciation	5-1
5.2	Results	5-1
6.	Base Case Simulation in the Northeast Domain	6-1
6.1	Technical Approach	6-1
6.1.1	Compilation of Models-3.....	6-1
6.1.2	Meteorological files.....	6-2

TABLE OF CONTENTS (continued)

6.1.3	Time-independent files	6-3
6.1.4	Initial conditions and boundary conditions.....	6-3
6.1.5	Emissions	6-5
6.2	Modeling Results	6-7
6.2.1	Simulation time	6-7
6.2.2	Gas-phase concentrations.....	6-7
6.2.3	PM results	6-11
7.	Contribution of Biogenic Emissions to O ₃ and PM _{2.5} in the Northeast Domain..	7-1
7.1	Description of the Sensitivity Studies	7-1
7.2	Results	7-1
7.2.1	O ₃	7-1
7.2.2	PM	7-8
8.	Conclusions.....	8-1
9.	References.....	9-1

LIST OF TABLES

Table 2-1.	Modifications to CBM-IV for the Odum/Griffin et al. SOA module	2-4
Table 2-2.	Partition constants of the Odum/Griffin et al. SOA module	2-5
Table 2-3.	Modifications to CBM-IV for the CMU/STI SOA module	2-8
Table 2-4.	Aerosol yield parameters and saturation concentrations of the CMU/STI module	2-9
Table 2-5.	Surrogate organic oxidation products used in the AEC gas/particle partition module	2-13
Table 2-6.	Description of MADRID 2	2-15
Table 3-1.	Boundary conditions for PM components at the surface ($\mu\text{g}/\text{m}^3$) for the Nashville simulation.....	3-5
Table 3-2.	Composition of terpenes in Atlanta used in Odum/Griffin et al. and MADRID 2 simulations.....	3-9
Table 3-3.	Determining emissions of alkanes, alkenes, and ketones from emissions (anthropogenic only) of CBM-IV species	3-10
Table 3-4.	Model performance statistics of one-hour average O_3 concentrations for the Models-3/CMAQ simulations of Nashville, Tennessee, 15-18 July 1995	3-13
Table 3-5.	Measured vs. predicted $\text{PM}_{2.5}$ and sulfate concentrations in Nashville.....	3-29
Table 3-6.	Summary of SOA predictions ($\mu\text{g m}^{-3}$) at three sites: Land Between Lakes (LBL), Nashville (NAS), and Youth, Inc. (YOU)	3-36
Table 3-7.	Summary of SOA ($\mu\text{g m}^{-3}$) partitions predicted by three absorption modules at three sites: Land Between Lakes (LBL), Nashville (NAS), and Youth, Inc. (YOU)	3-46
Table 4-1.	Boundary conditions used in the sensitivity simulations for the Nashville, TN domain	4-6
Table 4-2.	O_3 results for Nashville sensitivity cases	4-8

LIST OF TABLES (continued)

Table 4-3.	Predictions of SOA in the base and best estimate sensitivity simulations.....	4-15
Table 4-4.	PM _{2.5} on 16 July and 18 July in the base and best estimate sensitivity cases in Nashville.....	4-21
Table 5-1.	Alternative terpene speciation profile	5-2
Table 6-1.	Boundary conditions for PM components at the surface for the Northeast simulation (µg/m ³)	6-6
Table 6-2.	Model performance statistics of one-hour average O ₃ concentrations for the Models-3/CMAQ simulation of the Northeast domain, 13-15 July 1995	6-8
Table 6-3.	Measured vs. predicted PM _{2.5} and PM _{2.5} components, 15 July 1995 (µg/m ³).....	6-18
Table 7-1.	Boundary conditions used in the sensitivity simulations for the Northeast domain	7-2
Table 7-2.	O ₃ results for Northeast simulations	7-4
Table 7-3.	PM _{2.5} on 14 July and 15 July in the base and best estimate sensitivity cases in Washington, D.C.....	7-13

LIST OF FIGURES

Figure 3-1.	Temporal O ₃ profiles at Youth, Inc. and Nashville, TN, 16 to 18 July 1995	3-14
Figure 3-2.	Spatial distribution of O ₃ at 5 p.m. EST on 16 July 1995 and at 3 p.m. EST on 18 July 1995 simulated by CBM-IV.....	3-15
Figure 3-3.	Spatial distribution of O ₃ at 6 p.m. EST on 16 July 1995 and at 6 p.m. EST on 18 July 1995 simulated by CACM	3-16
Figure 3-4.	Isoprene at Youth, Inc.: observations and simulated values	3-18
Figure 3-5.	Temporal profiles of anthropogenic and biogenic condensable gases in Nashville, 16-18 July 1995 (a) Odum/Griffin et al. formulation, (b) CMU/STI formulation, and (c) MADRID 2	3-20
Figure 3-6.	Spatial distribution of 24-hour average PM _{2.5} on 16 July and 18 July 1995 (a) Odum/Griffin et al. SOA module and (b) MADRID 2	3-22
Figure 3-7.	Temporal profiles of PM _{2.5} in Nashville between 16 July and 18 July 1995 (a) Odum/Griffin et al. module, (b) CMU/STI module, and (c) MADRID 2	3-24
Figure 3-8.	Temporal profiles of PM _{2.5} components in Nashville between 16 July 1995 and 18 July 1995: (a) sulfate, (b) elemental carbon, (c) primary organic carbon, (d) SOA (Odum/Griffin et al. module), and (e) SOA (CMU/STI module)	3-25
Figure 3-9.	Temporal profiles of PM _{2.5} components in Nashville between 16 July 1995 and 18 July 1995: (a) sulfate, (b) elemental carbon, (c) primary organic carbon, (d) SOA (MADRID 2)	3-27
Figure 3-10.	24-Hour average composition of PM _{2.5} components in Nashville on 16 July and 18 July 1995	3-32
Figure 3-11.	Spatial distribution of 24-hour average SOA predicted by (a) Odum/Griffin et al., (b) CMU/STI and (c) AEC SOA modules on 16 July 1995.....	3-34
Figure 3-12.	SOA and condensable gases predictions at NAS and LBL by three modules	3-38

LIST OF FIGURES (continued)

Figure 3-13.	Temporal profiles of SOA as predicted by three modules in Nashville on 16-18 July 1995	3-42
Figure 3-14.	Hydrophilic (Type A) and hydrophobic (Type B) SOA predicted at three sites by the AEC SOA module of MADRID 2	3-43
Figure 3-15.	SOA and condensable gases predictions at NAS and LBL by the hydrophobic absorption module of AEC.....	3-45
Figure 3-16.	Hydrophilic SOA vs. particulate water predicted by MADRID 2 at LBL, NAS, and YOU.....	3-48
Figure 3-17.	Hydrophilic SOA vs. RH predicted by MADRID 2 at LBL, NAS, and YOU.....	3-49
Figure 3-18.	Time series of hydrophilic SOA, Surrogate 1, and RH predicted by MADRID 2 at LBL, NAS, and YOU.....	3-51
Figure 4-1.	Sensitivity simulation procedure	4-4
Figure 4-2.	O ₃ time series for the base case and best estimate sensitivity cases at (a) NAS, (b) YOU, and (c) LBL	4-12
Figure 4-3.	Differences in the concentrations of anthropogenic SOA and O ₃ between the base case and best estimate sensitivity case A	4-16
Figure 4-4.	Spatial distribution of 24-hour average PM _{2.5} (a) Base case on 16 July, (b) base case on 18 July, (c) best estimate sensitivity case A on 16 July, (d) best estimate sensitivity case A on 18 July, (e) best estimate sensitivity case B on 16 July, and (f) best estimate sensitivity case B on 18 July.....	4-18
Figure 5-1.	SOA distribution in the base case and sensitivity case with alternative terpene speciation on 16 July 1995	5-4
Figure 6-1.	Temporal O ₃ profiles at two IMPROVE sites from 13 July 1995 to 15 July 1995.....	6-9

LIST OF FIGURES (continued)

Figure 6-2.	Spatial distribution of O ₃ at 3 p.m. EST on 14 July 1995 and 15 July 1995	6-10
Figure 6-3.	Temporal profiles of anthropogenic and biogenic condensable gases at two IMPROVE sites, 13-15 July 1995.....	6-12
Figure 6-4.	Spatial distribution of 24-hour average PM _{2.5} on 14 July and 19-hour average PM _{2.5} on 15 July 1995	6-13
Figure 6-5.	Temporal profiles of PM _{2.5} at two IMPROVE sites, 13-15 July 1995	6-15
Figure 6-6.	Temporal profiles of PM _{2.5} components at the Edwin B. Forsythe NWR site, 13-15 July 1995: (a) sulfate, (b) elemental carbon (EC), (c) primary organic carbon (POC), (d) SOA (CMU/STI module)	6-16
Figure 6-7.	Average predicted composition of PM _{2.5} components at the Edwin B. Forsythe site and the location of maximum PM _{2.5} (near New York City) on 14 July 1995 (24-hour average) and 15 July 1995 (19-hour average).....	6-20
Figure 7-1.	O ₃ temporal profiles at Edwin B. Forsythe and Washington, D.C. in the base and best estimate sensitivity cases.....	7-7
Figure 7-2.	Spatial distribution of 24-hour average PM _{2.5} on 14 (left) and 15 (right) July 1995 in the base (top) and best estimate sensitivity case A (middle, and best estimate sensitivity case B (bottom).....	7-10

EXECUTIVE SUMMARY

This report presents a series of three-dimensional modeling studies aimed at improving the current understanding of the contribution of biogenic emissions to ozone (O_3) and particulate matter (PM). The specific objectives were to:

- ◆ Determine the likely range of O_3 concentrations in urban areas that can be attributed to biogenic emissions
- ◆ Assess the attainability of the new 8-hour O_3 National Ambient Air Quality Standards (NAAQS)
- ◆ Estimate the contribution of biogenic/natural emissions to $PM_{2.5}$
- ◆ Assess the uncertainties in the modeling of secondary organic aerosols (SOA) formation

The modeling studies were conducted for the Nashville/Tennessee domain and the NARSTO Northeast domain. Both domains feature significant regional biogenic emissions, and also anthropogenic emissions from urban areas, such as Nashville and New York, and from major point sources in the Nashville/Tennessee domain. The Models-3/Community Multiscale Air Quality (CMAQ) model was used as the host model. To represent the state of the science in $PM_{2.5}$ simulations, three new modules were implemented to simulate the formation of SOA. These include (1) the CMU/STI module, (2) the Odum/Griffin et al. module, and (3) the AER/EPRI/Caltech (AEC) module. The AEC module is implemented within the comprehensive PM model called the Model of Aerosol Dynamics, Reaction, Ionization, and Dissolution, Version 2 (MADRID 2). Each module was implemented with a unique chemical mechanism. Changes were made to the Carbon-Bond Mechanism, Version IV (CBM-IV) for the CMU/STI and Odum/Griffin et al. modules, and a new gas-phase mechanism, the Caltech Atmospheric Chemistry Mechanism (CACM) was implemented to support SOA formation in MADRID 2.

Both base case simulations built upon existing O_3 simulations, which were found to provide satisfactory performance. CACM predicted higher O_3 than CBM-IV, most

likely due to different treatments in these mechanisms for the oxidation of biogenic compounds, including isoprene. The Nashville/Tennessee base case simulation was evaluated against limited isoprene data at a semi-rural site. Isoprene predictions were found to agree with the measurements within a factor of two. This finding was consistent with our previous review (Lamb et al., 1999) on the accuracy of BEIS2. PM predictions were found to be commensurate with available data in the Nashville/Tennessee domain, but were lower than observed concentrations in the Northeast domain. Generalized PM emission speciation may result in some errors in predictions. Limited data from which to derive boundary conditions also contributed to uncertainties in PM predictions, because fine particles have long lifetimes in the absence of precipitation.

E.1 Contribution of Biogenic Emissions to O₃

In the Nashville/Tennessee and Northeast domains, sensitivity simulations were performed to estimate the contribution of biogenic emissions to O₃ and PM_{2.5}. In one sensitivity approach, a full perturbation approach was used, where all biogenic emissions were eliminated within the domain. In best estimate sensitivity case A, the influence of natural (biogenic and other non anthropogenic sources, e.g., volcanoes, lightning) emissions at the boundary was also removed. In a second sensitivity case (case B), we simulated an environment with only biogenic emissions and natural boundary conditions. Despite large contributions of biogenic compounds to the emissions of volatile organic compounds (VOC), the contributions of biogenic VOC to the domain average production of O₃ were small in both domains, as deduced from the difference between the base case and sensitivity case A. The contributions of biogenic compounds to the domain average O₃ concentrations were 4 ppb (6% of base case O₃) in Nashville and 12 ppb (16%) in the Northeast domain. Sensitivity cases B predicted domain-average O₃ contributions of 8 ppb (14%) for Nashville and 17 ppb (23%) for the Northeast. These contributions may be compared to the combined anthropogenic and biogenic background O₃ levels of 40 ppb in Nashville and almost 60 ppb in the Northeast, which were assumed at the boundary in the base case simulations. We postulated that large areas of each domain

were sensitive to the availability of NO_x. Therefore, O₃ was not very sensitive to biogenic emissions that consist mainly of VOC.

Urban areas tend to be more sensitive to VOC, since anthropogenic emissions of NO_x are more abundant. The contributions of biogenic emissions to peak O₃ concentrations at urban locations were higher than the domain average contributions in sensitivity case A. In Nashville, biogenic emissions were estimated to account for 34% of the peak one-hour O₃ concentrations, estimated by the deviation between the base case and sensitivity case A. The peak O₃ concentrations in sensitivity case B provided a lower estimate of the contribution of biogenic compounds to O₃ in Nashville (12%) because of the lower NO_x concentrations associated with these scenarios. Therefore, significant non-linearities exist in the formation of O₃ from biogenic and anthropogenic emissions. Different responses for the domain-average and the urban O₃ concentrations in the simulations indicate that the effects of biogenic emissions (of mostly VOC and a small amount of NO_x) on O₃ manifested mainly via their interaction with anthropogenic emissions of NO_x.

The corresponding fraction of O₃ in sensitivity simulation A attributable to biogenics was 22% of the base case value in Washington, D.C. In sensitivity simulation B for this domain, biogenic emissions were found to produce a maximum of 24 ppb of O₃ (21%) in Washington, D.C. These estimates are consistent with each other.

E.2 Attainability of the 8-hour NAAQS

In Nashville and Washington, D.C., biogenic emissions were estimated to account for 32% and 23%, respectively, of the maximum 8-hour O₃ concentrations. In sensitivity simulation A, the simulated maximum 8-hour average O₃ concentration in Nashville dropped from 83 ppb in the base case, exceeding the new NAAQS, to 56 ppb in the sensitivity case with no biogenic emissions. On the other hand, the maximum 8-hour concentration in sensitivity case B implies smaller biogenic contributions (11 ppb or 13%). Therefore, biogenic emissions may contribute significantly to non-attainment of the 8-hour NAAQS in urban areas like Nashville. In the Northeast domain, sensitivity case A indicates that biogenic emissions contributed about 24 ppb to the maximum 8-

hour average of 105 ppb in the Washington, D.C. base case. On the other hand, the maximum 8-hour concentration of O₃ produced by biogenic emissions was 21 ppb. Therefore, while biogenic emissions do not cause exceedances of the 8-hour average NAAQS per se, they contribute significantly to O₃ pollution caused by anthropogenic emissions.

E.3 Contribution of Biogenic/Natural Emissions to PM_{2.5}

Due to small contributions of SOA of biogenic origins to the total simulated PM_{2.5}, the direct contributions of biogenic emissions to the production of SOA within both domains were typically small. However, widespread emissions of reactive biogenic VOC in many parts of the domains affect the production of secondary inorganic PM (e.g., nitrate, sulfate, ammonium) and anthropogenic SOA via their effects on oxidants and radicals. In addition, the reduction of PM of natural origins at the boundary has a significant effect on the simulated PM concentrations within the domain owing to the long atmospheric lifetimes of fine PM. In Nashville, the contribution of biogenic and natural PM_{2.5} was approximately 2 µg m⁻³ averaged over 24 hours. In Washington, D.C., the 24-hour average PM_{2.5} concentrations decreased by approximately 6 µg m⁻³ with the removal of biogenic emissions and natural PM at the boundary.

In simulations with only biogenic and natural emissions, PM concentrations were only on the order 1 to 2 µg m⁻³. These concentrations represent the inflow of background PM from the boundary as well as some formation of secondary compounds. Primary emissions were completely eliminated in these simulations because current inventory only includes anthropogenic sources. In addition, the formation of secondary compounds was curtailed by reduced emissions of precursors as well as lower levels of oxidants.

E.4 Uncertainties in the Modeling of SOA Formation

Significant uncertainties in the modeling of SOA are highlighted in this work. The formation of SOA is sensitive to the mixture of precursors, including biogenic precursors, being modeled. Different terpene speciation profiles can cause a 50% change

in the predicted amount of SOA in the Odum/Griffin et al. module, which considers explicit terpene species. Therefore, a BEIS3 type emissions model with explicit terpene representation is desirable. The NO₃ reaction appeared to be an important mechanism for SOA formation. Further research should help elucidate the reaction mechanisms and the identities of the condensable products.

We compared the SOA predictions of the three modules incorporated into Models-3 in this project. Two of the modules, Odum/Griffin et al. and CMU/STI, were developed based on empirical data. In both cases, condensable products were not explicitly identified and were simulated as surrogates based on modified versions of the CBM-IV mechanism. They differ in the SOA precursors and condensable products simulated. Odum/Griffin et al. models a large number of biogenic precursors, while CMU/STI represents only one monoterpene precursor. CMU/STI models the formation of condensables from both primary species and secondary aromatic compounds. In contrast, Odum/Griffin et al. simulates only 2 classes of primary aromatic compounds.

The modeling approach of CACM, used with MADRID 2/AEC, consists in following several generations of condensable products explicitly. A fundamental approach is used in the gas/particle partition routine based on estimated properties of the explicit condensable products rather than on empirical data. One additional difference between the MADRID 2/AEC and the empirical approaches is that the formation of SOA by aqueous dissolution is modeled in MADRID 2/AEC in addition to absorption into an organic phase.

The predictions of three different SOA modules differed by as much as a factor of 40. For example, the domain average SOA concentrations on 16 July predicted by Odum/Griffin et al., CMU/STI, and MADRID 2 were 0.065, 0.63, and 2.39 $\mu\text{g m}^{-3}$, respectively. Of the three modules, only the AEC SOA module of MADRID 2 simulates the formation of hydrophilic SOA, and these compounds contribute significantly to the observed differences in SOA predictions. At present, the formation of water soluble condensable compounds and their gas/particle partition are major knowledge gaps.

Further experimental work is needed to define the identities of the partitioning compounds as well as the parameters for the gas/particle partition of SOA. Current modules differ significantly in both areas. For example, the Odum/Giffin et al. module

predicted higher formation of biogenic SOA than anthropogenic SOA, while the reverse was true in the CMU/STI module. The absorption parameters used in the CMU/STI and AEC modules favored partition into the particulate phase over the gas phase, but the opposite result was obtained in the Odum/Griffin et al. approach. Temperature dependence may be an important factor, since experimental smog chamber data (e.g., used in Odum/Griffin et al.) are typically obtained at high temperatures that may not be favorable to the condensation of SOA.

SOA may be formed via absorption, adsorption, aqueous dissolution, and saturation. Current modules fail to represent more than one or two of these pathways, and, except for MADRID 2, do not address the simultaneous partition due to several processes. Further model development and evaluation are clearly needed in this area.

1. INTRODUCTION

Since the establishment of the National Ambient Air Quality Standards (NAAQS) for oxidants and ozone (O₃) in the early seventies, the ambient concentrations of O₃ have decreased substantially in most areas due to reduced emissions of O₃ precursors, nitrogen oxides (NO_x) and volatile organic compounds (VOC), from anthropogenic sources.

More recently, regulatory efforts have been expanded to particulate matter (PM), especially fine PM of aerodynamic diameter of 2.5 μm or less (PM_{2.5}). While O₃ is formed in the atmosphere, fine particles may be of primary or secondary origins. Therefore, reductions in PM may require reductions in both primary PM and gaseous precursors of secondary PM. Secondary PM includes sulfate, nitrate, and organic compounds; these species together with ammonium can comprise much of PM_{2.5} in areas beyond the zone of influence of PM sources. The dominant component of secondary PM_{2.5} is geographically variable. In the western U.S., nitrate is typically more abundant, while sulfate tends to be the dominant secondary component in eastern U.S. The contributions of organic compounds may be comparable to sulfate at some locations, e.g., in the Upper Midwest Class I Areas (Pun et al., 2001a). While current measurement technologies do not allow the distinction between primary and secondary organic compounds, various analyses suggest that the fraction of secondary organic aerosols (SOA) may be high in locations downwind of major VOC emissions, especially in summer when photochemistry is active.

As anthropogenic emissions of O₃ precursors, PM, and PM precursors continue to decrease in the U.S., the fraction of O₃ and PM attributable to natural sources may become significant in some locations, reducing the efficacy that can be expected from future controls of anthropogenic sources. We addressed this issue by conducting modeling studies of O₃ and PM_{2.5} formation in two distinct domains: the Nashville, Tennessee domain and the NARSTO/Northeast domain. The specific objectives of this work were to:

- Determine the fraction of O₃ that can be attributed to biogenic emissions
- Assess the attainability of an 8-hour O₃ NAAQS of 80 ppb

- Estimate the contribution of biogenic SOA to PM_{2.5}
- Assess the uncertainties in the modeling of SOA formation from biogenic precursor emissions

In our Phase I report to the Coordinating Research Council (CRC) (Lamb et al., 1999), we reviewed the state of the science in biogenic emissions and the atmospheric fate of biogenic compounds, including their chemistry and formation of SOA from condensable products. The modeling studies discussed here complement our understanding by addressing the influence of biogenic compounds on ambient O₃ and PM based on state-of-the-science models. The air quality model used here, Models-3/Community Multiscale Air Quality Modeling System (CMAQ), represents one of the best available tools. Nevertheless, we improved its formulation for PM_{2.5} simulations by incorporating some enhancements in SOA chemistry and gas/particle partition to ensure that the current state of knowledge is properly reflected in these modeling studies. These enhancements are presented in Section 2. In Sections 3 to 5, we present our modeling results for the Nashville domain. Section 3 presents our approach to this modeling study and the evaluation of model performance for the base case. In addition to evaluating the model for O₃ and PM, we compared the simulated concentrations of isoprene to observations. Ambient isoprene measurements during the 1995 Southern Oxidant Study (SOS) provide an opportunity for a limited model evaluation of the emission model BEIS2 (BEIS2 was used in this study to generate the biogenic portion of the VOC emission inputs). In addition, we compare results obtained with three different SOA modules. Section 4 presents the sensitivity studies conducted to address the contribution of biogenic emissions to O₃ and PM. We present in Section 5 an uncertainty analysis that pertains to the speciation of monoterpenes, a major area of uncertainty in current biogenic emission inventory models. Modeling studies for the Northeast domain are discussed in Sections 6 and 7. Section 6 presents our technical approach and the model performance evaluation for the base case simulation. The sensitivity studies discussed in Section 7 address the contributions of biogenic emissions to O₃ and PM. In the concluding section (Section 8), we present key areas of information gaps pertinent to the modeling of O₃ and SOA attributable to biogenic sources.

2. IMPLEMENTATION OF NEW SECONDARY ORGANIC AEROSOL MODULES INTO MODELS-3/CMAQ

The implementation of three new SOA modules is discussed in this section. Two modules were obtained from the published literature, and a third was developed at AER. The two modules obtained from the literature are: (1) a SOA module based on the California Institute of Technology (Caltech) smog chamber data (Odum et al., 1997; Griffin et al., 1999) and (2) the CRC-sponsored SOA module of Strader et al. (1998), which is a version of the Carnegie-Mellon University (CMU) SOA (Strader et al., 1999) module that was simplified by Sonoma Technology, Inc. (STI). Hereafter, we will refer to these modules as the Odum/Griffin et al. and CMU/STI modules. A new and more detailed SOA module was developed at AER under funding from EPRI and the California Air Resources Board (CARB) (via a subcontract with Caltech, Professor John Seinfeld, Principal Investigator). The AER/EPRI/Caltech SOA module is hereafter referred to as the AEC module.

The Carbon-Bond Mechanism, Version IV (CBM-IV) gas-phase chemical kinetic mechanism was used in the PM simulations with Odum/Griffin et al. and CMU/STI SOA partition formulations. To perform PM simulations, modifications were made to this mechanism to account for condensable products that are not treated in the original mechanism formulation. Current gas-phase mechanisms, including CBM-IV, have been evaluated against smog chamber data that do not involve significant amounts of PM formation. On the other hand, smog chamber studies that address PM formation do not report the effect of PM precursors on O₃ formation. Consequently, the effects of the PM-forming reactions on O₃ formation are not well understood. Therefore, in this study, the reactions that were added to simulate PM formation were formulated in such a way that they have no effect on the chemistry of O₃ and radicals. We present the modifications made to CBM-IV for the Odum/Griffin et al. and CMU/STI SOA modules in Sections 2.1.1 and 2.2.1, respectively.

The new SOA partition modules of Odum/Griffin et al. and CMU/STI are discussed in Sections 2.1.2 and 2.2.2, respectively. These modules were developed according to the Models-3 coding standards and implemented within the existing modal

aerosol module of Models-3/CMAQ. Since condensation is the main pathway for SOA formation, we assumed that all SOA will be present in fine particles. We further assumed equilibrium partition of SOA between the gas phase and the particulate phase, which is appropriate for condensation on fine particles.

The new AEC SOA module is implemented within Version 2 of MADRID (Model of Aerosol Dynamics, Reaction, Ionization, and Dissolution) (Zhang et al., 2000; Pun et al., 2001b). The SOA module is interfaced with a new gas-phase chemical mechanism developed at Caltech (R. Griffin and J. Seinfeld, personal communication, 2000). In the host model, Models-3/CMAQ, the particle size distribution for MADRID 2 is represented using the sectional approach. In addition to the advanced treatment of SOA, MADRID 2 also treats the gas/particle thermodynamic equilibrium of sodium and chloride in addition to sulfate, nitrate, ammonium, and water. Section 2.3 presents the chemical mechanism, SOA module, and PM module used in this new air quality model.

Dry deposition of the added condensable compounds are treated as discussed in Section 2.4.

2.1 Odum/Griffin et al. Module

2.1.1 Gas-phase chemistry

Using empirical SOA data from the Caltech smog chamber, Odum et al. (1997) developed an absorption model that can be used to describe the formation of PM from the oxidation of many aromatic compounds. In this formulation, aromatic compounds are grouped into two classes: the high yield class contains aromatic compounds with few substitutions, while the low yield class consists of highly substituted compounds. Two condensable products are modeled for each class of aromatic compounds. Therefore, four fitted parameters are used in this model for each precursor class, two are stoichiometric coefficients and the other two are gas/particle partition constants for the condensable products. The condensable products are surrogate compounds and their chemical formulas are not identified explicitly.

In CBM-IV, the two classes of aerosol precursors are represented by toluene and xylenes, respectively. Two condensable products were added to the existing reactions of the aromatic species: TOLAER1 and TOLAER2 for toluene oxidation and XYLAER1 and XYLAER2 for xylene oxidation. The stoichiometric coefficients determined experimentally by Odum et al. are listed in Table 2-1. These stoichiometric coefficients are defined in terms of $\mu\text{g}/\text{m}^3$ of condensable product formed per $\mu\text{g}/\text{m}^3$ of precursor reacted. The reactions are formulated as if the stoichiometric coefficients are in ppm/ppm units, thereby assuming that the molecular weights (MW) of the products are the same as those of the precursors.

Griffin et al. (1999) applied the same partition model to numerous biogenic compounds, and determined the stoichiometric coefficients and gas/particle partition parameters of 34 surrogate condensable products from 12 biogenic precursor compounds. The new biogenic reactions generating condensable products are listed in Table 2-1, together with the kinetic rate constants compiled in our Phase I report (Lamb et al., 1999). Note that OH, O₃, and NO₃ are regenerated in these reactions, so that the inclusion of biogenic reactions has no net effect on the photochemistry of the system.

2.1.2 Gas/particle partition

In the Odum/Griffin et al. module, the following equation governs the gas/particle partition of each of the 38 condensable species listed in Table 2-2:

$$K_i = \frac{A_i / M_{\text{sum}}}{G_i} \quad (2-1)$$

where K_i ($\text{m}^3/\mu\text{g}$) is the partition coefficient obtained from the smog chamber experiments (see Table 2-2), A_i ($\mu\text{g}/\text{m}^3$ air) is the mass concentration of species i in the particle phase, G_i ($\mu\text{g}/\text{m}^3$ air) is the mass concentration of species i in the gas phase, and M_{sum} ($\mu\text{g}/\text{m}^3$ air) is the sum of primary organic compounds (assumed to be non-volatile) and secondary organic compounds (assumed to be semi-volatile) in the particulate phase that serve as the organic absorbing medium. Theoretically, M_{sum} can vary as A_i 's vary.

Table 2-1. Modifications to CBM-IV for the Odum/Griffin et al. SOA module.

Anthropogenic reactions with new products		
TOL + OH → 0.08 XO2 + 0.36 CRES + 0.44 HO2 + 0.56 TO2 + 0.71 TOLAER1 + 0.138 TOLAER2		
XYL + OH → 0.7 HO2 + 0.5 XO2 + 0.2 CRES + 0.8 MGLY + 1.1 PAR + 0.3 TO2 + 0.038 XYLAER1 + 0.167 XYLAER2		
Biogenic compound (molecular weight)	New biogenic reactions	Rate constants⁽¹⁾ (cm³ molec⁻¹ s⁻¹)
Carene (136)	CAR + OH → 0.054 CARAER1 + 0.517 CARAER2 + OH	8.8 x 10 ⁻¹¹
	CAR + O3 → 0.128 CARAER3 + 0.068 CARAER4 + O3	3.7 x 10 ⁻¹⁷
	CAR + NO3 → 0.743 CARAER5 + 0.257 CARAER6 + NO3	9.1 x 10 ⁻¹²
Caryophyllene (204)	CRP + OH → 1.0 CRPAER + OH	1.97 x 10 ⁻¹⁰
Humulene (206)	HUM + OH → 1.0 HUMAER + OH	2.93 x 10 ⁻¹⁰
Limonene (136)	LIM + OH → 0.239 LIMAER1 + 0.363 LIMAER2 + OH	1.71 x 10 ⁻¹⁰
Linalool (154)	LNL + OH → 0.073 LNLAER1 + 0.053 LNLAER2 + OH	1.59 x 10 ⁻¹⁰
Ocimene (136)	OCI + OH → 0.045 OCIAER1 + 0.149 OCIAER2 + OH	2.52 x 10 ⁻¹⁰
α-pinene (136)	APIN + OH → 0.038 APINAER1 + 0.326 APINAER2 + OH	5.37 x 10 ⁻¹¹
	APIN + O3 → 0.125 APINAER3 + 0.102 APINAER4 + O3	8.66 x 10 ⁻¹⁷
β-pinene (136)	BPIN + OH → 0.13 BPINAER1 + 0.0406 BPINAER2 + OH	7.89 x 10 ⁻¹¹
	BPIN + O3 → 0.026 BPINAER3 + 0.485 BPINAER4 + O3	1.36 x 10 ⁻¹⁷
	BPIN + NO3 → 1.0 BPINAER5 + NO3	2.31 x 10 ⁻¹²
Sabinene (136)	SAB + OH → 0.067 SABAER1 + 0.399 SABAER2 + OH	1.17 x 10 ⁻¹⁰
	SAB + O3 → 0.037 SABAER3 + 0.239 SABAER4 + O3	8.6 x 10 ⁻¹⁷
	SAB + NO3 → 1.0 SABAER5 + NO3	1.0 x 10 ⁻¹¹
Terpinene (136)	TER + OH → 0.091 TERAER1 + 0.367 TERAER2 + OH	2.7 x 10 ⁻¹⁰
Terpinenol (154)	TPO + OH → 0.049 TPOAER1 + 0.063 TPOAER2 + OH	1.59 x 10 ⁻¹⁰
Terpinolene (136)	TPL + OH → 0.046 TPLAER1 + 0.034 TPLAER2 + OH	2.25 x 10 ⁻¹⁰

(1) Lamb et al. (1999)

Table 2-2. Partition constants of the Odum/Griffin et al. SOA module (Odum et al., 1997; Griffin et al., 1999).

Condensable Species	K (m ³ /μg)
TOLAER1	0.053
TOLAER2	0.0019
XYLAER1	0.042
XYLAER2	0.0014
CARAER1	0.043
CARAER2	0.0042
CARAER3	0.337
CARAER4	0.0036
CARAER5	0.0088
CARAER6	0.0091
CRPAER	0.0416
HUMAER	0.0501
LIMAER1	0.055
LIMAER2	0.0053
LNLAER1	0.049
LNLAER2	0.0210
APINAER1	0.171
APINAER2	0.0040
APINAER3	0.088
APINAER4	0.0788
BPINAER1	0.044
BPINAER2	0.0049
BPINAER3	0.195
BPINAER4	0.0030
BPINAER5	0.0163
SABAER1	0.258
SABAER2	0.0038
SABAER3	0.819
SABAER4	0.0001
SABAER5	0.0115
OCIAER1	0.174
OCIAER2	0.0041
TPOAER1	0.159
TPOAER2	0.0045
TERAER1	0.081
TERAER2	0.0046
TPLAER1	0.185
TPLAER2	0.0024

Therefore, an iterative procedure would be necessary to solve the partition equations simultaneously for all condensing species. In the interest of computational resources, however, M_{sum} is calculated based on the concentration and composition of PM at the beginning of the time step in each grid cell, and held constant for the partition calculation. The system of 38 equations is therefore decoupled, and can be solved explicitly as follows:

$$A_i = \frac{C_i K_i M_{sum}}{(1 + K_i M_{sum})} \quad (2-2)$$

where C_i is the total concentration ($\mu\text{g}/\text{m}^3$ air) of species i in the gas phase and the particulate phase available for partitioning. Decoupling the calculation of M_{sum} from the determination of A_i results in minimal error if M_{sum} is dominated by primary organic aerosols or if the concentration and composition of organic particles change slowly with time.

2.2 CMU/STI Module

2.2.1 Gas-phase chemistry

In Strader et al. (1998), SOA formation from alkanes, alkenes, and secondary aromatic products (such as phenol, cresol, and nitrophenol) is modeled in addition to that from aromatics and terpenes. Since CBM-IV does not explicitly treat alkane and alkene species, it was necessary to map individual species to the CBM-IV functional groups. Based on the composition of ambient VOC in the Nashville area, the formation of condensables from two classes of alkanes was mapped to the reaction of PAR with OH and the condensables from two alkene classes were mapped to the reactions of OLE with OH, O_3 and O. In addition to condensable products, a new volatile product, benzaldehyde (BZA), was added to the reactions of TOL and XYL. Condensable products were included in the CRES and TERP reactions. NPHN, which is the surrogate for nitrophenol and nitrocresol, was added as a product of the CRO + NO_2 reaction. New

reactions include the reactions of BZA and radicals derived from it, and the reactions of phenol (PHEN) and nitrophenol (NPHN). Radicals and O₃ are always regenerated in these new reactions, so that they do not affect O₃ chemistry. These new reactions were typically obtained from CBM-X (Gery et al., 1988), the more comprehensive version of CBM-IV. Six condensable products are formed: CG1 and CG2 are formed from the oxidation of toluene; CG1 and CG3 are formed from the oxidation of xylenes, CG4 is formed from alkanes reacting with OH, alkenes reacting with O₃, O, and NO₃, and in the reactions of aromatic secondary products (cresol, benzaldehyde, phenol and nitrophenol); CG5 and CG6 are included as terpene products. In the CMU/STI module, the stoichiometric coefficients are given as μg/m³ of condensable product per ppm of precursor reacted. Using the molecular weight (MW) provided for the condensable species by Strader et al. (1998), the stoichiometric coefficients were converted to ppm/ppm units at room temperature in the implementation of the CBM-IV mechanism. The modifications to CBM-IV are listed in Table 2-3.

2.2.2 Gas/particle partition

The formulation of gas/particle partition in the CMU/STI module is also based on absorption theory. However, an ideal solution and Raoult's law are assumed for the organic particulate phase. Therefore, the partition relationships are defined based on the saturation vapor pressure of the condensable species, and the gas-phase concentration is defined to be equal to the product of the species mole fraction in the liquid phase and the pure liquid saturation vapor pressure:

$$G_i = \frac{A_i/MW_i}{\sum_{j=1}^n A_j/MW_j} \cdot c_i^0 = x_i c_i^0 \quad (2-3)$$

where MW_i is the molecular weight of species i, x_i is the mole fraction of i in the liquid phase, and c_i⁰ is the pure liquid saturation vapor concentration in μg/m³ (Table 2-4). Since the mole fractions are defined based on condensable compounds only, the SOA

Table 2-3. Modifications to CBM-IV for the CMU/STI SOA module.

Anthropogenic and biogenic reactions with new products		
PAR + OH → 0.87 XO ₂ + 0.13 XO ₂ N + 0.16 HO ₂ + 0.11 ALD ₂ + 0.76 ROR + (-0.11) PAR + 4.729 x 10 ⁻⁴ CG ₄		
OLE + OH → FORM + ALD ₂ + XO ₂ + HO ₂ + (-1) PAR + 1.549 x 10 ⁻³ CG ₄		
OLE + O ₃ → 0.5 ALD ₂ + 0.74 FORM + 0.33 CO + 0.44 HO ₂ + 0.22 XO ₂ + 0.1 OH + (-1) PAR + 1.549 x 10 ⁻³ CG ₄		
OLE + O → 0.63 ALD ₂ + 0.38 HO ₂ + 0.28 XO ₂ + 0.3 CO + 0.2 FORM + 0.02 XO ₂ N + 0.22 PAR + 0.2 OH + 1.549 x 10 ⁻³ CG ₄		
OLE + NO ₃ → 0.91 XO ₂ + 0.02 XO ₂ N + ALD ₂ + FORM + (-1) PAR + NO ₂ + 1.549 x 10 ⁻³ CG ₄		
TOL + OH → 0.08 XO ₂ + 0.36 CRES + 0.44 HO ₂ + 0.56 TO ₂ + 0.083 CG ₁ + 0.173 CG ₂		
XYL + OH → 0.7 HO ₂ + 0.5 XO ₂ + 0.2 CRES + 0.8 MGLY + 1.1 PAR + 0.3 TO ₂ + 0.0571 CG ₁ + 0.209 CG ₃ + 0.1 BZA		
CRES + OH → 0.4 CRO + 0.6 XO ₂ + 0.6 HO ₂ + 0.3 OPEN + 0.0457 CG ₄		
CRES + NO ₃ → CRO + HNO ₃ + 0.0457 CG ₄		
CRO + NO ₂ → NTR + NPHN		
TERP + OH → OH + 0.121 CG ₅ + 1.609 x 10 ⁻⁵ CG ₆		
TERP + NO ₃ → NO ₃ + 0.121 CG ₅ + 1.609 x 10 ⁻⁵ CG ₆		
TERP + O ₃ → O ₃ + 0.121 CG ₅ + 1.609 x 10 ⁻⁵ CG ₆		
New secondary compounds	New reactions	Rate constants⁽¹⁾ (cm³ molec⁻¹ s⁻¹)
Benzaldehyde	BZA + OH → 1.034 x 10 ⁻³ CG ₄ + BZO ₂ + OH	1.36 x 10 ⁻¹¹
	BZA + NO ₃ → 1.034 x 10 ⁻³ CG ₄ + BZO ₂ + NO ₃	1.40 x 10 ⁻¹² (T/300) ⁻¹ e ^{-1886/T}
Peroxybenzyl radical	BZO ₂ + NO → PHO + NO	2.52 x 10 ⁻¹²
	BZO ₂ + HO ₂ → PHEN + HO ₂	3.40 x 10 ⁻¹³ (T/300) ⁻¹ e ^{800/T}
	BZO ₂ + C ₂ O ₃ → PHEN + C ₂ O ₃	2.80 x 10 ⁻¹² (T/300) ⁻¹ e ^{530/T}
	BZO ₂ + XO ₂ → PHEN + XO ₂	1.86 x 10 ⁻¹¹ (T/300) ⁻¹ e ^{530/T}
Phenoxy radical	PHO + HO ₂ → PHEN + HO ₂	3.40 x 10 ⁻¹³ (T/300) ⁻¹ e ^{800/T}
	PHO → PHEN	1.0 x 10 ⁻¹³
	PHO + NO ₂ → NPHN + NO ₂	1.36 x 10 ⁻¹¹
Phenol	PHEN + OH → 0.0397 CG ₄ + OH	2.63 x 10 ⁻¹¹ (T/300) ⁻¹
	PHEN + NO ₃ → 0.0397 CG ₄ + NO ₃	3.59 x 10 ⁻¹² (T/300) ⁻¹
Nitrophenol	NPHN + NO ₃ → 0.059 CG ₄ + NO ₃	3.59 x 10 ⁻¹² (T/300) ⁻¹

(1) source: CBM-X

Table 2-4. Aerosol yield parameters and saturation concentrations of the CMU/STI module (Strader et al., 1998).

Condensable Species	Saturation Concentration ($\mu\text{g m}^{-3}$)
SOA1	0.023
SOA2	0.572
SOA3	0.776
SOA4	0.007
SOA5	0.008
SOA6	0.008

dissolve in a solution of secondary compounds. In this equation, MW_i/c_i^0 plays the role of K_i in the Odum/Griffin et al. formulation. The module is formulated in a manner similar to that of the Odum/Griffin et al. module, and the denominator is treated as constant for a given time step in the partition calculation. Since only SOA forms the absorbing medium, a special case where no SOA is initially present (all $A_i = 0$) is included, where we assume an initial concentration of the absorbing medium and iterate to obtain the concentration of the absorbing medium.

2.3 MADRID 2 with the AER/EPRI/Caltech SOA Module

2.3.1 Gas-phase chemistry

A new gas-phase chemical kinetic mechanism, the Caltech Atmospheric Chemistry Mechanism (CACM), was obtained from Robert Griffin and John Seinfeld, Caltech (private communication, 2000). This mechanism contains 361 reactions among 189 species and provides detailed descriptions of the chemistry of alkanes (3 classes), alkenes (2 classes), aromatics (2 classes), alcohols (3 classes), isoprene, and terpenes (2 classes). Several generations of products are described, including the formation of highly polar products with multiple functional groups. In the past, gas-phase mechanisms have been designed to model O_3 formation and secondary organic compounds have typically not been modeled in detail. For the purpose of modeling SOA, however, it is important to represent the formation of multifunctional compounds that have low vapor pressures and are expected to form SOA by condensing onto existing particles or forming new ones. Some multifunctional compounds may also have hydrophilic properties and can dissolve into aqueous particles. Therefore, CACM is uniquely suitable for modeling SOA because 42 condensable second- and third-generation products are explicitly represented, including 14 with sufficient solubility to dissolve into aqueous particles.

2.3.2 Gas/particle partition

The AEC SOA module (EPRI, 1999) simulates an external mixture of hydrophilic and hydrophobic particles. Hydrophilic condensable organic compounds partition into existing aqueous particles when liquid water is available (e.g., associated with inorganic components). This partition is governed by Henry's Law, and takes into account the activity coefficient of the molecular solute, which is calculated using UNIFAC (Lyman et al., 1990). The dissociation of condensable organic compounds with acidic functional groups increases their partition into the aqueous phase. When no liquid water is available, hydrophilic condensable products will undergo absorption, similar to the partition of hydrophobic compounds, discussed below. Hydrophilic SOA are associated with additional particulate water when the ambient relative humidity is above the deliquescence humidity of any individual organic compound in the particulate phase. Since the addition of organic ions and water will affect the partition of inorganic components, such as nitrate and ammonium, this module interacts with an inorganic equilibrium partition model, such as SCAPE2 (Meng et al., 1998) or ISORROPIA (Nenes et al., 1999), to simulate organic-inorganic interactions.

Hydrophobic condensable organic compounds are absorbed into particles and are modeled using equilibrium partition between the particulate phase and the gas phase, as represented in Equation 2-1.

The particulate-phase concentration A_i is calculated based on the partition coefficient K_i , the gas-phase concentration G_i , and M_{sum} , the sum of SOA and any primary organic material that may serve as the absorbing organic medium. The partition constant is calculated following Pankow (1994):

$$K_i = \frac{760 RT}{10^6 P_i^{\text{sat}} \gamma_i (MW)_{\text{om}}} \quad (2-4)$$

Key parameters include the saturation vapor pressure (P_i^{sat}) of the partitioning compounds, the UNIFAC-derived activity coefficient (γ_i) of the partitioning compound in the particulate phase, and the average molecular weight (MW_{om}) of the organic material into which the condensable compound is absorbed.

Both the hydrophilic and hydrophobic SOA modules require the simultaneous solution of partition equations for several compounds. A globally convergent Newton/line search method is implemented in the AEC module. In the interest of computational resources in 3-D applications, some simplifications are provided as options. The amount of water associated with hydrophilic organic compounds is calculated by assuming that the water associated with each hydrophilic compound in a binary solution is additive (i.e., using the ZSR equation). In the hydrophobic module, M_{sum} in Equation 2-1 is calculated based on the concentration and composition of PM at the beginning of the time step in each grid cell, and held constant for the partition calculation. This option is similar to the approach used in the Odum/Griffin et al. SOA module and should only result in minimal error if M_{sum} is dominated by primary organic aerosols, or if the concentration and composition of organic particles change slowly with time. Further information regarding the formulation of the AEC module can be found in EPRI (1999).

A surrogate compound approach is used for the interface of AEC with CACM. We represented the 42 condensable organic products of CACM using 10 surrogate compounds, grouped according to their affinity (5 surrogate species for 28 explicit hydrophobic compounds and 5 surrogate species for 14 hydrophilic compounds), origins (anthropogenic vs. biogenic), size (number of carbons), volatility, and dissociation properties (Pun et al., 2000). Each surrogate compound takes up the characteristic size and functional groups of the explicit compounds it represents, as shown in Table 2-5. Due to the paucity of property data for complex organic compounds, partition parameters, such as Henry's law constants and saturation vapor pressures, are estimated using group contribution methods. Dissociation constants and deliquescence relative humidities are assigned based on analogy to simpler compounds.

Although the calculations are performed using surrogate species in the aerosol module, gas-phase and particulate-phase concentrations of the explicit species are tracked in the model. Each explicit condensable species is partitioned into the particulate phase and gas phase based on the behavior of the surrogate species at the end of the call to the partition module, so that the number of moles is conserved between the explicit and surrogate representations.

Table 2-5. Surrogate organic oxidation products used in the AEC gas/particle partition module.

Surrogate	Description	#C	COOH	C=O	CHO	OH	ONO ₂	NO ₂	C=C
A1	water soluble, anthropogenic, dissociative, low #C	3	2						
A2	water soluble, anthropogenic, dissociative, high #C	8	2		1				2
A3	water soluble, anthropogenic, non-dissociative	8			2	1			2
A4	water soluble, biogenic, dissociative	9	1	1		1			1
A5	water soluble, biogenic, non-dissociative	10		1	1	1			
B1	Hydrophobic, anthropogenic, benzene-based, low volatility	9	1(a)			1(a)		1(a)	
B2	Hydrophobic, anthropogenic, benzene-based, higher volatility	9	1(a)		1(a)				
B3	Hydrophobic, anthropogenic, naphthalene-based	12					1		
B4	Hydrophobic, anthropogenic, aliphatic	16				1	1		
B5	Hydrophobic, biogenic, aliphatic	10		1		1			1

(a) attached to the aromatic ring as opposed to a side chain alkyl substituent.

2.3.3 Sectional PM model

The AEC SOA module is implemented within Version 2 of the Model for Aerosol Dynamics, Reaction, Ionization, and Dissolution (MADRID 2), a sectional PM model developed at AER (Zhang et al., 2000; Pun et al., 2001b). A summary of the PM module is provided in Table 2-6. This model is comprehensive and provides different options for simulating various processes described in the aerosol dynamics equation. For 3-D modeling, the options selected here (noted in Table 2-6) represent a compromise between computational speed and accuracy. Secondary organic components are assumed to partition only into the fine section of the two-section model.

Multiple iterations are used in the Newton/line search method to solve the simultaneous equations in the AEC routine for aqueous SOA formation, increasing significantly the computational burden for the three-dimensional model. To facilitate 3-D computations, we have decreased the frequency for PM calculations from every time step (5 to 6 minutes) to once every hour. Changing the time step should result in only minimal errors due to removal of condensable material by dry deposition of gases instead of particle deposition.

2.4 Dry Deposition

Dry deposition of condensable gases and organic particles is included in the simulations. Condensable gases typically contain multiple functional groups, such as aldehyde, acid, and alcohol groups. Without information on the identities of these compounds, deposition velocities of the organic gases are assigned by analogy. The deposition velocity of higher aldehydes, calculated by the Models-3/CMAQ meteorological pre-processor, was used for all condensable gases in the Odum/Griffin et al. and CMU/STI formulations, irrespective of the precursor.

For the condensable products formed in CACM, most aliphatic secondary compounds were assigned dry deposition velocities based on their major functional groups, following one of three classes of compounds: aldehydes, nitrates, and acids.

Table 2-6. Description of MADRID 2.

Process	Module (Options are indicated with numbers)	Comments
Gas-phase chemistry	CACM	Modified to account for additional VOC for SOA formation
Coagulation	None	Coagulation is negligible compared to other processes under most conditions.
Nucleation	1. New particle formation theory of McMurry and Friedlander (1979) 2. None ^a	
Gas-particle thermodynamic equilibrium for inorganic species	1. SCAPE2 (sulfate, nitrate, ammonium, sodium, magnesium, potassium, calcium, chloride, carbonate, water) 2. ISORROPIA (sulfate, nitrate, ammonium, sodium, chloride, water) ^a	SCAPE2 is currently being revised. The current version may fail to converge under some conditions (e.g., low relative humidity). ISORROPIA may lead to incorrect predictions of particulate nitrate under some conditions.
Gas-particle equilibrium for organic species	Mechanistic formulation with 10 surrogate species coupled with inorganic aerosol module	see Section 2.3.2
Gas/particle mass transfer for inorganic species	1. Kinetic algorithm 2. Hybrid algorithm ^a 3. Full equilibrium algorithm	The kinetic algorithm is computationally demanding and may not be suitable for most 3-D simulations. Two condensational growth algorithms are available with the kinetic algorithm (see below).
Gas/particle mass transfer for organic species	Hybrid algorithm	SOA formation occurs primarily on fine particles; therefore, a kinetic approach that allows better treatment for cases with coarse/fine particles mass transfer is not necessary.

Table 2-6. Description of MADRID 2 (continued).

Process	Module (Options are indicated with numbers)	Comments
Condensational growth/shrinkage by volatilization	Diffusion-limited condensation/volatilization with options for the advection algorithm and the growth law Finite difference algorithm when hybrid or full equilibrium algorithm is used for mass transfer ^a Advection algorithm when kinetic algorithm is used for mass transfer 1. Bott's algorithm 2. QSTSE algorithm Growth law 1. CIT growth law ^a 2. Fuchs-Sutugin growth law	QSTSE does not apply to the 2-section option.
Dry deposition	Integrated flux approach of Venkatram and Pleim (1999)	see Section 3.4
Aerosol size distribution	Sectional with at least 2 size sections 1. 2-section representation (fine and coarse particles) ^a 2. Multi-section representation ^a	The Stokes diameter is used to define the size section boundaries; note that the PM _{2.5} and PM ₁₀ definitions are based on the aerodynamic diameter.

(a) Options chosen for 3-D modeling.

Aromatic compounds were not assigned any deposition, following the lack of deposition for phenol and cresols in previous simulations.

Organic components in particles are assumed to settle at the same rate as PM_{2.5} particles. Therefore, the calculation of deposition velocity of fine PM was modified in Models-3 to include organic particulate species.

3. BASE CASE SIMULATION IN THE NASHVILLE, TN DOMAIN

Air quality simulations of the Nashville/Western Tennessee region were conducted for O₃ and PM using Models-3/CMAQ. The PM simulation builds upon the O₃ base case simulation that was completed in June 1999 under EPRI funding. As discussed in Section 2, modifications were made to Models-3/CMAQ to incorporate more recent formulations for SOA formation and corresponding changes in the gas-phase chemical mechanisms to simulate the formation of condensable gases.

We present in this section the results of the three Models-3 simulations conducted with these SOA modules for the 14-18 July 1995 episode. Biogenic emissions were obtained with BEIS2.

3.1 Technical Approach

3.1.1 Compilation of Models-3

Once the new reactions for CBM-IV are keyed into the graphical user interface (GUI), Models-3 automatically generates various include files that are needed for compiling the CMAQ code. Several include files contain information about the identity number of species involved in each reaction and the stoichiometric coefficients of the reactants and products. Four sets of include files are generated for gas-phase, particulate-phase, non-reactive, and tracer compounds. Each set includes a species list, and specifications for advection, dry deposition, diffusion, emissions, IC and BC, scavenging, and wet deposition. In addition, include files are used to control the file output of concentration and dry deposition results. Also, species in different phases are matched to one another in the include files.

CACM was also implemented into Models-3/CMAQ using the chemistry reader program of Models-3. The GUI generated the include files associated with the reactions. We developed additional chemistry routines to treat reactions involving variable stoichiometric coefficients (competitive pathways and products) and reaction rate constants with complicated functional forms that are not currently defined in the Models-

3 chemistry reader. Modifications were made to the chemistry solver to interface with the new subroutines.

CACM contains 19 photolysis reactions. The photolysis rates were provided by Caltech as a look-up table based on the solar zenith angle. Models-3/CMAQ requires photolysis rates as a look-up table based on hours. Therefore, we calculated the photolysis rates at each hour based on the time of sunrise/sunset and the solar declination angle.

3.1.2 Meteorological files

Meteorological inputs were generated from an MM5 simulation conducted with four-dimensional data assimilation by AER under an EPRI-sponsored project (Karamchandani et al., 2000). The general meteorology was characterized by a large anticyclone centered over the eastern United States. During the episode, wind flows shifted from weak southeasterly on 14 July to westerly and northwesterly (16-17 July) to northerly (18 July) and finally to easterly on 19 July. Afternoon temperatures were in the high 80's and low 90's. The boundary layer contained sufficient moisture to form some cumulus clouds and sporadic thunder storms.

The MM5 simulation started at 00 UTC on 14 July 1995 and ran for 125 hours to cover the period from local midnight on 14 July to local midnight on 19 July. A three-level nested domain (36, 12, and 4 km horizontal resolution) was used. All three domains were based on the Lambert Conformal (LC) projection and were approximately centered over Nashville, TN.

Physical parameterizations used included the Blackadar scheme for the planetary boundary layer (PBL) diffusion, an explicit moisture scheme with simple ice physics, cumulus convection parameterized by the Grell scheme, and long- and short-wave radiation schemes. In the FDDA simulation, the nudging towards observations was performed using a radius of influence for each observation of 50 km in the horizontal and 0.001 sigma units in the vertical for ± 40 minutes around the observation time. The data used for the observation nudging consisted of both surface and upper-air observations from the SOS dataset, with sites located in and around Tennessee, and the standard

monitoring network as archived at the National Center for Atmospheric Research (NCAR). The SOS data used included hourly averaged temperature, relative humidity, and wind fields from 8 surface stations and hourly consensus average of wind speed and direction from 4 profiler stations with either 101 m or 60 m vertical resolution. Standard National Weather Service (NWS) data from the innermost two domains were available every 3 hours (surface) or 12 hours (soundings).

3.1.3 Time-independent files

Time-independent files, such as land-use and elevation definitions, were obtained from previous simulations conducted under an EPRI-sponsored project (Karamchandani et al., 2000). A new domain was used for the PM simulation. This domain contains 100 x 65 grid cells and is slightly reduced at the northern boundary from the previous simulations. This choice was dictated by the domain covered by area source and biogenic emissions available from simulations conducted at the Tennessee Valley Authority (TVA).

3.1.4 Initial conditions and boundary conditions

Initial conditions (IC) and boundary conditions (BC) files are needed for PM and PM precursors that were not included in the earlier O₃ simulation. These species include individual terpenes, sulfur dioxide (SO₂), ammonia (NH₃), PM_{2.5}, and PM₁₀. Isoprene BC were added since biogenic compounds are of interest in this study (default values were used in earlier O₃-only simulations).

The concentrations of individual terpene species are in general small; therefore, we used a default value of 0.0 ppb for their IC and BC. For SO₂ and NH₃, few or no measurements are available. Therefore, the IC and BC were defined based on the simulated steady-state concentrations from within-domain emissions in a test run with zero IC and BC, where applicable. For NH₃, the domain mean concentration ranges from 0.7 ppb to ~2 ppb, with higher concentrations observed at night. We used a constant value of 2 ppb for both the IC and BC. SO₂ builds up in a simulation with zero IC,

reaching 2.8 ppb after 24 hours of simulation time due to emissions within the modeling domain. We used a temporally averaged concentration of 2 ppb as the IC of the base case simulation. Limited SO₂ data are available from two of the IMPROVE network sites just outside the modeling domain, Great Smoky Mountains and Mammoth Cave. Concentrations recorded at these National Park sites seemed highly variable and ranged from 0.1 to 1.7 ppb around the modeling domain. Therefore, we chose 1 ppb as the BC for the base case simulation. For the vertical profiles, we assumed that the mixing ratio of the gaseous species is constant with height for the IC and BC.

Data are available from the IMPROVE networks for PM₁₀, PM_{2.5}, and PM_{2.5} components, i.e., sulfate, nitrate, elemental carbon (EC), organic carbon (OC), and elemental species. The monitoring schedule of the IMPROVE network was twice a week on Wednesdays and Saturdays. This base case simulation covers the period from 14 July 1995 (Friday) to 18 July 1995 (Tuesday). Therefore, we selected the ground-level BC using the data from 15 July 1995 (Saturday) at five National Park sites. The sites at Great Smoky Mountains and Shining Rock represent the eastern BC. Mammoth Cave in Kentucky was used as the northern BC. The southern BC was derived from Sipsey, south of the domain. The western BC was obtained from Upper Buffalo in Arkansas. The distribution of PM and PM components as a function of height is based on the default profiles used in the Models-3/CMAQ IC and BC (EPA, 1999). The IC for the PM components were determined as the average of all 4 boundaries. Table 3-1 presents the BC of the PM components at the surface.

Isoprene emissions are temperature- and light-dependent. The lack of isoprene emissions at night, combined with its rapid chemical reactions with O₃ (late in the day) and NO₃ (nighttime), makes 0.0 ppb a reasonable IC at the beginning of the simulation at midnight. However, BC need to be defined. In a simulation with zero IC and BC, isoprene concentrations always dropped to below 1 ppb at night. During the day, however, the domain average isoprene concentration builds up, and concentrations range from 2 ppb in the late morning to 3.5 ppb in the late afternoon. We selected the following BC. From midnight until noon, we used a BC of 0 ppb. From 1 p.m. to 8 p.m. local time, we used a boundary concentration of 3 ppb. After 8 p.m., the concentration drops back to 0 ppb.

Table 3-1. Boundary conditions for PM components at the surface ($\mu\text{g}/\text{m}^3$) for the Nashville simulation.

Boundary	North	East	South	West
Site(s)	Mammoth Cave	Great Smoky Mountains, Shining Rock	Sipsey	Upper Buffalo
Sulfate ⁽¹⁾	13.178	14.025	14.385	9.462
Ammonium ⁽¹⁾	5.000	5.309	5.451	3.595
Nitrate ⁽¹⁾	0.202	0.171	0.194	0.163
Organic compounds ⁽¹⁾	4.095	7.898	4.730	5.750
Elemental carbon ⁽¹⁾	0.520	0.575	0.880	0.410
Unspecified PM _{2.5} ⁽¹⁾	12.395	8.968	3.010	5.650
Unspecified coarse PM ⁽²⁾	0.756	0.633	1.788	0.939
Sea salt ⁽³⁾	0.749	0.522	2.243	0.524
Soil ⁽³⁾	6.055	5.175	13.849	7.927

(1) PM_{2.5} composition, assigned to the accumulation mode or fine section.

(2) 10% of all PM_{coarse} ($\text{PM}_{\text{coarse}} = \text{PM}_{10} - \text{PM}_{2.5}$) (Jacobson, 1997)

(3) Sea salt and soil make up 90% of all PM_{coarse} ($\text{PM}_{\text{coarse}} = \text{PM}_{10} - \text{PM}_{2.5}$), relative contribution calculated from the ratio of sea salt to soil in PM_{2.5} measurements.

For the AEC SOA module (MADRID 2) application, IC and BC files were developed for PM and PM precursors that were not included in the earlier Models-3/CMAQ simulations. These species include individual organic compounds (alkanes, alkenes, aromatics, monoterpenes) of CACM and PM components in two size sections.

For anthropogenic organic compounds, we developed IC and BC in a manner similar to that used for the development of the emissions files (see next section). Where applicable, we applied the existing IC and BC directly by mapping the equivalent species between CBM-IV and CACM. For alkanes, ketones, and alkenes, we applied factors to existing IC and BC files of the CBM-IV species PAR, OLE, etc. Since the anthropogenic or biogenic origin of the ambient gases represented in the IC and BC could not be determined, the factors used for primary emissions were applied directly. That is equivalent to assuming that the ambient concentrations are dominated by anthropogenic emissions. This assumption is justified by the fact that biogenic compounds are typically more reactive than anthropogenic compounds and thus biogenic ambient concentrations are relatively small.

For particles, the same IMPROVE network data for PM₁₀, PM_{2.5}, and some PM_{2.5} components, i.e., sulfate, nitrate, EC, OC, and elemental species are used in both the sectional and modal simulations, as shown in Table 3-1.

3.1.5 Emissions

Emissions files were prepared for PM_{2.5}, PM₁₀, SO₂, NH₃, and individual terpene species compatible with the Odum/Griffin et al., CMU/STI, or AEC SOA modules. County-level emissions of NH₃, SO₂, PM_{2.5}, and PM₁₀ were obtained from EPA's National Emission Trends (NET) database (Tom McMullen, EPA, personal communication, 1999), grouped by source category codes (SCC).

Area sources were processed as follows. Using ACCESS, a seasonal factor, a day-of-week factor and a diurnal profile (obtained from Tom Braverman, EPA) were applied to each source category. Emissions from different source categories were aggregated at the county level. Spatial allocation was performed using a UNIX pre-

processor developed at AER to produce gridded and temporally-resolved emissions from the county emissions.

Point sources were selected from the database and processed with Models-3's emissions model SMOKE. Temporal profiles were applied based on season, day-of-week, and time-of-day. SMOKE also calculates the release point of the elevated point sources. As a result, a three-dimensional file is generated for point source emissions.

We applied these procedures to the point source and area source NO_x emissions and we compared the combined NO_x emissions file to the original base case NO_x emissions file obtained from TVA. Since the two files differed by less than 1%, we concluded that the procedures to generate area and point source emissions were accurate. The point source and area source procedures were then applied to generate PM₁₀, PM_{2.5}, NH₃, and SO₂ emissions files. Note that the seasonal factors for fertilizer and livestock categories recommended by Tom Pierce of EPA were applied here.

Emissions files were prepared for PM components in two sections for the application of MADRID 2. The three-dimensional emissions of PM_{2.5} and PM₁₀ prepared for the model PM simulations were processed into fine PM and coarse PM sections using a modal-to-sectional PM emission processor developed at AER. The default chemical composition of each PM section was obtained from the original Models-3 formulation.

For biogenic compounds, isoprene emissions are obtained directly from BEIS2. Terpene emissions from BEIS2 are represented as some combination of CBM-IV species, such as ALD2, PAR, and OLE. The default chemical speciation of monoterpenes gives 0.5 mole OLE, 6 moles PAR, and 1.5 moles ALD2 per mole of monoterpene. To model SOA formation using the Odum/Griffin et al. module, the concentrations of individual terpene species, rather than the lumped structure groups, are needed. From the BEIS2 gridded and temporally-resolved emission estimate of ALD2, the molar emissions of all monoterpenes were calculated. A single terpene class is modeled in the SOA module of CMU/STI. This terpene species is further processed to obtain the emissions of individual terpenes and oxygenate species required by the Odum/Griffin et al. SOA module and two monoterpene classes required by the AEC module.

Chemical speciation of biogenic emissions is a research topic that has attracted much attention during the past few years. Unfortunately, information is still scarce

because terpene species are very difficult to measure in the ambient and not all terpenes species that are emitted have been positively identified. The terpene speciation used for the Nashville is based on Helmig et al. (1999). They identified over 10 monoterpene and sesquiterpene compounds emitted from an Atlanta forest. This composition was used to speciate the BEIS2 terpene emissions (see Table 3-2). Compared to other land types in the Helmig study, the Atlanta forest emits more sesquiterpenes. Emissions of linalool and terpinenol were not measured at this location. A small amount of emissions (0.7% of total terpene emissions) was assumed for each. For use with the AEC module, these emissions were then classified as either high aerosol yield monoterpenes (BIOH, aerosol yield higher than that of α -pinene) or low aerosol yield monoterpenes (BIOL) (see Table 3-2). The emissions of biogenic organic compounds are determined as a fraction of the total monoterpene emissions from BEIS2 (e.g., BIOH = 0.60 x TERP; BIOL = 0.27 x TERP; unreactives = 0.13 x TERP).

The new chemistry mechanism, CACM, models many more organic species than the CBM-IV mechanisms used in previous simulations. We speciated existing emissions of anthropogenic organic compounds as follows. Speciated emissions were prepared for several classes of alkanes, alkenes, ketones, aromatics, etc. We used the emissions of PAR, OLE, TOL, XYL, etc., from previous CBM-IV simulations as a starting point. Many CACM species correspond in a unique manner to CBM-IV species. For example, the emissions of TOL were assigned to the emissions of high aerosol yield aromatic compounds (AROH). The emissions of XYL were assigned to the emissions of low aerosol yield aromatic compounds (AROL). Both PAR and OLE comprise emissions from anthropogenic and biogenic sources in the CBM-IV representation. Alkanes and alkenes are typically of anthropogenic origins. Therefore, we separate biogenic emissions out from the anthropogenic emissions of PAR and OLE by calculating the difference between the total emissions and the biogenic emissions obtained from BEIS2. Next, we applied factors (listed in Table 3-3) to PAR and OLE to obtain emissions of various classes of alkanes, ketones, and alkenes. These factors are calculated based on the fraction of PAR or OLE contributed from each model class in the California South Coast Air Basin, assuming that the speciation of anthropogenic compounds are similar in the two areas.

Table 3-2. Composition of terpenes in Atlanta used in the Odum/Griffin et al. and MADRID 2 simulations.

Compound	Odum/Griffin et al. Model Species	MADRID 2 Model Group	Mole %
α -pinene	APIN	BIOL	7.6
sabinene	SAB	BIOH	0.4
β -pinene ⁽¹⁾	BPIN	BIOH	5.4
3-carene	CAR	BIOH	0.09
terpinene	TER	BIOH	13.6
d-limonene ⁽¹⁾	LIM	BIOH	11.6
ocimene	OCI	BIOL	17.9
terpinolene	TPL	BIOL	0.7
linalool ⁽²⁾	LNL	BIOL	0.7
terpinenol ⁽²⁾	TPO	BIOL	0.7
sesquiterpenes	HUM, CRP ⁽³⁾	BIOH	28.3
unreactives	--	--	13.2

(1) includes other structurally similar compounds.

(2) emission factors for linalool and terpinenol assign by analogy to terpinolene.

(3) equally divided between humulene and caryophyllene in the Odum/Griffin et al. simulation.

Table 3-3. Determining emissions of alkanes, alkenes, and ketones from emissions (anthropogenic only) of CBM-IV species.

Organic compounds	CACM model name	CBM-IV species from which emissions are calculated	Factor⁽¹⁾
Alkanes, C3 – C6	ALKL	PAR	0.12
Alkanes, C6 – C9	ALKM	PAR	0.031
Alkanes, > C9	ALKH	PAR	0.00042
Ketones (C3 – C6)	MEK	PAR	0.0079
Ketones (> C6)	KETH	PAR	0.0068
Alkenes (C3 – C6)	OLEL	OLE	0.96
Alkenes (> C6)	OLEH	OLE	0.044

(1) factors account for composition and difference in number of carbons between CBM-IV and CACM species

3.2 Simulation Results

3.2.1 Simulation time

Simulating PM with the original aerosol module can add significant computational time to a Models-3/CMAQ simulation compared to an O₃-only simulation. For example, an 80% increase in simulation time was observed in a previous simulation of the California South Coast Air Quality Study (SCAQS) episode of 1987 with the EPA default SOA module. The new SOA partition modules of Odum/Griffin et al. and CMU/STI add comparatively small computational requirements to the PM simulation. The 5-day Nashville simulation from 14 July to 19 July 1995 was completed in 80 hours with the Odum/Griffin et al. module and in 67 hours with the CMU/STI module, as opposed to 32 hours for the O₃-only simulation.

The comprehensive CACM mechanism and MADRID 2 with the AEC SOA module added significant computational time to a Models-3/CMAQ simulation compared to a simulation based on CBM-IV and a simple SOA module such as the CMU/STI module. On a Sun Ultra 60 workstation, the 5-day Nashville simulation from 14 July to 18 July 1995 was completed in about 500 CPU hours, as opposed to less than 100 hours with CBM-IV and the Odum/Griffin et al. module or the CMU/STI module. Because of a larger number of model species, the gas-phase mechanism CACM alone can be responsible for a factor of four increase in computational time, from our past experience with a SCAQS simulation. The new SOA partition module adds about 50% more computational requirements, due primarily to the solution of simultaneous equations. Note that the QSSA numerical solver was used for the gas-phase chemistry. The implementation in Models-3/CMAQ of faster numerical solvers at EPA and AER will allow significant reductions in the computational times mentioned above.

3.2.2 O₃ concentrations

As expected, O₃ results are quite similar in the CBM-IV simulations to those from the O₃-only base case. Slight differences are observed at the boundary, where new

isoprene BC were used. Identical O₃ predictions are obtained in the simulations with the two new SOA modules using CBM-IV. Measurements showed a domain maximum O₃ concentration of 124 ppb at Youth, Inc. on 16 July 1995. The domain-wide predicted maximum one-hour O₃ concentration is 105 ppb on 16 July 1995 (~15% bias) and 121 ppb over the five-day simulation on 14 July 1995. Table 3-4 summarizes the model performance statistics of one-hour average ozone concentrations. Figure 3-1 shows the temporal profiles of O₃ at selected monitoring sites. Spatial plots at the time of maximum O₃ on 16 July and 18 July 1995 are presented in Figure 3-2 for the CBM-IV simulations. O₃ tends to be highest downwind of major sources, including major point sources and the Nashville urban area, and lowest in the western part of the domain.

The O₃ concentrations predicted by CACM share a lot of common spatial characteristics with those predicted in the earlier CBM-IV simulations. As shown in Table 3-4, the O₃ model performance is also similar. Spatial plots at the time of maximum O₃ on 16 July and 18 July 1995 are presented in Figure 3-3. Higher O₃ was observed in the eastern half of the domain. The spatially averaged O₃ concentrations simulated with CACM are greater than the CBM-IV simulated values, and high O₃ in excess of 80 ppb was observed over a larger area. The higher O₃ predictions by CACM are possibly due to the difference in the treatment of biogenic reactions in the two mechanisms. Isoprene reactions are represented in greater detail in CACM than in CBM-IV, and the explicit representation of monoterpene reactions is likely to result in different O₃ formation than the OLE, PAR, and ALD2 reactions used to represent them in CBM-IV. Since biogenic emissions are widespread in the Nashville domain, it is not surprising that changes in the representation of biogenic VOC reactions may lead to different levels of O₃. The domain-wide predicted maximum one-hour O₃ concentration is 118 ppb on 16 July 1995, which represents a -5% bias compared to the observed maximum concentration of 124 ppb at Youth, Inc. The domain-wide maximum one-hour O₃ concentration is 132 ppb over the five-day simulation on 18 July 1995 at a location south of the Cumberland power plant. Figure 3-1 shows the temporal profiles of O₃ at selected monitoring sites. The predicted O₃ concentrations were very similar at these sites to those from the CBM-IV-based simulations. On 16 July 1995, both mechanisms underpredict the peak O₃ concentrations. On the 17 to 18 July 1995, CACM predicted O₃

Table 3-4. Model performance statistics of one-hour average O₃ concentrations for the Models-3/CMAQ simulations of Nashville/Tennessee, 15-18 July 1995 (source: Karamchandani et al., 2000).

	CBM-IV	CACM
Paired peak error ⁽¹⁾	-14%	-14%
Gross error	20%	17%
Fractional gross error	0.2	0.17
Bias	4%	4%
Fractional Bias	0.01	0.02

(1) Paired in both space and time

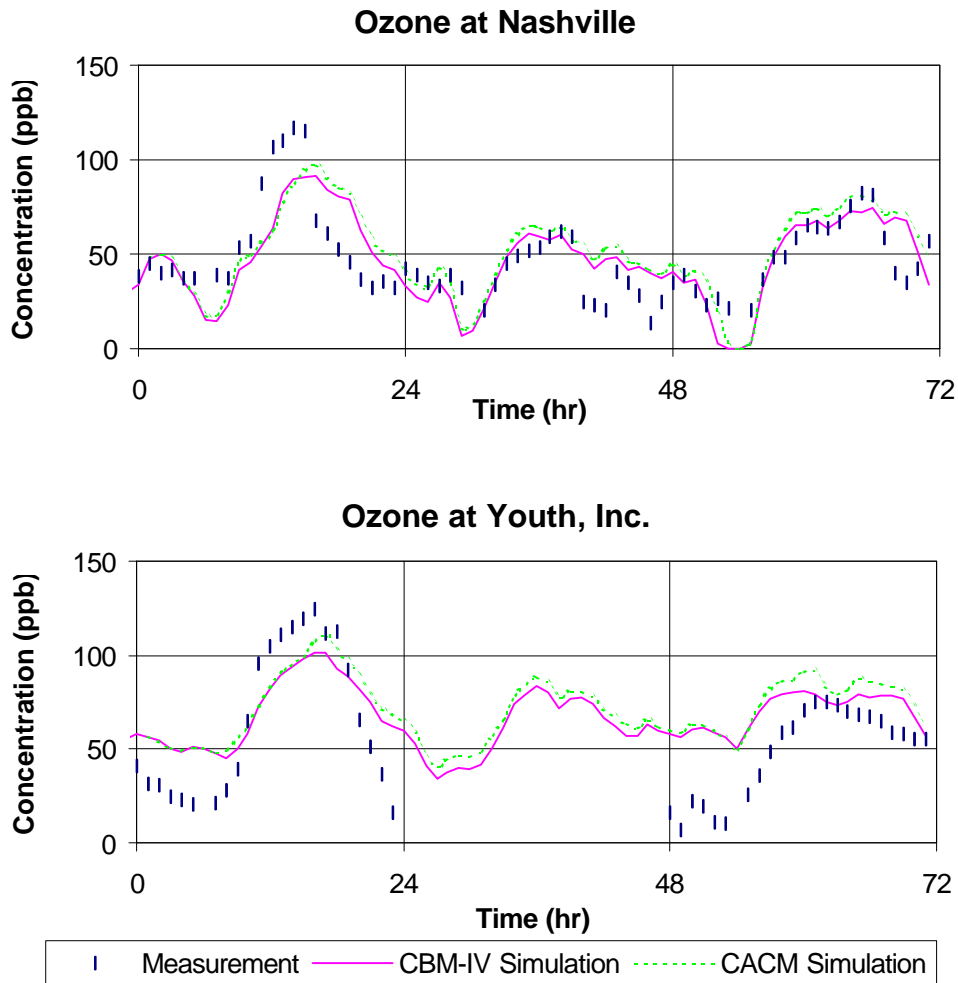


Figure 3-1. Temporal O₃ profiles at Youth, Inc. and Nashville, TN, 16 to 18 July 1995.

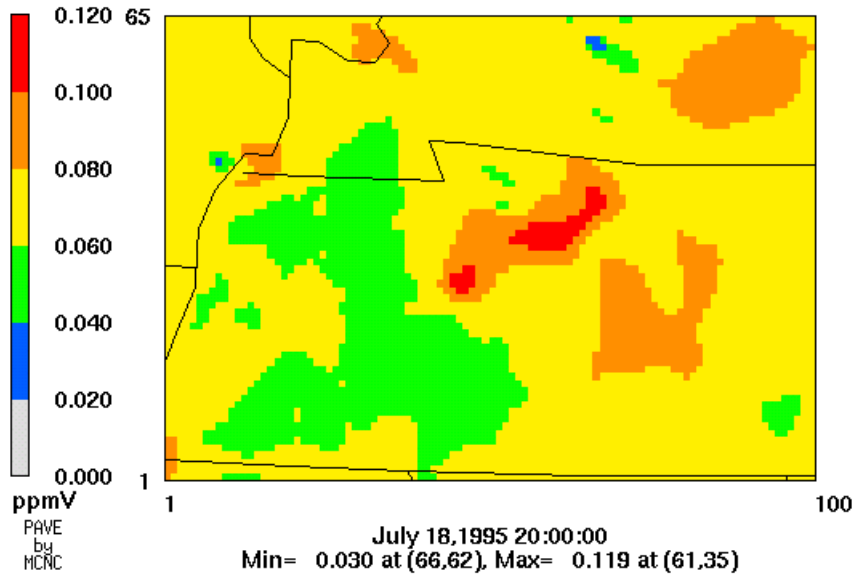
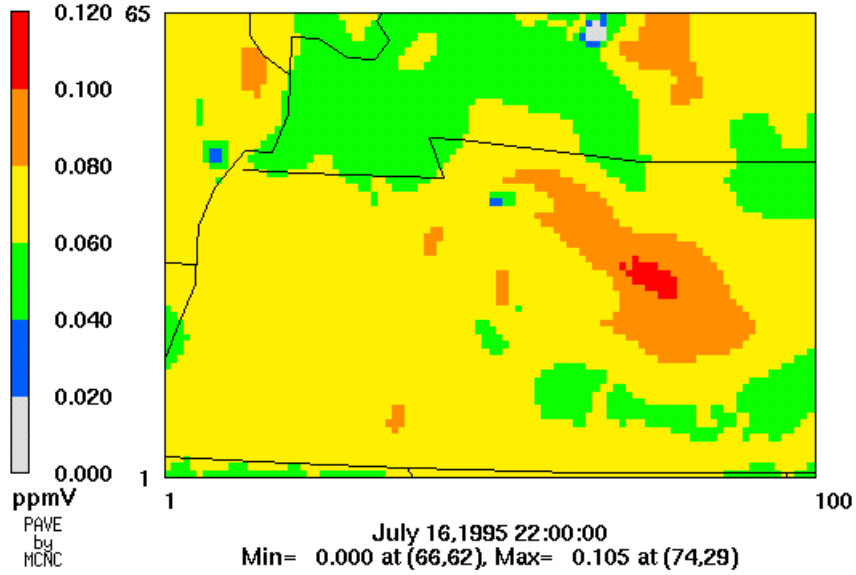


Figure 3-2. Spatial distribution of O₃ at 5 p.m. EST on 16 July 1995 and at 3 p.m. EST on 18 July 1995 simulated by CBM-IV.

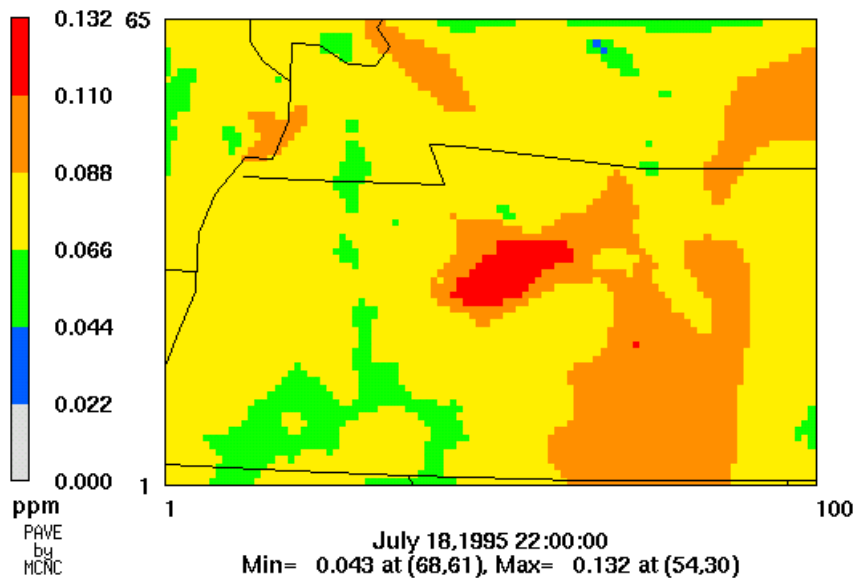
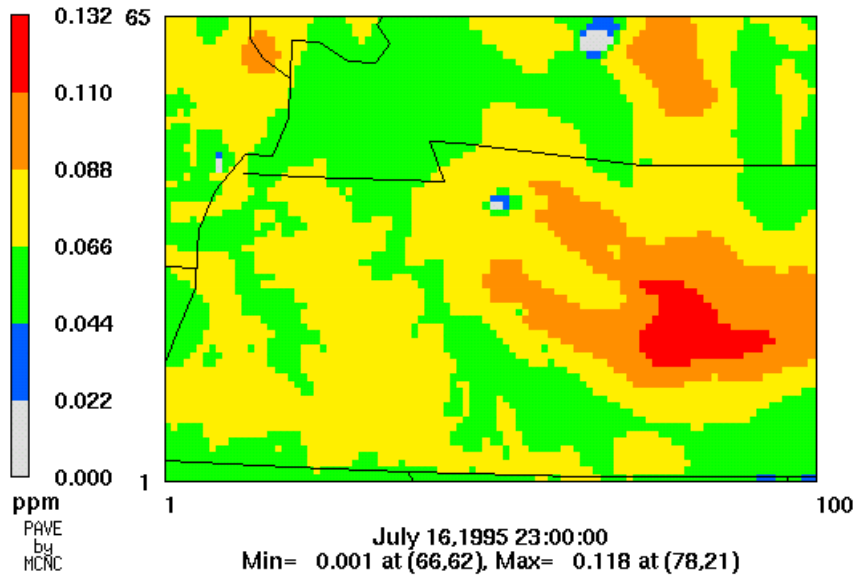


Figure 3-3. Spatial distribution of O₃ at 6 p.m. EST on 16 July 1995 and at 6 p.m. EST on 18 July 1995 simulated by CACM.

concentrations that are a few ppb higher than the CBM-IV simulations. Predictions from both mechanisms agree well with observed data in Nashville on 17 and 18 July.

3.2.3 Biogenic compounds

Some ambient measurements of biogenic VOC were obtained during the 1995 Southern Oxidant Study (SOS). Helmig et al. (1998) measured isoprene and several monoterpene species, including α -pinene, β -pinene, and limonene, at a forest site near Oak Ridge, TN. Starn et al. (1998) measured isoprene at Youth Inc., a semirural location downwind of Nashville that was occasionally affected by urban emissions. The Oak Ridge site lies outside of the current modeling domain. The isoprene data at Youth, Inc. were used to provide some indication in terms of the model's performance in the simulation of biogenic VOC precursors.

Shown in Figure 3-4 are the observations of isoprene and the model simulated values. The model was able to reproduce the correct magnitude and the overall trend of isoprene concentrations. However, the model was not able to predict the peak isoprene concentrations that occurred in the early afternoon on July 18, and missed the early afternoon peak on July 19. A possible reason for this discrepancy between modeled and measured values is the fact that the modeled values represent a volume-average concentration with a 4 km horizontal resolution whereas the measured values may represent more localized events.

These results are consistent with our earlier assessment that isoprene emissions estimated with BEIS2 and similar models are generally accurate within a factor of two and that the atmospheric chemistry is fairly well established (Lamb et al., 1999).

Monoterpenes are emitted most abundantly from forest-covered areas. The emissions are highest during the day. Simulated concentrations exhibit a diurnal cycle where low concentrations are observed during the day. Peak concentrations are simulated in the evening (e.g., 8 p.m.), probably due to reduced mixing as the nocturnal boundary layer sets in. Anthropogenic precursors usually exhibit peak concentrations during the morning (e.g., 5 to 9 a.m.), as a direct result of emissions, or at night due to reduced mixing.

Youth, Inc.

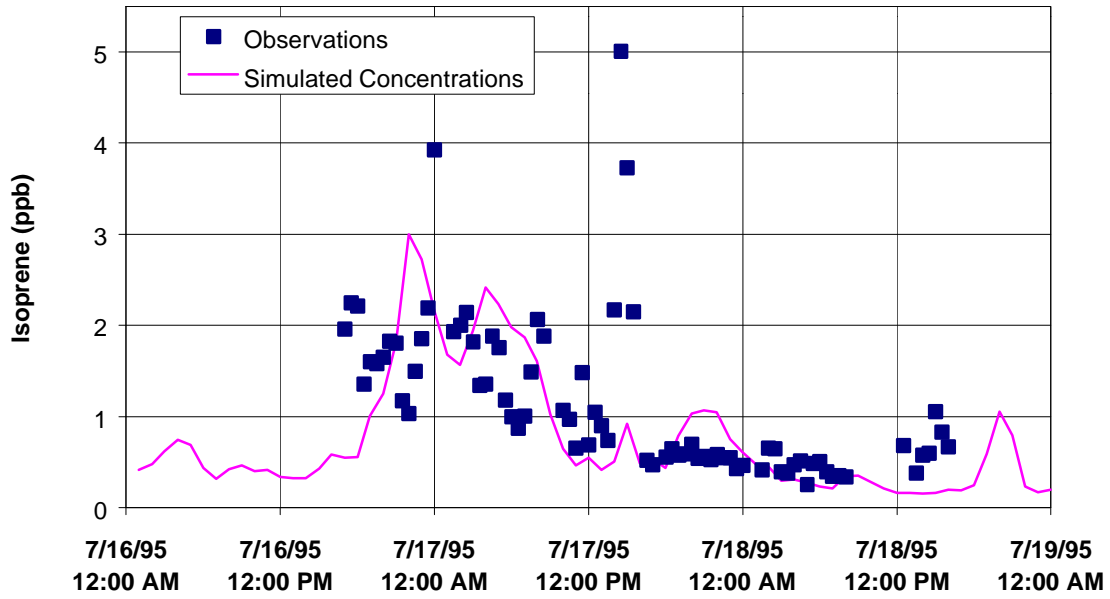


Figure 3-4. Isoprene at Youth, Inc.: observations and simulated values.

3.2.4 Condensable gases

The biogenic organic condensable gases, as predicted by the Odum/Griffin et al. module, display a different temporal profile than the precursors. The diurnal cycle is not as well-defined as for the terpene precursor gases, although peak concentrations also tend to occur at night. Anthropogenic condensable compounds tend to exhibit higher concentrations during the day. Figure 3-5a shows temporal profiles of biogenic and anthropogenic condensable gases at Nashville, as predicted by the Odum/Griffin et al. formulation. At this location, biogenic condensable gases (sum of 34 compounds) are typically more abundant than their anthropogenic counterparts (4 compounds from the reactions of toluene and xylenes).

The CMU/STI module predicts very different results, even though the total emissions of anthropogenic and biogenic precursor compounds are similar to those used in Odum/Griffin et al. The concentrations of gas-phase condensable compounds are small compared to the Odum/Griffin et al. module predictions. While anthropogenic compounds are only lower by a factor of two, biogenic condensables are two orders of magnitudes lower. As a result, biogenic condensable gases predicted by CMU/STI are also about two orders of magnitude lower in concentration than the anthropogenic gases. The reason for the low concentrations of biogenic condensables in the gas phase is that the initial condensables have partitioned heavily into the particulate phase (see Section 3.3). Both biogenic and anthropogenic compounds display strong diurnal trends. High concentrations of anthropogenic compounds are predicted during the day, and biogenic secondary compounds are abundant at night.

Peak concentrations of condensable gases of anthropogenic origins tend to occur in the late afternoons or early evenings (6 – 8 p.m.) in the MADRID 2/AEC simulation. At some locations, high concentrations persist into the night or a secondary morning peak of anthropogenic condensable compounds can be predicted on some days. Biogenic condensable compounds are more widespread. Peak concentrations of biogenic condensables also occur at night or early in the morning, typically later than the time of peak concentrations of terpenes. Figure 3-5c shows temporal profiles of biogenic and anthropogenic condensable gases at Nashville. At this location, anthropogenic

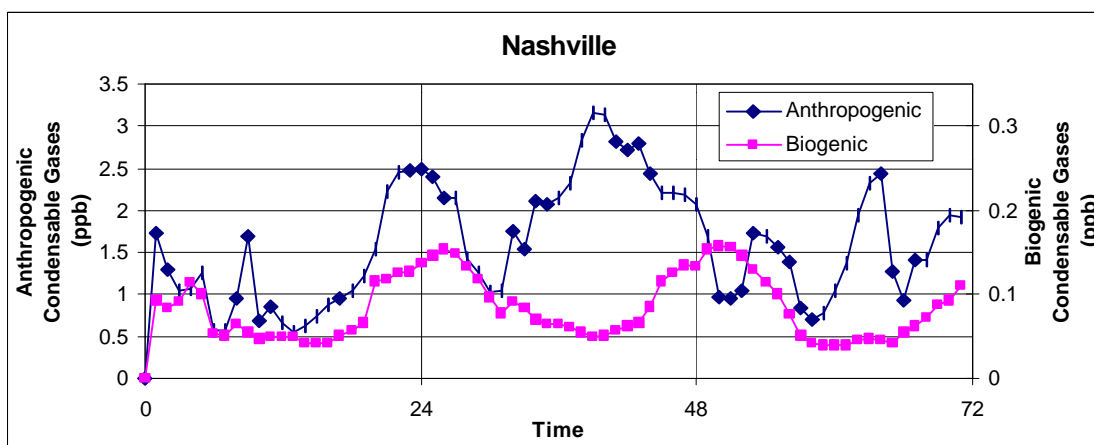
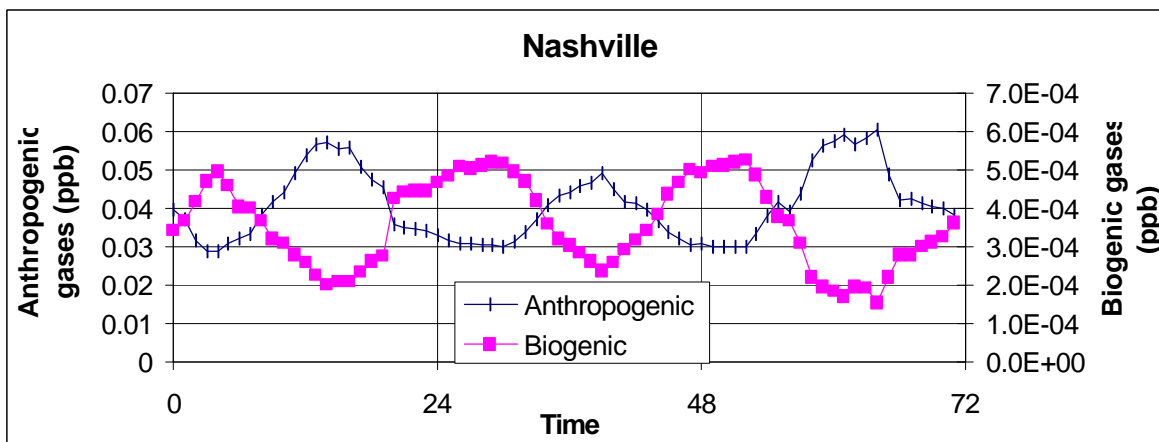
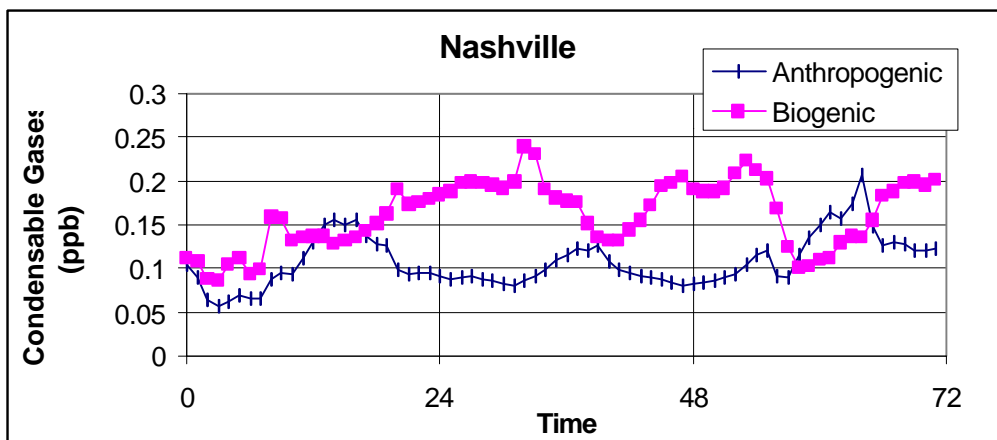


Figure 3-5. Temporal profiles of anthropogenic and biogenic condensable gases in Nashville, 16-18 July 1995. (a) Odum/Griffin et al. formulation, (b) CMU/STI formulation, and (c) MADRID 2.

condensable gases are typically more abundant than their biogenic counterparts by a factor of 5 to 10.

3.2.5 PM

Figure 3-6a shows the spatial distribution of the 24-hour average $PM_{2.5}$ on 16 July and 18 July 1995 predicted by the CBM-IV simulation with the Odum/Griffin et al. SOA module. Similar spatial distribution was simulated by the CMU/STI module with slightly higher PM concentrations. Figure 3-6b shows the spatial distribution of the 24-hour average $PM_{2.5}$ on 16 July and 18 July 1995 as predicted by MADRID 2. In general, the 24-hour average $PM_{2.5}$ concentrations predicted by MADRID 2 are higher than those predicted by the modal PM modules. In the spatial plots of Figures 3-6a and 3-6b, $PM_{2.5}$ concentrations are typically higher in the eastern part of the domain.

Figures 3-7 to 3-9 show the temporal profiles of $PM_{2.5}$ and various PM components. $PM_{2.5}$ tends to accumulate at night and during early morning. The two CBM-IV simulations predicted very similar $PM_{2.5}$ mass (Figure 3-7). The CMU/STI module predicts higher SOA and thus slightly higher $PM_{2.5}$ and PM_{10} . $PM_{2.5}$ predictions in the MADRID 2 simulation are typically higher than those of the CMU/STI simulation. The difference in the above-mentioned time period is due to SOA formation (discussed later) and its effect on inorganic components, e.g., nitrate and ammonium, via the association of SOA with additional particulate water. $PM_{2.5}$ tends to accumulate at night and during early morning.

During the Metropolitan Acid Aerosol Characterization Study (MAACS) (Hsu et al., 1997), 6 stations were operational in Nashville in the summer of 1995 to measure 24-hour average PM_{10} , $PM_{2.5}$, and PM sulfate. For $PM_{2.5}$, the ranges of values observed during the modeling period were $17 \mu\text{g}/\text{m}^3$ (18 July 1995) to $36 \mu\text{g}/\text{m}^3$ (15 July 1995). Table 3-5 lists the observed and predicted concentrations of $PM_{2.5}$ and sulfate. $PM_{2.5}$ concentrations are underpredicted (by $\sim 10\%$) on the first two days in the CBM-IV simulations. On the second day, while the Odum/Griffin et al. and CMU/STI simulations slightly underpredicted $PM_{2.5}$, which was measured at two sites, the sectional MADRID 2

(a)

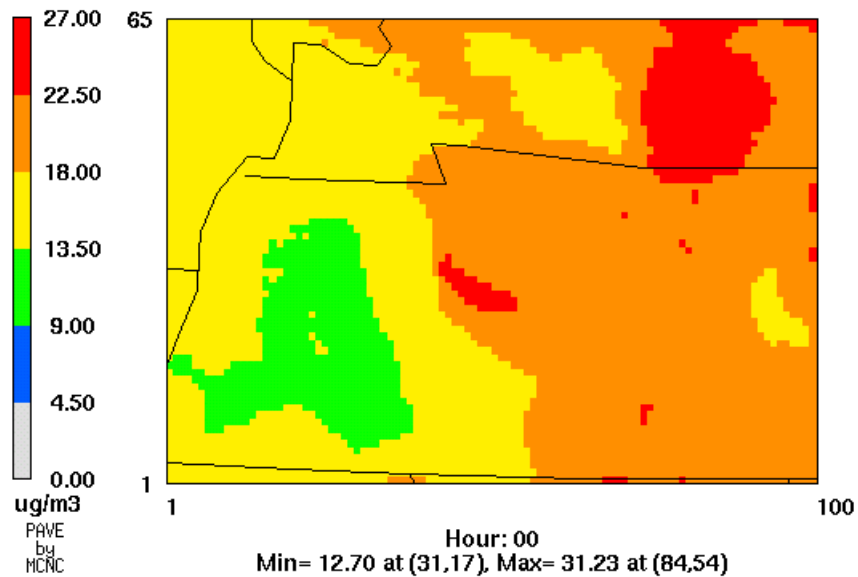
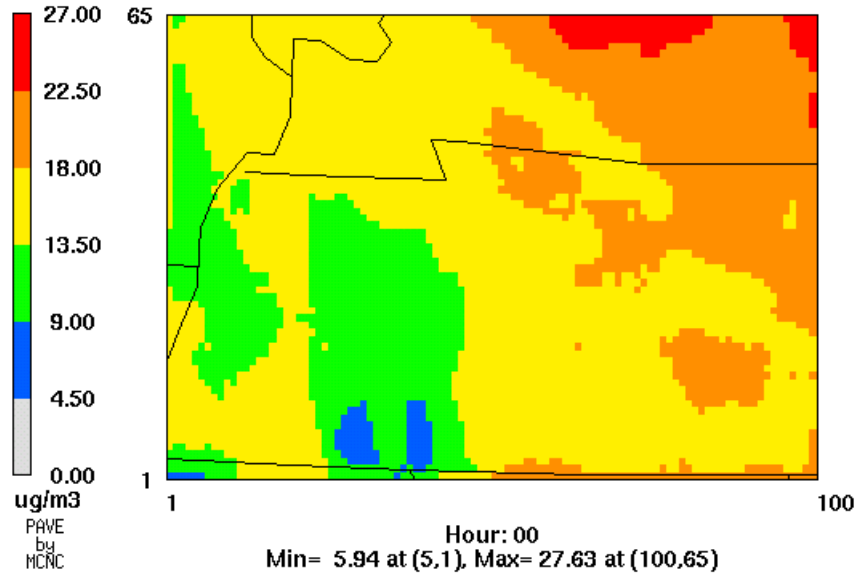


Figure 3-6. Spatial distribution of 24-hour average PM_{2.5} on 16 July and 18 July 1995: (a) Odum/Griffin et al. SOA module and (b) MADRID 2.

(b)

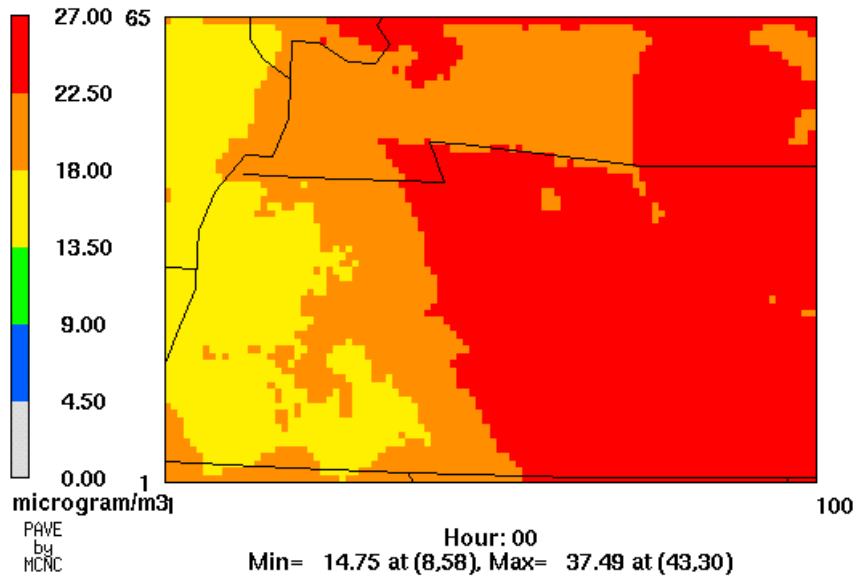
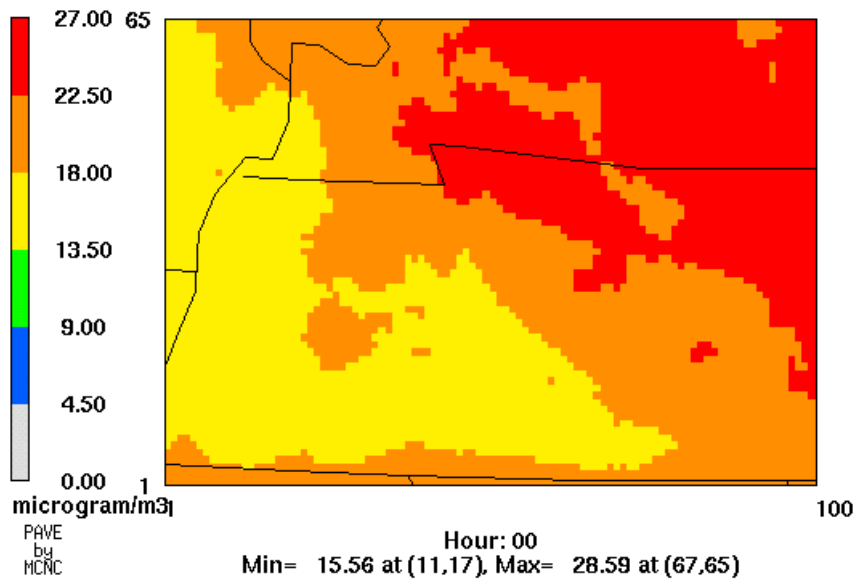


Figure 3-6. Spatial distribution of 24-hour average PM_{2.5} on 16 July and 18 July 1995: (a) Odum/Griffin et al. SOA module and (b) MADRID 2 (continued).

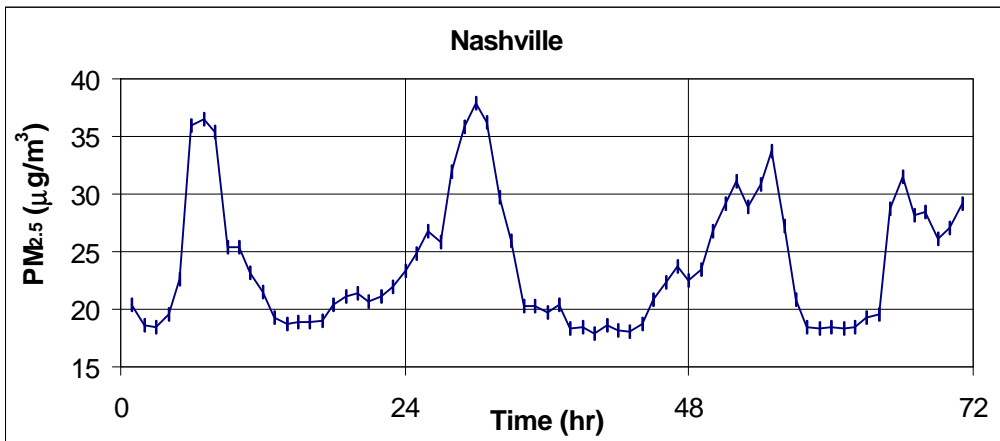
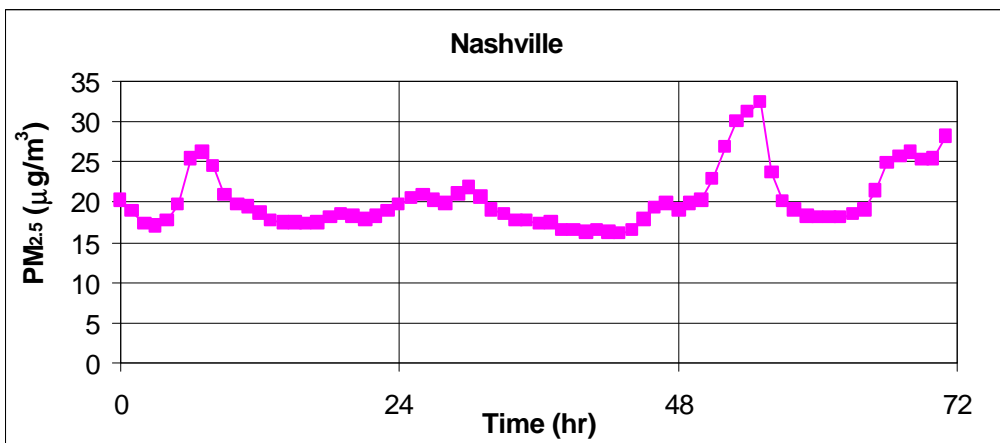
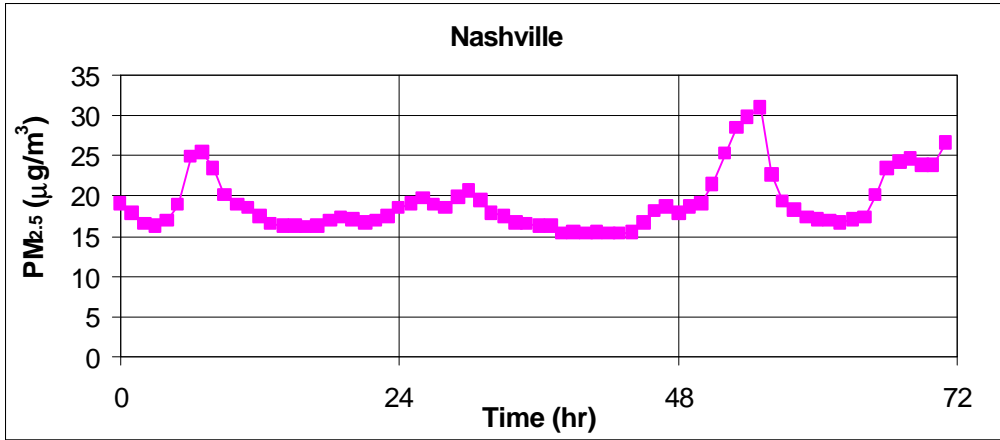


Figure 3-7. Temporal profiles of $PM_{2.5}$ in Nashville between 16 July and 18 July 1995. (a) Odum/Griffin et al. module, (b) CMU/STI module, and (c) MADRID 2.

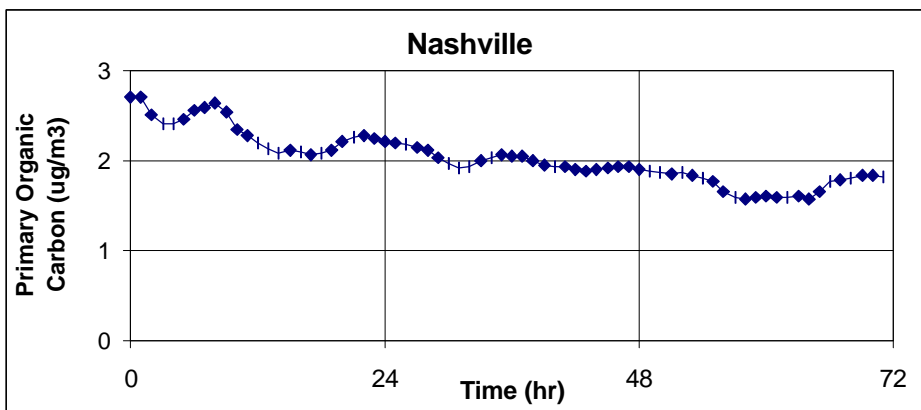
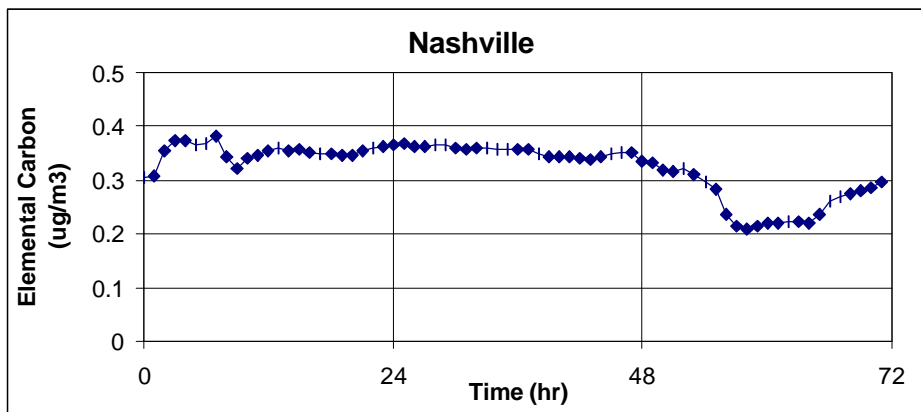
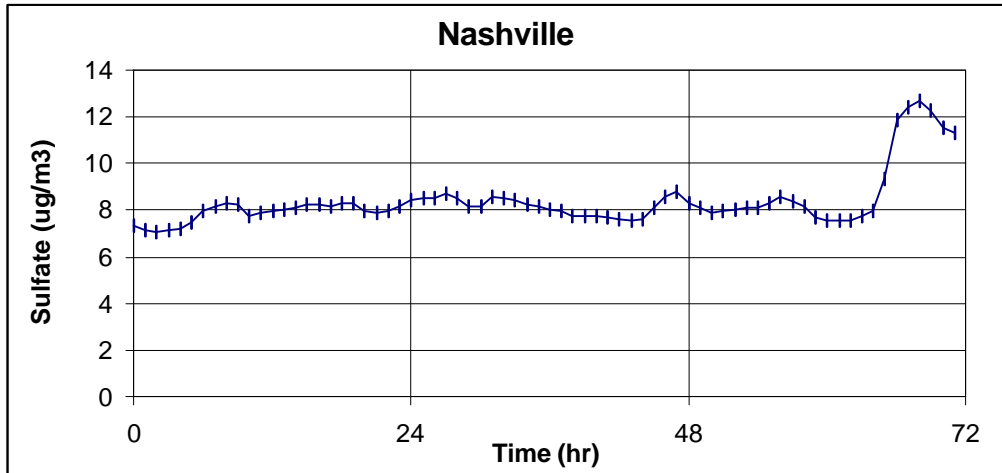


Figure 3-8. Temporal profiles of PM_{2.5} components in Nashville between 16 July 1995 and 18 July 1995 with CBM-IV gas-phase chemistry: (a) sulfate, (b) elemental carbon, (c) primary organic carbon, (d) SOA (Odum/Griffin et al. module), and (e) SOA (CMU/STI module).

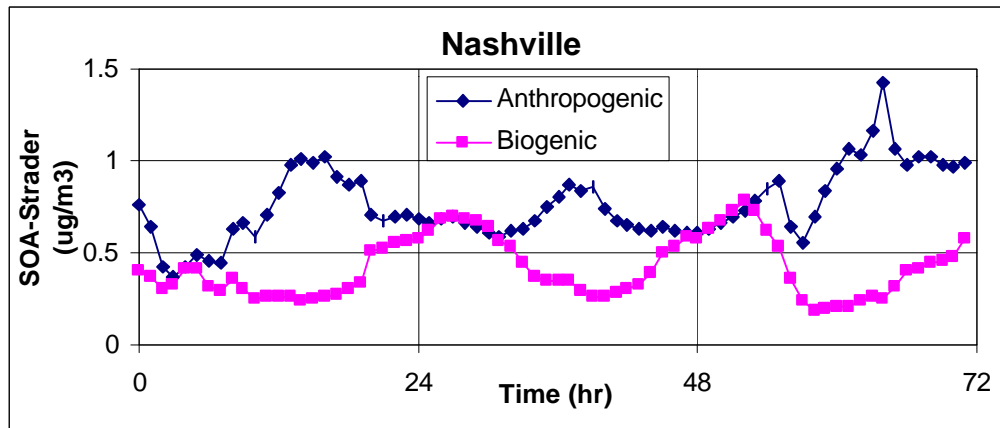
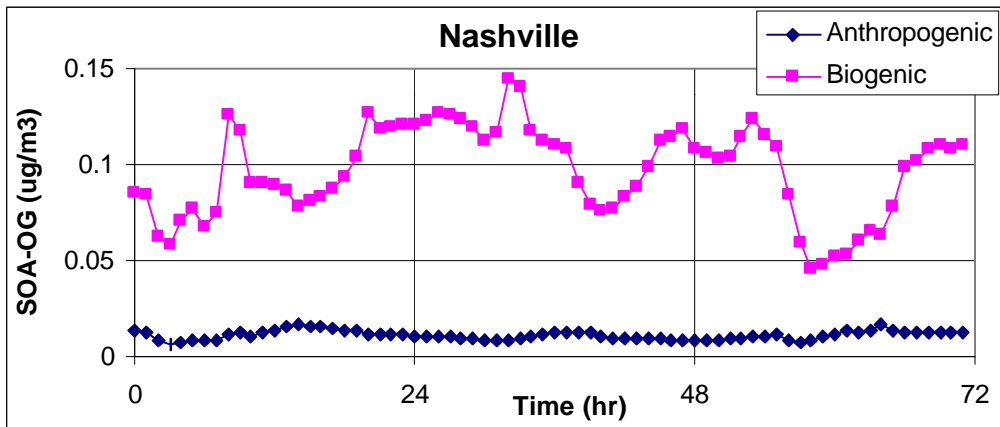


Figure 3-8. Temporal profiles of $PM_{2.5}$ components in Nashville between 16 July 1995 and 18 July 1995 with CBM-IV gas-phase chemistry: (a) sulfate, (b) elemental carbon, (c) primary organic carbon, (d) SOA (Odum/Griffin et al. module), and (e) SOA (CMU/STI module) (continued).

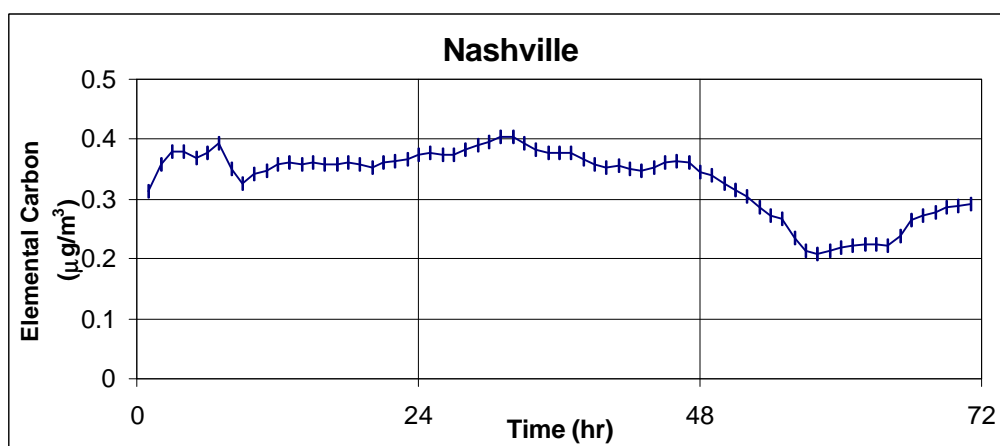
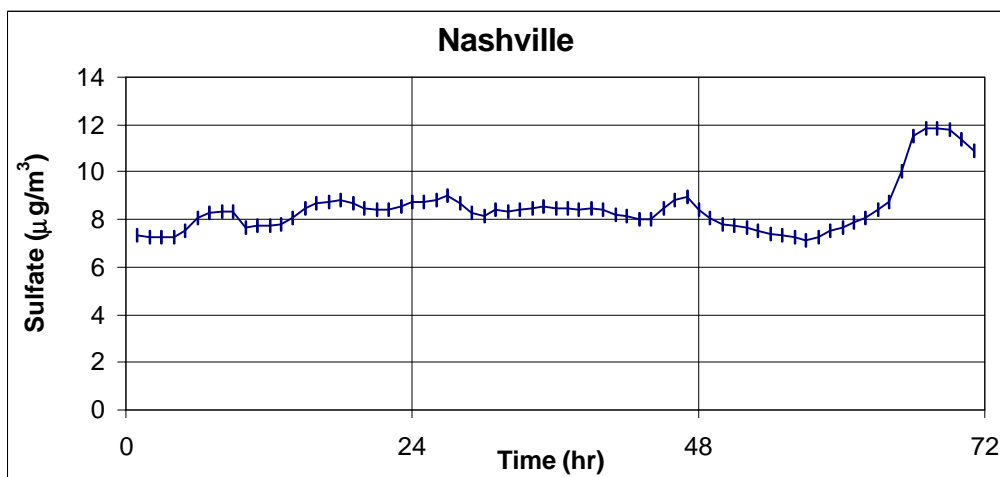


Figure 3-9. Temporal profiles of PM_{2.5} components in Nashville between 16 July 1995 and 18 July 1995 with CACM gas-phase chemistry: (a) sulfate, (b) elemental carbon, (c) primary organic carbon, (d) SOA (MADRID 2).

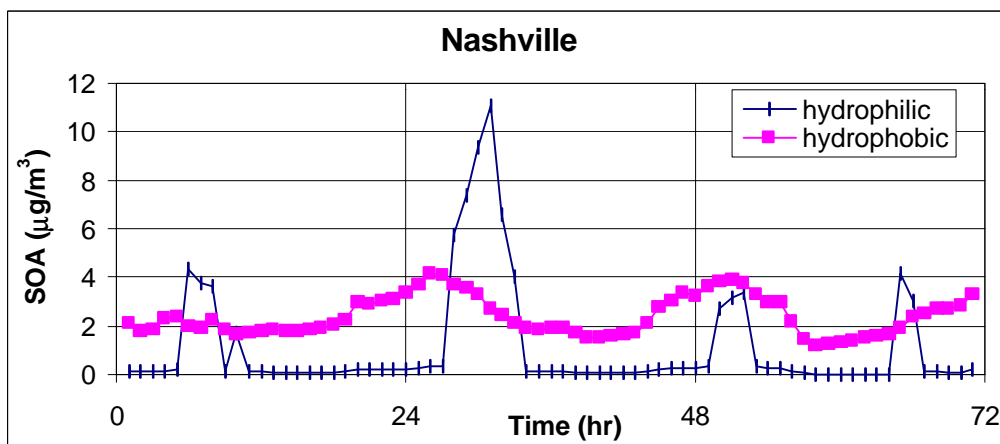
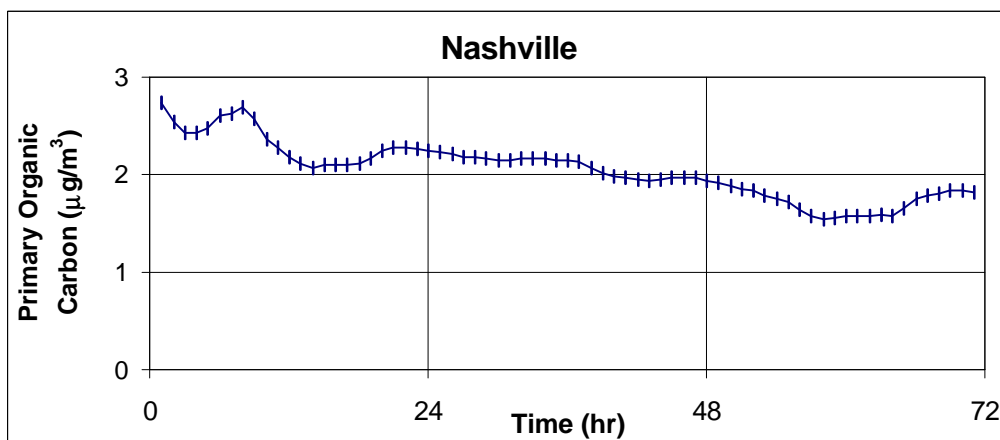


Figure 3-9. Temporal profiles of PM_{2.5} components in Nashville between 16 July 1995 and 18 July 1995 with CACM gas-phase chemistry: (a) sulfate, (b) elemental carbon, (c) primary organic carbon, (d) SOA (MADRID 2) (continued).

Table 3-5. Measured vs. predicted PM_{2.5} and sulfate concentrations in Nashville.

	PM _{2.5} (µg/m ³)	Sulfate (µg/m ³)
16 July 95		
Observed ^(a)	20.4 – 29.5 (5)	8.2 – 15.2 (6)
Predicted (Odum/Griffin et al.)	18.3	7.9
Predicted (CMU/STI)	19.3	7.9
Predicted (AEC)	22.8	8.1
17 July 95		
Observed ^(a)	18.8 – 19.0 (2)	6.4 – 6.8 (2)
Predicted (Odum/Griffin et al.)	17.4	8.2
Predicted (CMU/STI)	18.5	8.2
Predicted (AEC)	23.9	8.5
18 July 95		
Observed ^(a)	16.7 – 24.1 (6)	6.6 – 8.7 (6)
Predicted (Odum/Griffin et al.)	21.7	9.1
Predicted (CMU/STI)	23.0	9.1
Predicted (AEC)	25.5	8.8

(a) Number of MAACS stations in parentheses.

simulation overpredicted PM_{2.5}. The predictions of Odum/Griffin et al. and CMU/STI agree well with measured PM_{2.5} on the third day, while MADRID 2 overpredicted by 5%.

The significant observed decrease in sulfate and PM_{2.5} from 16 to 17 July is not reproduced by the model. This may be due to the fact that we assumed constant BC for particulate concentrations due to a paucity of data. The relatively long atmospheric residence time of fine particles implies that the BC will affect the fine particle concentrations within the modeling domain. Therefore, it is possible that upwind concentrations of fine particles were greater on July 16 than on July 17.

A range of 7 µg/m³ (17 July 1995) to 16 µg/m³ (16 July 1995) was observed for particulate sulfate during MAACS. With an average concentration of 7.9 to 9.1 µg/m³ for the Odum/Griffin et al. and the CMU/STI simulations and 8.1 to 8.8 µg/m³ for the MADRID 2 simulation, sulfate predictions are also consistent with the observations of Hsu et al. during MAACS. All three models predicted similar temporal trends in Nashville. On individual days, sulfate may be overpredicted (e.g., July 17) or underpredicted (July 16 and July 18).

Figure 3-7 depicts the temporal profile of the simulated concentrations of several constituents of PM_{2.5}: sulfate, elemental carbon, primary organic carbon, and secondary organic carbon in the Odum/Griffin et al. and CMU/STI simulations. For the SOA constituent, results are presented for both the Odum/Griffin et al. module and CMU/STI module. The CMU/STI module leads to more SOA formation than the Odum/Griffin et al. module, primarily because the former module favors increased partitioning of condensables toward the particulate phase compared to the latter module.

Figure 3-8 depicts the temporal profiles of the MADRID 2 simulated concentrations in Nashville corresponding to Figure 3-7. For the SOA constituent, results are presented for hydrophilic and hydrophobic SOA. The diurnal predictions of primary components, such as elemental carbon and primary organic carbon, agree well with the CBM-IV simulations (Figure 3-7). No significant diurnal profiles are observed for these components.

SOA shows significant diurnal fluctuations in the MADRID 2 simulation. High concentrations of hydrophilic SOA are observed in the mornings of 16 and 17 July and before dawn and in the early evening of 18 July 1995. Hydrophobic SOA accumulated at

night on 17 and 18 July 1995 to a maximum concentration of about $4.2 \mu\text{g m}^{-3}$ at this location. Daytime concentrations of hydrophobic SOA are about 1 to $2 \mu\text{g m}^{-3}$.

As shown in Figure 3-10, sulfate is a significant component of $\text{PM}_{2.5}$ in Nashville. The second most abundant component in the Odum/Griffin et al. and CMU/STI simulations is ammonium on 16 July and other/unidentified on 18 July 1995, accounting for 17-18% and 23-24% of the $\text{PM}_{2.5}$ mass, respectively. Ammonium (13 to 14%) ranks behind other/unidentified (14 to 22%) in the MADRID 2 simulation. Some differences are observed in the predictions of PM components between the Odum/Griffin et al. approach and the CMU/STI approach, due to small changes in PM deposition velocity resulting from the discrepancies in the SOA predictions. Sulfate predictions in the MADRID 2 simulation are higher than those in the previous simulations by an average of less than $1 \mu\text{g m}^{-3}$ on the first two days and lower by $0.3 \mu\text{g m}^{-3}$ on the last day (also see Table 3-4). Overall, the MADRID simulation predicts more nitrate than the CBM-IV simulations (13-14% vs. 6-8%). The difference in sulfate and nitrate predictions is caused by different gas-phase mechanisms and differences in the dry deposition algorithms used in the sectional and modal approaches. Additionally, including hydrophilic SOA in aqueous particles also serves to enhance the partition of ammonium nitrate due to additional particulate water associated with organic compounds.

SOA tends to account for a small fraction of $\text{PM}_{2.5}$ in Nashville, negligible as predicted by the Odum/Griffin et al. module, about 6% in the CMU/STI case, and 12-13% in the MADRID 2 simulation. In the CACM/AEC simulation, SOA is the fourth most abundant component. The contribution of SOA to $\text{PM}_{2.5}$ in the CBM-IV simulations ranks 6th in contribution below primary organic compounds and nitrate (Figure 3-10).

As predicted by the AEC module, hydrophobic SOA are formed in greater amounts than hydrophilic SOA in Nashville. At this location, hydrophobic SOA is dominated by biogenic components. However, the maximum hydrophilic SOA is more than $10 \mu\text{g m}^{-3}$ in the morning of July 17 (see Figure 3-9), which exceeds the amount of hydrophobic SOA at the time. Total SOA, about $14 \mu\text{g m}^{-3}$, account for much of the difference in the $\text{PM}_{2.5}$ predictions of the CMU/STI and AEC modules seen in Figure 3-7 at this time. The 24-hour average SOA composition as predicted by AEC was

Odum/Griffin et al.

CMU/STI

AEC

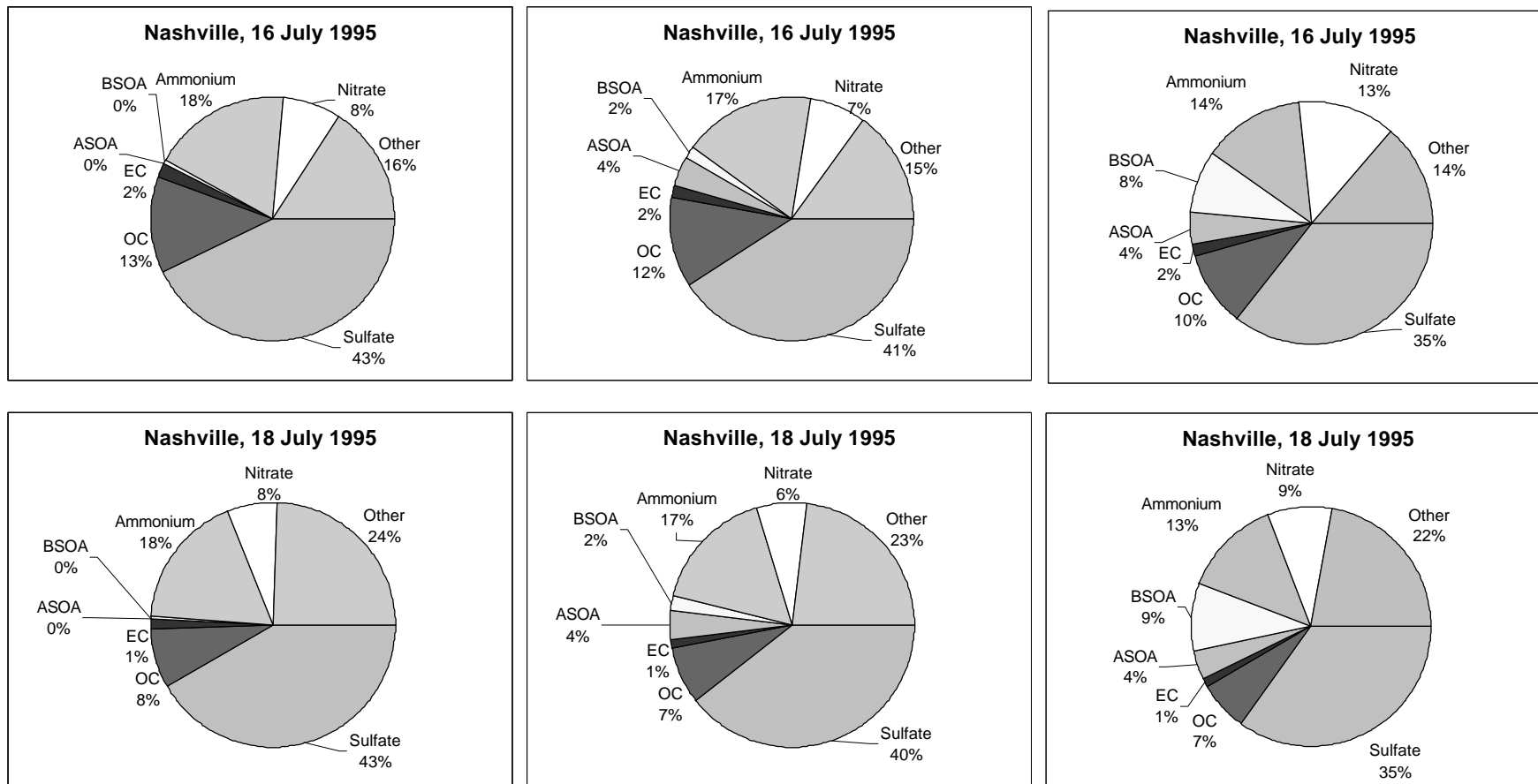


Figure 3-10. 24-hour average composition of PM_{2.5} components in Nashville on 16 July and 18 July 1995. OC is primary organic carbon, EC is elemental carbon, ASOA is anthropogenic SOA and BSOA is biogenic SOA predicted by the Odum/Griffin et al. module (left hand side), the CMU/STI module (middle), and the AEC module (right hand side).

significantly higher in Nashville than that predicted by the CMU/STI module, which was in turn higher than the predictions of the Odum/Griffin et al. module (2.8 to 3.2 $\mu\text{g m}^{-3}$ vs. 1.1 to 1.3 $\mu\text{g m}^{-3}$ vs. 0.1 $\mu\text{g m}^{-3}$). The yield of SOA may be different due to the representation of SOA precursors (especially biogenic compounds) in the three models, the formation of condensable compounds by different chemical mechanisms, or different gas/particle partition of organic compounds. For example, the yield of SOA may be limited, in the case of the Odum/Griffin et al. module, by the availability of absorbing organic compounds. The differences in SOA predictions are explored in detail in Section 3.3.

Large uncertainties are associated with biogenic VOC emissions inventories. The availability of biogenic SOA precursors may limit the amount of SOA that can be formed. Furthermore, the speciation of terpenes used in the Odum/Griffin et al. module was modeled after an Atlanta forest: this is an additional source of uncertainty in the biogenic emissions, which will be further investigated in Section 5.

3.3 Detailed Comparison of Results from Three SOA Modules

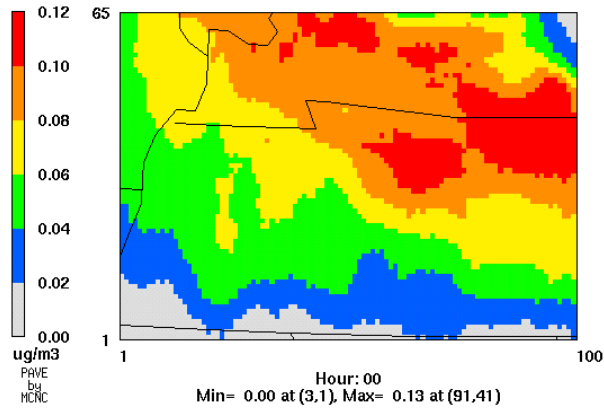
The Odum/Griffin et al., CMU/STI, and AEC modules predicted different SOA characteristics due to their different formulation. This section presents a more detailed analysis and comparison of the SOA concentrations in terms of quantity, distribution, origins, and partition.

3.3.1 Spatial distribution of SOA

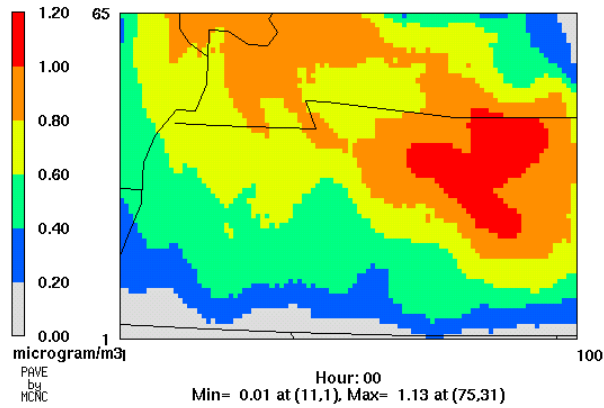
Different spatial distributions were expected because the modules simulated different mixtures of SOA. The spatial distribution of 24-hour average SOA concentrations on 16 July 1995 as predicted by the three SOA modules are presented in Figure 3-11. Different concentration scales are used in these spatial plots because of the difference in the simulated SOA concentrations.

On 16 July, the simulated domain maximum 24-hour average SOA concentrations were 0.13 $\mu\text{g m}^{-3}$, 1.13 $\mu\text{g m}^{-3}$, and 5.15 $\mu\text{g m}^{-3}$, respectively, for the Odum/Griffin et al.

(a) Odum/Griffin



(b) CMU/STI



(c) AEC

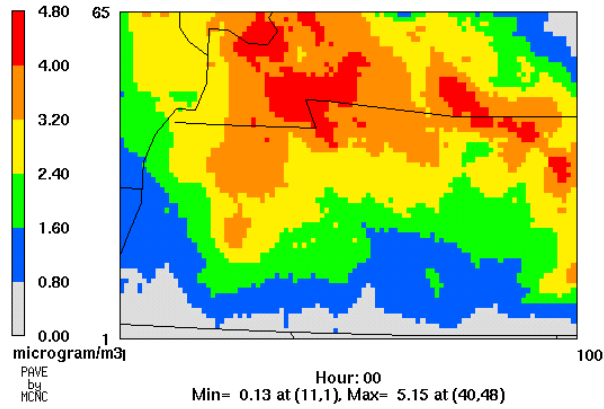


Figure 3-11. Spatial distribution of 24-hour average SOA predicted by (a) Odum/Griffin et al., (b) CMU/STI and (c) AEC SOA modules on 16 July 1995.

module, the CMU/STI module, and the AEC module. The domain average 24-hour SOA concentrations were $0.065 \mu\text{g m}^{-3}$, $0.63 \mu\text{g m}^{-3}$, and $2.39 \mu\text{g m}^{-3}$, respectively. The AEC module predicted more SOA at all times and all locations within the modeling domain than the Odum/Griffin et al. module. The CMU/STI module also predicted more SOA than the Odum/Griffin et al. module except close to the boundaries. While the AEC module predicted higher SOA formation overall, the CMU/STI module predicted slightly higher SOA formation than the AEC module during some afternoon hours.

Gradients of SOA concentrations were observed in all three cases from north (higher concentrations) to south, possibly indicating the general build up of SOA as a result of wind flows. The CMU/STI module predicted a more distinct urban plume of SOA downwind of Nashville, TN compared to the Odum/Griffin et al. module. On the other hand, the AEC module did not predict a distinct plume emanating from the Nashville metropolitan area. In this simulation, SOA tended to be more widespread, an indication of the predominance of biogenic SOA.

We selected three sites for further analyses: an urban location, Nashville (NAS); a semi-rural location that is at times affected by the Nashville urban plume, Youth, Inc. (YOU); and a rural location, Land Between Lakes (LBL). The average SOA concentrations predicted by the three modules at these three sites are summarized in Table 3-6. The Odum/Griffin et al. module predicted the highest SOA concentrations in Nashville on two out of three days. On the last simulation day, the SOA concentration at LBL was higher than at the other two sites. On average, Nashville was predicted to have the highest SOA concentrations of the three sites. The CMU/STI module predicted high concentrations of SOA at YOU and low concentrations of SOA at LBL on the first two days. On the last simulation day, the SOA concentration at NAS exceeded that at the other two sites. On average, LBL was predicted to have lower SOA than NAS and YOU. The AEC module predicted the highest SOA at LBL followed by NAS; lower concentrations were observed at YOU in all three days. Thus, we can conclude that the three SOA modules predicted different geographical distributions of SOA, and these differences were time-dependent.

Table 3-6. Summary of SOA predictions ($\mu\text{g m}^{-3}$) at three sites: Land Between Lakes (LBL), Nashville (NAS), and Youth, Inc. (YOU)

	Odum/Griffin et al.			CMU/STI			AEC		
	LBL	NAS	YOU	LBL	NAS	YOU	LBL	NAS	YOU
16 July 1995	0.088	0.107	0.088	0.78	1.05	1.12	3.95	2.82	2.05
17 July 1995	0.082	0.124	0.119	0.92	1.15	1.25	4.61	4.53	4.04
18 July 1995	0.115	0.099	0.080	1.14	1.28	1.13	3.41	3.25	1.99
Average	0.095	0.110	0.096	0.95	1.16	1.17	3.99	3.55	2.70

3.3.2 Production of condensable compounds

The total condensable compounds (sum of SOA and condensable gases that may be converted to SOA under favorable partition conditions) of each of the three modules may be used to estimate the SOA production potential. This analysis will reveal fundamental differences in the chemistry of organic compounds leading to the production of condensable products. With the exception of dry deposition of particles vs. gases, the comparison of condensable compounds is independent of the partition process.

The concentrations of individual condensable gases were output from the simulation. Because Models-3/CMAQ kept track of gases in ppm units and particulate matter in $\mu\text{g m}^{-3}$ units, we converted the gas-phase concentrations to mass units using an average temperature of 300.0 K at the surface. The input temperature range was 293 to 310 K; therefore, the maximum conversion error due to the use of a fixed temperature was about 3.5%.

On 16 July 1995, the domain average concentrations of all condensable gases were predicted to be $0.89 \mu\text{g m}^{-3}$, $0.18 \mu\text{g m}^{-3}$, and $5.57 \mu\text{g m}^{-3}$, respectively, for CBM-IV with Odum/Griffin et al., CBM-IV with CMU/STI, and CACM with AEC. As discussed in Section 3.3.1, the domain average SOA concentrations were $0.065 \mu\text{g m}^{-3}$, $0.63 \mu\text{g m}^{-3}$ and $2.39 \mu\text{g m}^{-3}$. Therefore, CACM produced a total of $8.0 \mu\text{g m}^{-3}$ of condensable products, which was 8.3 and 9.8 times those produced in the two CBM-IV mechanisms. This large difference illustrates a fundamental gap in our current understanding of SOA formation, as compiled in CACM and deduced from the available experimental data used in the formulation of the Odum/Griffin et al. and CMU/STI modules.

The temporal profiles of SOA and condensable gases in Nashville and Land Between Lakes are depicted in Figure 3-12. The concentrations of SOA and condensable gases at Youth, Inc. were very similar to those in Nashville. Total condensable products simulated by the two CBM-based mechanisms were very similar, in the range of $1\text{-}2 \mu\text{g m}^{-3}$. The Odum/Griffin et al. module in fact predicted slightly larger amounts of total condensable products at these sites, despite predicting significantly lower SOA. The AEC module predicted more condensable gases as well as more SOA than the other two modules. The concentration of total condensable products predicted by AEC displays

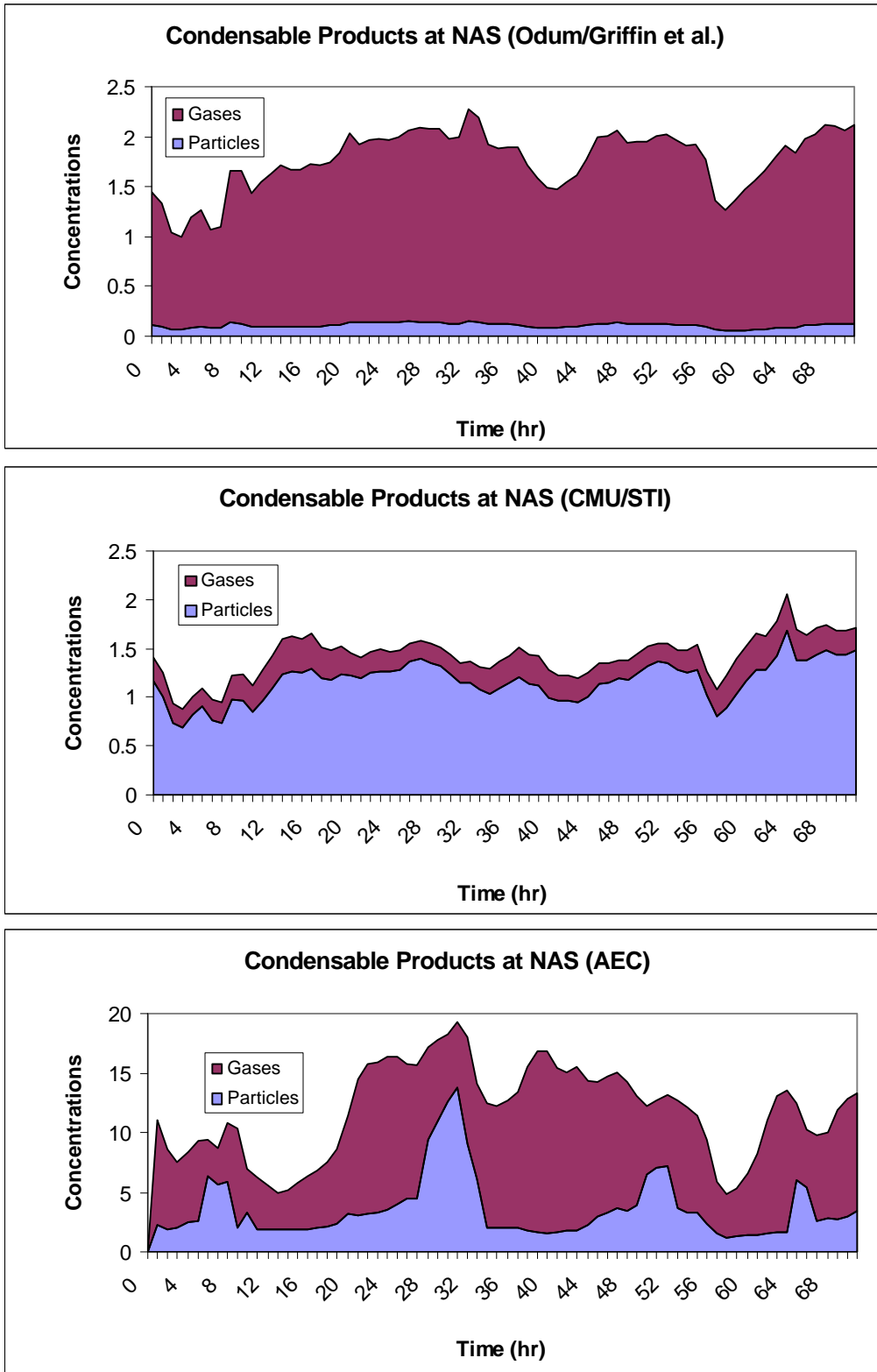


Figure 3-12. SOA and condensable gases predictions at NAS and LBL by three modules.

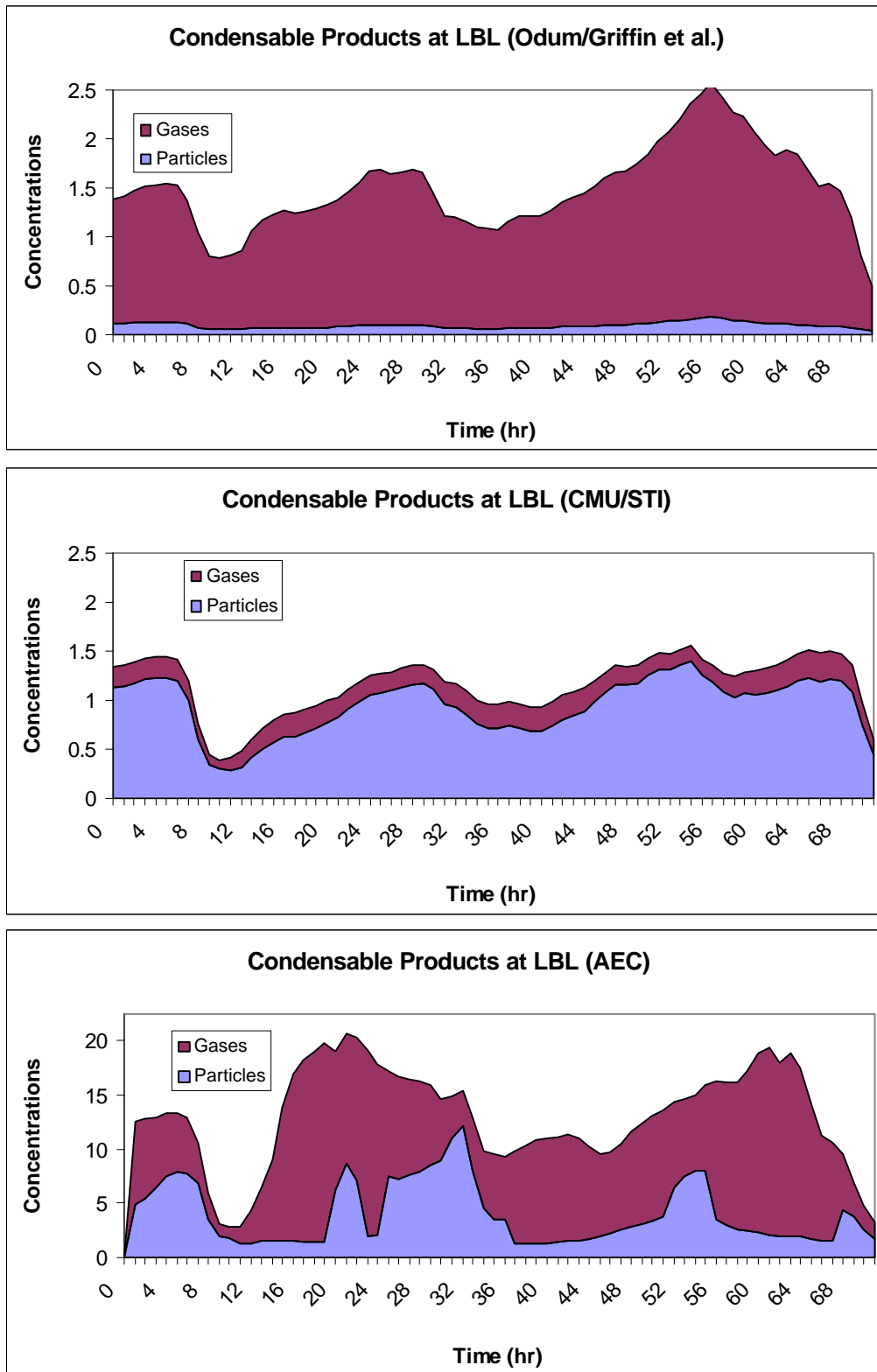


Figure 3-12. SOA and condensable gases predictions at NAS and LBL by three modules (continued).

much stronger temporal variations than the other two modules. The average condensable product concentrations at these two sites were approximately 8-9 $\mu\text{g m}^{-3}$. Therefore, CACM could potentially produce a lot more SOA than the mechanisms based on CBM-IV.

Of the 34 condensable products simulated in CACM, a lumped organic acid with fewer than 6 carbon atoms contributed to a significant portion of the condensable compounds simulated within the domain. The acid is produced from both anthropogenic and biogenic sources, including ethene, olefins, and second generation products of isoprene. This small acid is hydrophilic and quite volatile; therefore, it does not contribute significantly to SOA production except when conditions are favorable for its dissolution into the aqueous phase (see Section 3.3.5). This is also true with many other hydrophilic biogenic compounds. Their relative abundance in the gas phase was higher than that in the particulate phase on average.

3.3.3 Origins of SOA

Different anthropogenic and biogenic SOA precursors and condensable products are modeled in different models. CACM and CMU/STI model several classes of anthropogenic precursors, including alkanes, alkenes, and aromatic compounds. Odum/Griffin et al. includes only SOA production from aromatic compounds but not the other anthropogenic compounds listed above. On the other hand, SOA formation from 12 terpene compounds is represented in Odum/Griffin et al., while CACM models only two groups of monoterpenes, and CMU/STI only one. In the modified CBM-IV mechanisms, only one generation of condensable products is predicted, and the yields of condensable products are determined from smog chamber measurements. CACM utilizes a mechanistic approach and models several generations of condensable products. Although uncertainties in the mechanism are significant because the reactions of complex secondary organic compounds have not been as thoroughly studied as those of primary compounds, this level of mechanistic detail may eventually be necessary for the accurate representation of condensable organic compounds.

The Odum/Griffin et al. module predicts that biogenic SOA is the dominant component of total SOA, accounting for 90% of SOA at most locations. The CMU/STI simulation produces larger amounts of SOA, especially anthropogenic SOA, which is about twice the concentration of biogenic SOA. More condensable products are produced with the CMU/STI module from anthropogenic precursors because alkanes, alkenes, and secondary aromatic compounds produce SOA in addition to the primary aromatics modeled in the Odum/Griffin et al. module. The AEC module predicts that slightly more biogenic SOA (about 52% of total SOA averaged over three days) than anthropogenic SOA are formed on a domain-wide basis. Note that since the small acid, which can be a significant component of hydrophilic SOA when RH is high, is counted as anthropogenic even though it can originate from both anthropogenic and biogenic emissions, the fraction of biogenic SOA may in fact be slightly higher as predicted by the MADRID 2/AEC module. Significant differences, as illustrated in Figure 3-13, are observed in both the total amount and the anthropogenic or biogenic origins of the SOA predicted by the three modules.

3.3.4 Different implementations of absorption

Different formulations of the absorption theory were used in the Odum/Griffin et al., CMU/STI, and AEC modules. It is of interest to identify the range of predictions that resulted from using different parameters for the same theoretical formulation. The AEC module uses the partition theory to predict SOA formation for all hydrophobic condensable compounds and for hydrophilic compounds when no existing aqueous phase has already been predicted for the inorganic particles. Since predictions of high hydrophilic SOA seemed to be associated with nighttime periods of high relative humidity, and the average concentration of hydrophilic SOA was lower than that of hydrophobic SOA (see Figure 3-14), we anticipated that the formation of hydrophilic SOA was dominated by dissolution rather than by absorption. We analyzed the partition of hydrophobic SOA to approximate the effects of partition by absorption in the AEC module.

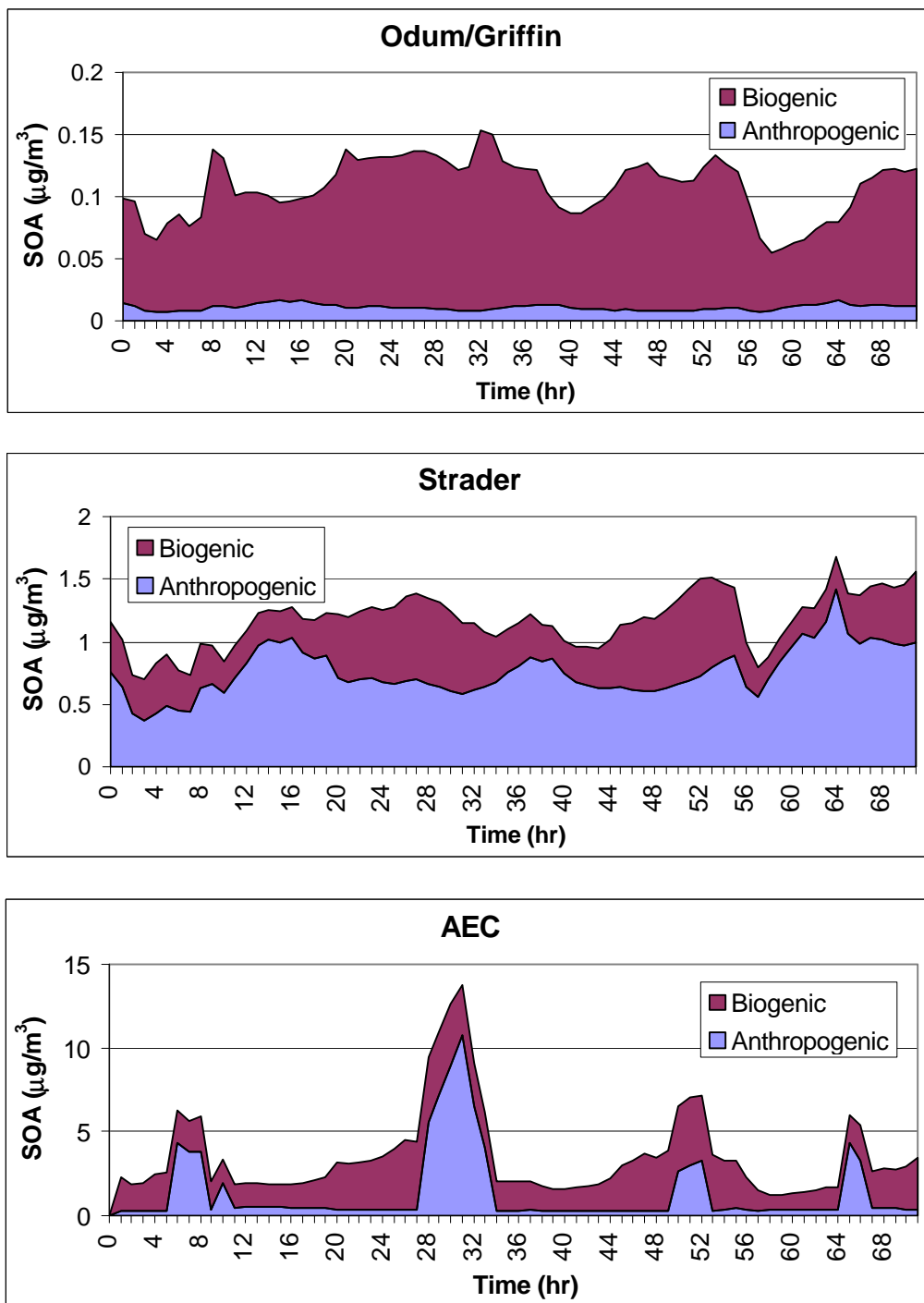


Figure 3-13. Temporal profiles of SOA as predicted by three modules in Nashville on 16 – 18 July 1995.

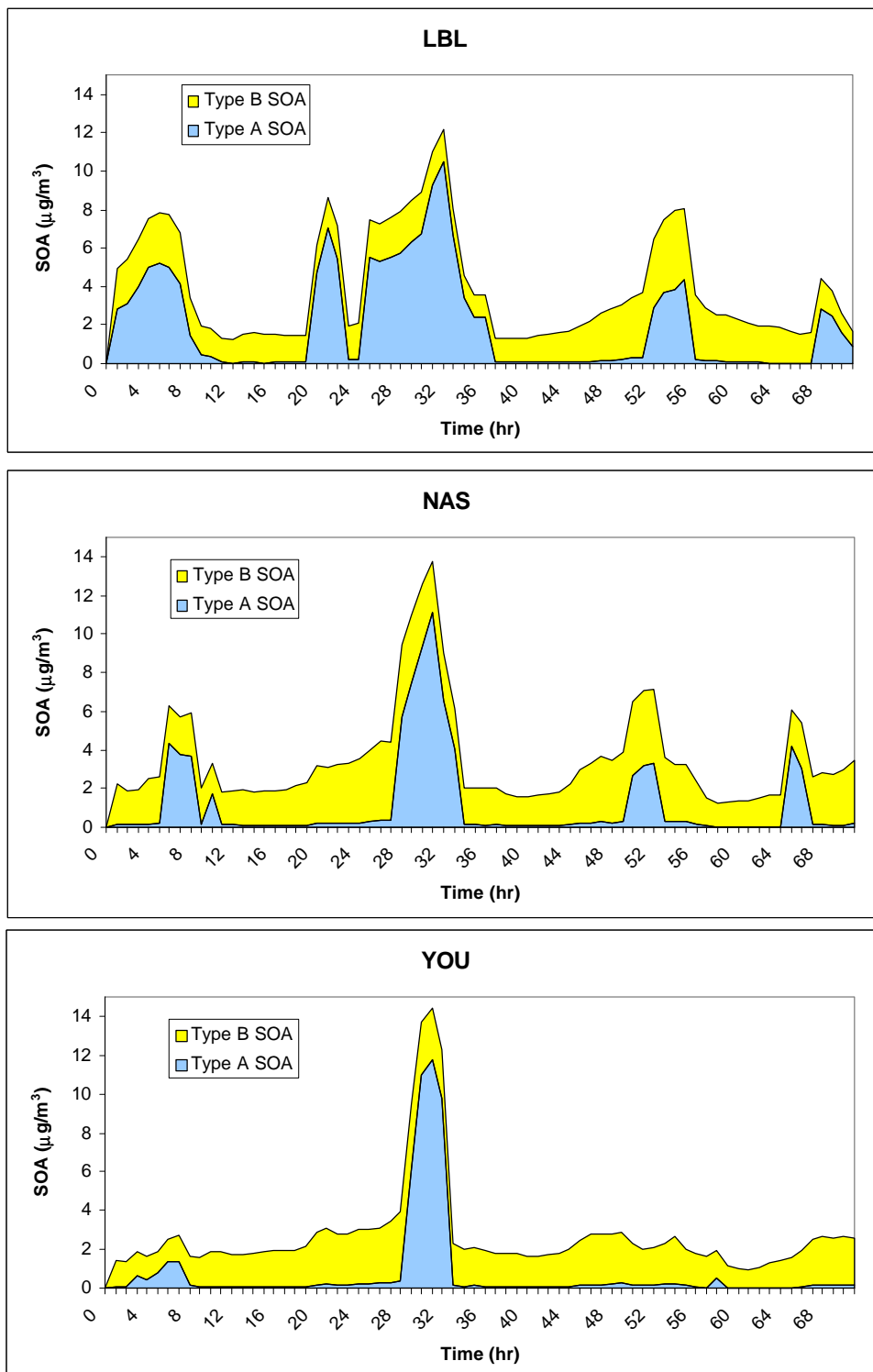


Figure 3-14. Hydrophilic (Type A) and hydrophobic (Type B) SOA predicted at three sites by the AEC SOA module of MADRID 2.

Figure 3-15 shows the partition of hydrophobic condensable products at LBL and NAS, in a format that is comparable to Figure 3-12. Although the hydrophobic SOA only accounted for a fraction of the SOA predicted by the AEC module, the total amount of hydrophobic condensable products exceeded the total amounts predicted by the Odum/Griffin et al. and CMU/STI modules. Nevertheless, we will analyze in this section the partitioning of products between the two phases. Shown in Table 3-7 are the average amounts of condensable gases and SOA predicted by the absorption modules. The partitioning characteristics between the gas and particle phases were remarkably similar for each module at different sites, despite differences in the amounts of total condensable products. The hydrophobic absorption module in AEC resulted in the highest proportion of condensable products (88-89% by mass) in the particle phase. The CMU/STI module partitioned about 80% to 82% of the total condensable mass into the aerosol phase at urban and rural sites. The Odum/Griffin et al. module tended to favor partitioning into the gas phase, with only 6% to 7% of the condensable products forming SOA. Differences in the partition parameters contribute to the differences in gas/particle distribution of the condensable products. In particular, temperature dependence may be an important factor, since experimental smog chamber data (e.g., used in Odum/Griffin et al.) are typically obtained at high temperatures that may not be favorable to the condensation of SOA.

According to the partitioning algorithm of Odum/Griffin et al., Equation 2-1, the presence of primary organic compounds enhances the partitioning of SOA into the particle phase. Primary organic aerosols tend to be underpredicted relative to the observed data from the National Park sites (used as IC and BC). In a previous application of Models-3 to the Los Angeles basin, the primary organic emissions were found to be underrepresented in the model relative to the measured concentrations as well. We attribute this underprediction to the default composition assumed for PM_{2.5} emissions within Models-3/CMAQ. The differences in the partitioning of condensable products between the gas phase and the particle phase explained some of the differences in the amount of SOA produced by the three modules.

Despite different amounts of condensable organic compounds and different mixtures, the fraction of SOA predicted by each module was very constant at locations

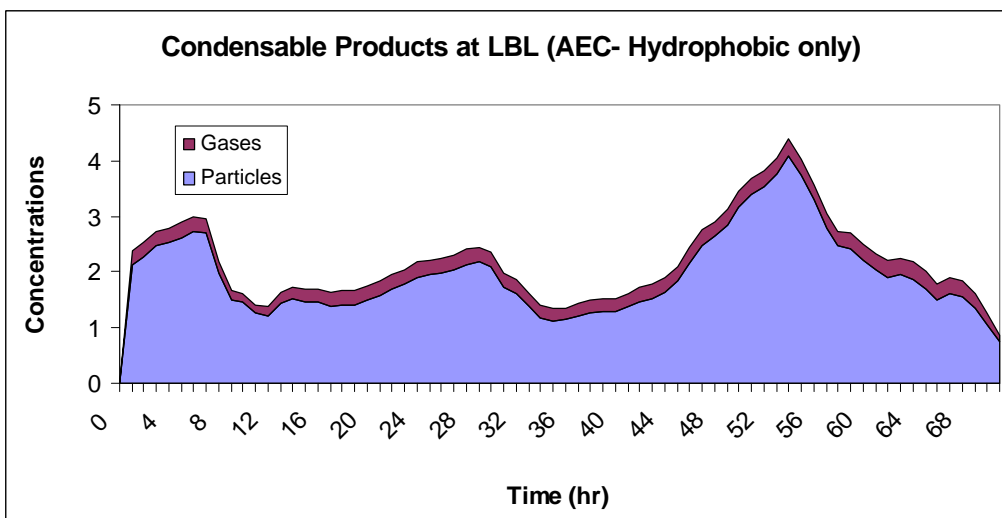
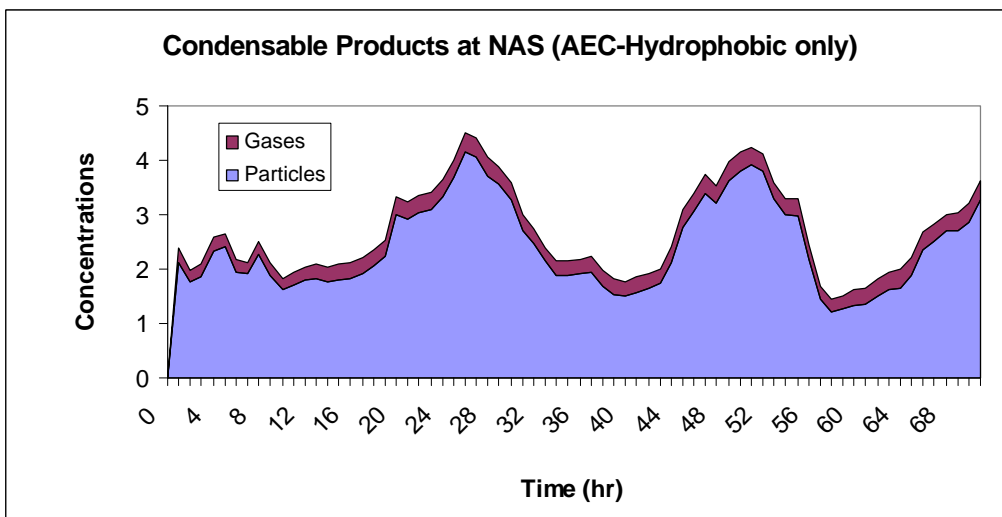


Figure 3-15. SOA and condensable gases predictions at NAS and LBL by the hydrophobic absorption module of AEC.

Table 3-7. Summary of SOA ($\mu\text{g m}^{-3}$) partitions predicted by three absorption modules at three sites: Land Between Lakes (LBL), Nashville (NAS), and Youth, Inc. (YOU).

	Odum/Griffin et al.			CMU/STI			AEC (Hydrophobic SOA module only)		
	LBL	NAS	YOU	LBL	NAS	YOU	LBL	NAS	YOU
16 July 1995									
SOA	0.09	0.11	0.09	0.78	1.05	1.12	1.80	2.13	1.77
Condensable Gases	1.17	1.45	1.31	0.20	0.26	0.26	0.23	0.26	0.24
SOA as % of total condensables	7%	7%	6%	80%	80%	81%	89%	89%	88%
3-day average									
SOA	0.10	0.11	0.10	0.95	1.16	1.17	1.96	2.40	1.99
Condensable Gases	1.40	1.65	1.53	0.21	0.26	0.26	0.25	0.29	0.28
SOA as % of total condensables	6%	6%	6%	82%	82%	82%	89%	89%	88%

ranging from urban to rural. One reason seemed to be that condensable gases and SOA tended to be regionally distributed (Figure 3-11). Another related reason seemed to be that the composition of SOA and condensable gases was more spatially homogeneous than the distribution of the organic precursors would indicate. For example, the fraction of condensable (gas + particles) products of biogenic origins was predicted to be 79% at LBL and 75% in Nashville by the Odum/Griffin et al. module. The analogous values were 35% at LBL and 29% in Nashville with the CMU/STI module, and 83% at both LBL and NAS with the hydrophobic condensables in the AEC module.

3.3.5 Formation of SOA by dissolution

As shown in Figure 3-14, hydrophilic SOA tended to be formed in spurts, contributing to very spiky SOA concentration temporal profiles predicted by the AEC module. The formation of hydrophilic SOA seemed to be limited by the conversion of the condensable gases to particles. Much of the condensable gases in Figure 3-12 were hydrophilic, since hydrophobic gases (Figure 3-15) were quite low in concentrations.

Because the availability of particulate water is a key variable for the dissolution of hydrophilic SOA (they form an organic solution by absorption only when no preexisting aqueous particles are simulated), we show in Figure 3-16 cross plots of the amount of hydrophilic SOA vs. particulate water. Note that particulate water output by Models-3/CMAQ is the sum of the water associated with aqueous inorganic particles and that associated with hydrophilic organic compounds in the aqueous solution. High concentrations (above $4 \mu\text{g m}^{-3}$) of hydrophilic SOA were typically associated with high particulate water predictions (e.g., above $30 \mu\text{g m}^{-3}$), and low concentrations (below $0.5 \mu\text{g m}^{-3}$) of hydrophilic SOA were associated with low particulate water predictions (e.g., below $20 \mu\text{g m}^{-3}$). However, intermediate water content could be associated with a range of SOA concentrations. This discontinuous transition behavior seemed to be associated with the deliquescence of one of the surrogates at 79% relative humidity. Figure 3-17 shows the cross plots between the total amounts of hydrophilic SOA at three sites and the relative humidity (RH). (Since RH was not a direct input/output for Models-3, the values plotted in Figure 3-17 were calculated based on temperature and mixing ratios of water

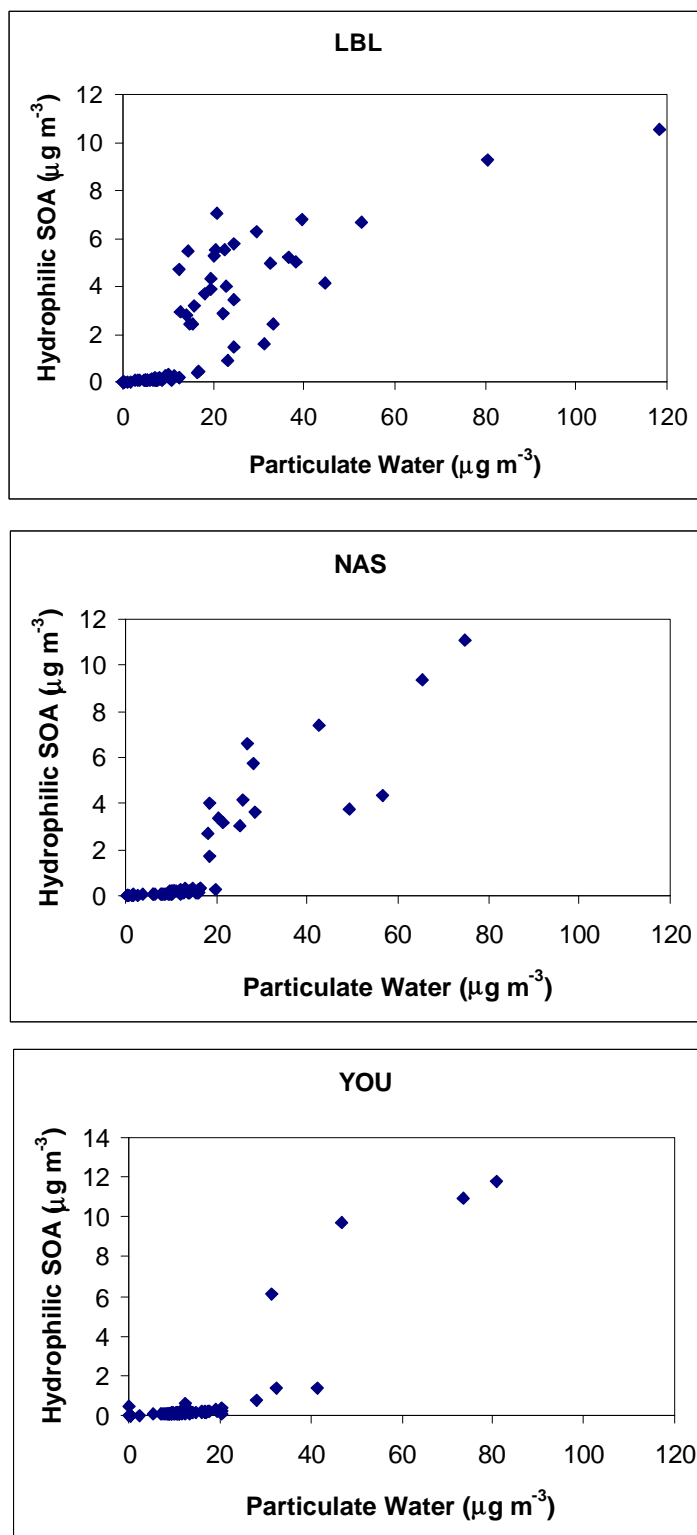


Figure 3-16. Hydrophilic SOA vs. particulate water predicted by MADRID 2 at LBL, NAS, and YOU.

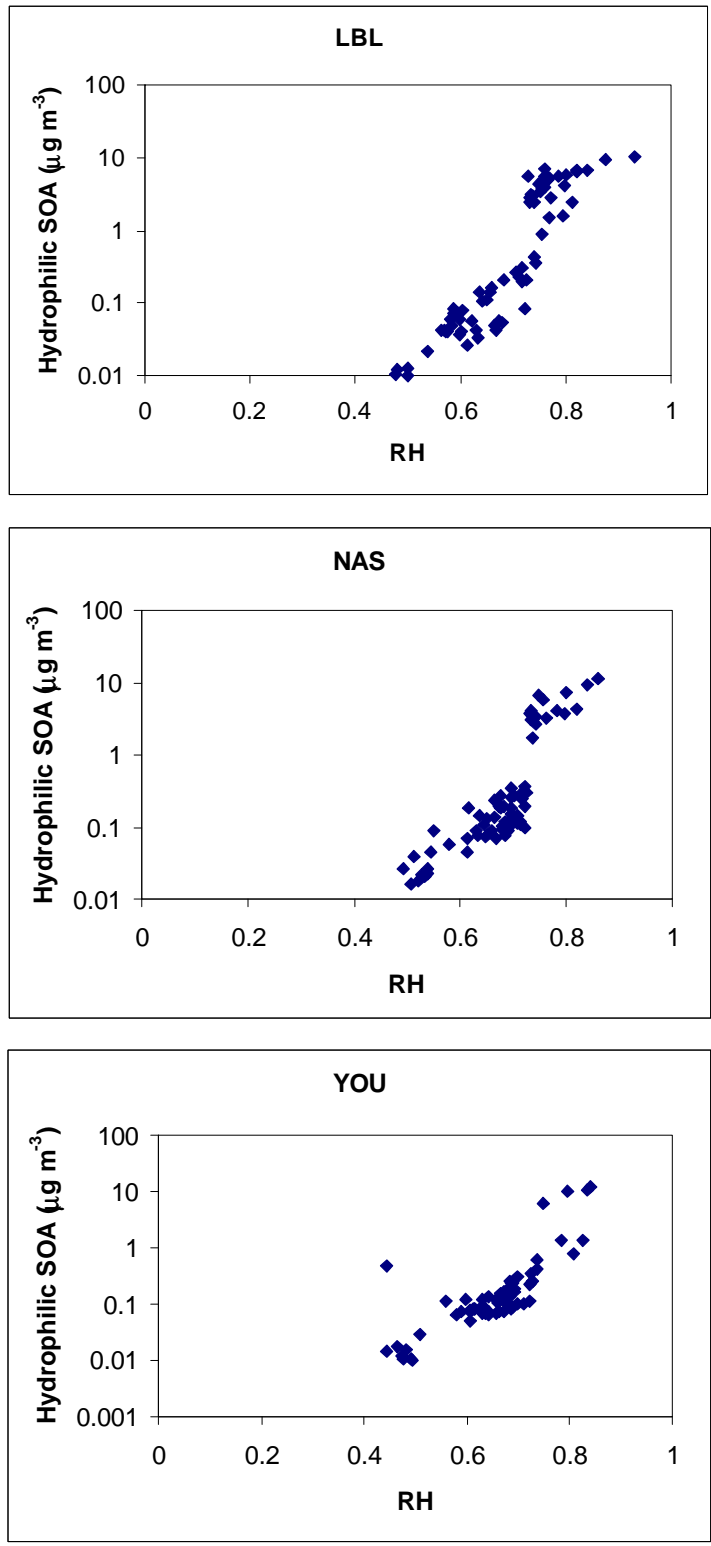


Figure 3-17. Hydrophilic SOA vs. RH predicted by MADRID 2 at LBL, NAS, and YOU.

vapor (Seinfeld, 1986) and could be slightly different from the RH values used in the model.) A sharp rise in SOA can be seen at all three sites at RH close to 80% from SOA concentrations in the range of $0.1 \mu\text{g m}^{-3}$ to a few $\mu\text{g m}^{-3}$.

The time series of hydrophilic SOA and the deliquescent surrogate compound (Surrogate 1, a short chain diacid) are shown in Figure 3-18. Surrogate 1 constituted a large fraction of the hydrophilic SOA on average. But it did not partition into the particulate phase most of the time. Significant concentrations of Surrogate 1 were only predicted when RH exceeded the deliquescence humidity of this compound. When this happened, there was a large increase in the SOA concentrations, indicating the abundance of this compound in the gas phase available for the formation of SOA under favorable conditions. These results point out the importance of correctly characterizing the partitioning properties of condensable compounds.

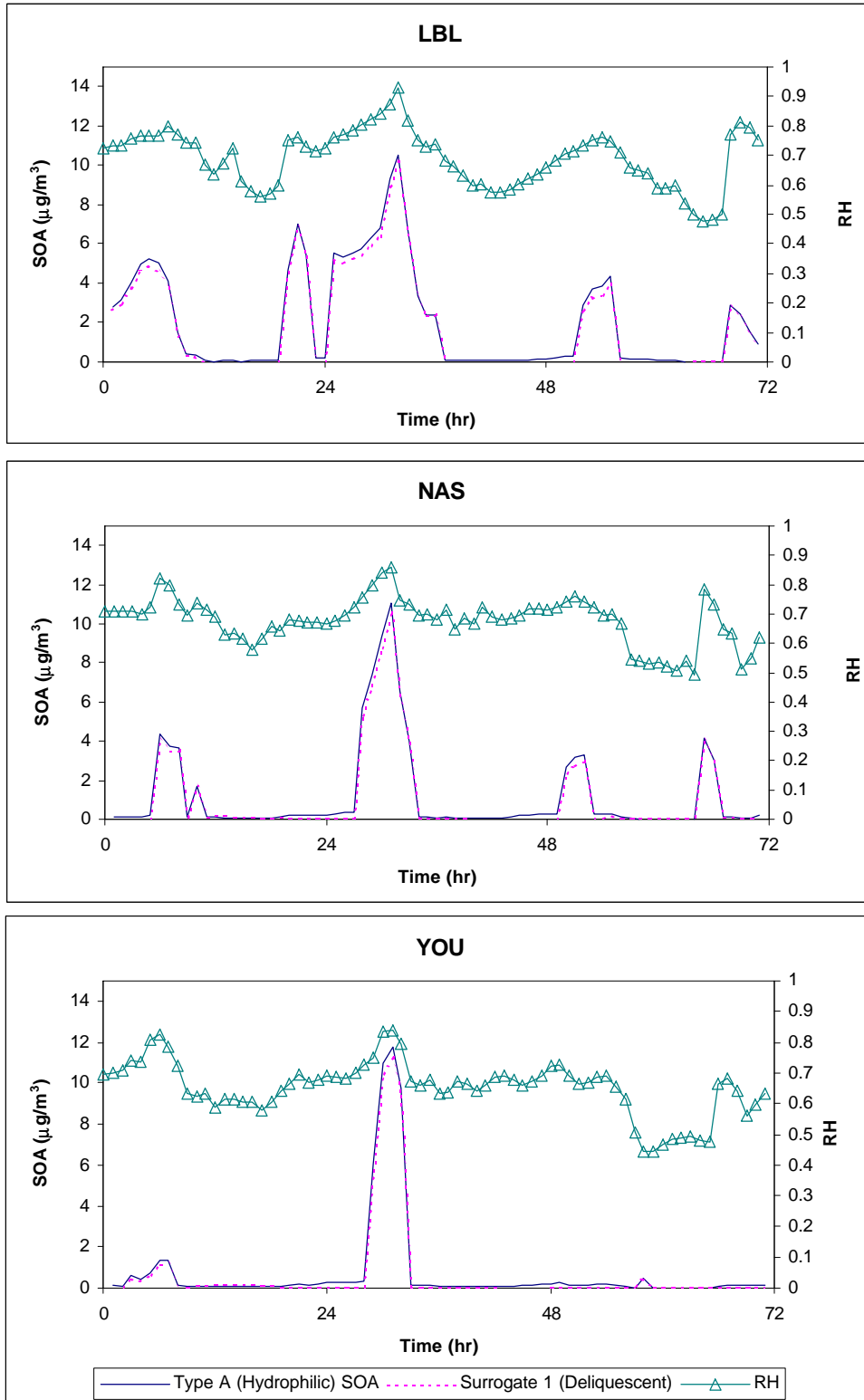


Figure 3-18. Time series of hydrophilic SOA, Surrogate 1, and RH predicted by MADRID 2 at LBL, NAS, and YOU.

4. CONTRIBUTION OF BIOGENIC EMISSIONS TO O₃ AND PM_{2.5} IN THE NASHVILLE DOMAIN

4.1 Description of the Sensitivity Studies

4.1.1 Modeling scenarios

To investigate the contribution of biogenic emissions to O₃ and PM_{2.5}, we elected to use the CMU/STI SOA formulation. Two SOA modules were coupled with CBM-IV whereas one was coupled with CACM (see Section 2). CBM-IV has been widely used for O₃ studies, and is, therefore, selected for these sensitivity studies. The two SOA modules coupled with CBM-IV give identical results in O₃ concentrations. The CMU/STI module predicts higher SOA concentrations and, therefore, should give an upper limit of the effect of biogenic emissions on PM_{2.5} production. It was, therefore, selected for these sensitivity studies.

Several approaches can be used to estimate the contribution of biogenic emissions to O₃ and PM_{2.5} using modeling studies. First, one can treat the current situation as a base case, and remove biogenic emissions to calculate their contribution to O₃ and PM. Biogenic emissions account for about 8% of the total NO_x emissions. Biogenic VOC, including isoprene and monoterpenes, account for 67%, 88%, and 78% of the domain-wide emissions of paraffinic carbons (PAR), higher aldehydes (ALD2), and olefins (OLE), respectively, when converted to CBM-IV model species. In removing these emissions, we calculate the contribution of biogenic emissions to O₃ and PM concentrations under current conditions. One should note, however, that this contribution estimate may vary if we perturb the biogenic emissions slightly (e.g., -10%) or totally (i.e., -100%). By selecting a total perturbation (i.e., no biogenic emissions), we are able to address the “global” sensitivity and bypass the possible issue of nonlinearity in the effect of biogenic emissions on O₃ and PM. This is an appropriate approach since we are interested in the contribution of all biogenic emissions on O₃ and PM.

A second approach consists in simulating the natural atmosphere with no human influence. The O₃ and PM concentrations calculated in such a simulation would

represent the absolute contribution from biogenic emissions. There are, however, several drawbacks to this approach: (1) current urban-to-regional scale air quality models have never been evaluated under such conditions and the validity of those models in such applications is uncertain (for example, global models systematically underestimate O₃ concentrations by 5 to 10 ppb, Jacob and Wang, 1998), and (2) biogenic emissions interact with anthropogenic emissions to produce O₃ and PM_{2.5}. Therefore, simulating an atmosphere with only biogenic emissions may not be of relevance since a natural atmosphere with no human influence does not currently exist.

A third general category of approaches includes techniques that can “tag” each O₃ (or PM) molecule to a specific source or calculate the sensitivity coefficient of O₃ (or PM) to biogenic emissions. However, as stated above, the non-linearity of the response of O₃ and PM_{2.5} to changes in biogenic and anthropogenic emissions will lead to different results depending on the source attribution or local sensitivity techniques being used.

We elected to bound the problem by applying the first two approaches. The contribution of biogenic emissions and natural boundary conditions (BC) to O₃ and PM deduced by removing these components from the base case is expected to be different from the concentrations of O₃ and PM in a simulation with natural BC and only biogenic emissions, due to non-linearity in the chemical production of secondary air pollutants. The range of values predicted in these simulations for biogenic influences on O₃ and PM should, therefore, provide reasonable bounds for the answer we seek.

We will consider three sensitivity cases:

- Lower limit sensitivity case with no biogenic emissions but with base case BC (i.e., BC include the contribution of natural species)
- Best estimate sensitivity case A with no biogenic emissions and no natural contribution to BC; i.e., an anthropogenic scenario
- Best estimate sensitivity case B with no anthropogenic emissions and no anthropogenic contribution to BC; i.e., a biogenic/natural scenario

4.1.2 Treatment of the boundary conditions

In a model simulation, O₃ and PM concentrations predicted within a modeling domain result from (1) emissions of O₃ precursors, PM and PM precursors within the domain, (2) transport of O₃ and PM into the domain by advection across the domain boundaries and (3) production within the domain by precursors transported into the domain by advection. If the contribution of the advected components (i.e., BC) is small compared to that of the domain emissions, the contribution of biogenic emissions can be estimated by conducting sensitivity simulations with no biogenic or no anthropogenic emissions. On the other hand, if the contribution of the BC is significant, a procedure is needed to separate out the anthropogenic and biogenic components in the BC.

For VOC and NO_x, we used the following approach. Some precursors are exclusively anthropogenic (e.g., aromatic compounds) or biogenic (e.g., isoprene). Others are common to both anthropogenic and biogenic sources (e.g., NO_x and, in the CBM-IV formulation, PAR, OLE, and ALD2). For these compounds, we assumed that the fraction of the BC originating from anthropogenic activities was identical to the anthropogenic fraction of the emissions within the domain.

Fine particulate species have very long atmospheric lifetimes; therefore, the influence of the BC may dominate the simulated PM_{2.5} concentrations. We assumed that the background PM concentrations observed at remote locations represent natural sources of PM, which include biogenic emissions as well as other sources, such as volcanoes and sea salt. The anthropogenic fraction of the PM BC was assumed to be the difference between the observed values and the background values. (Note that for SOA, the BC were set to zero in the base case, to evaluate the formation of SOA from emissions within the domain.) The same approach was used for gaseous species that have long atmospheric lifetimes, such as carbon monoxide (CO) and ammonia (NH₃).

Separating the anthropogenic and biogenic components in the BC is especially challenging for O₃. In this domain, 40 ppb of O₃ is assumed at the boundary in the base simulation. The procedure used here is depicted in Figure 4-1. We assumed that the relative influence of anthropogenic and biogenic precursors in the BC was the same as the relative effect of anthropogenic and biogenic emissions within the domain. We further assumed that the influence of anthropogenic emissions was reflected in the difference in domain- and episode-averaged O₃ concentrations between the base case

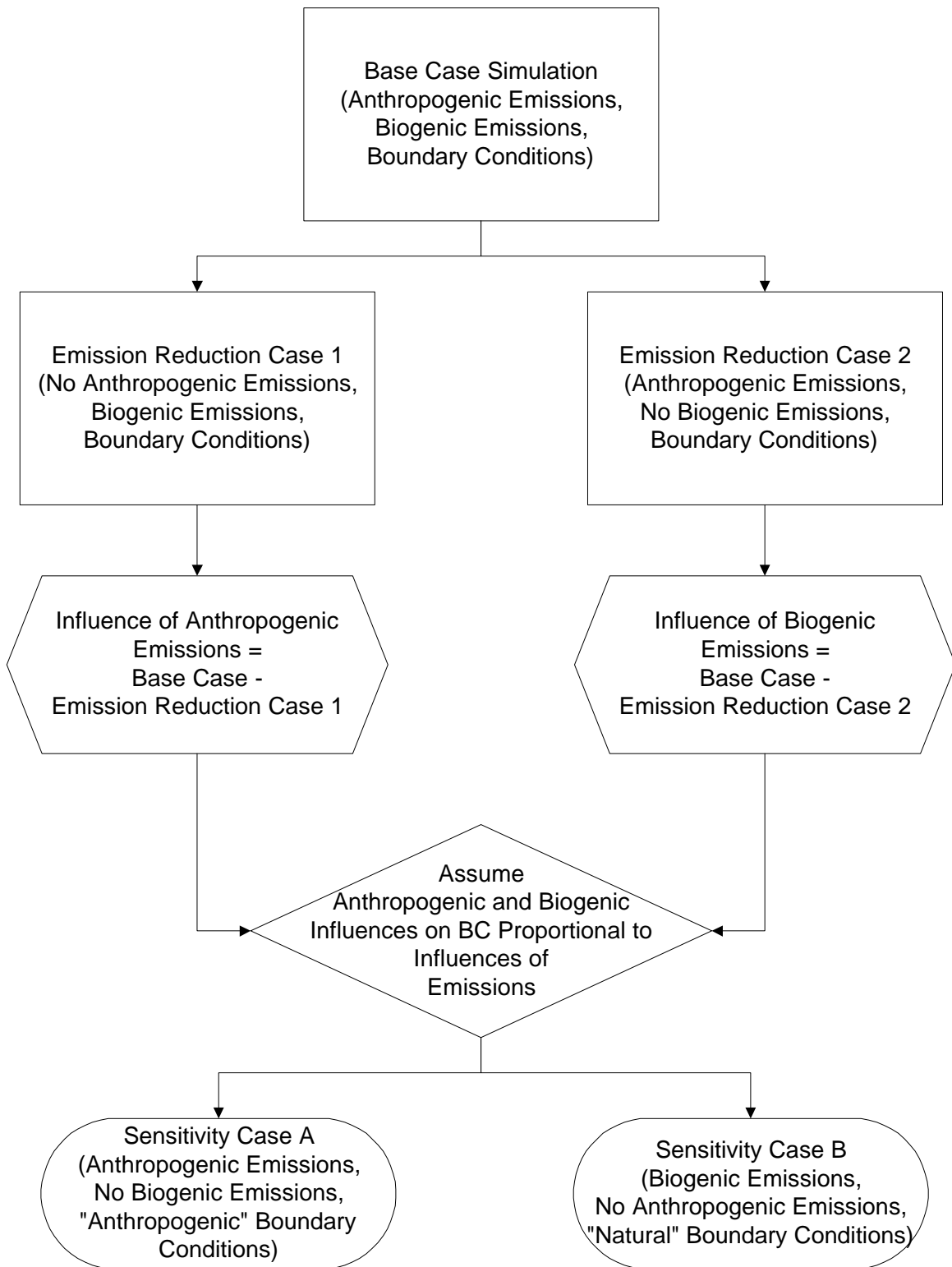


Figure 4-1. Sensitivity simulation procedure.

simulation and a simulation without anthropogenic emissions (biogenic emissions + BC influenced by both anthropogenic and biogenic factors). Similarly, the influence of biogenic emissions was assumed to be reflected in the difference in domain- and episode-averaged O₃ concentrations between the base case simulation and a simulation with no biogenic emissions. The results (i.e., spatially and temporally averaged O₃ concentrations) of these simulations were then used to define the anthropogenic vs. biogenic contributions to O₃ in the BC. We summarize in Table 4-1 the BC used in sensitivity simulations A (no biogenic emission, no biogenic influence at the boundary) and B, which is the exact complement of that in case A, with no anthropogenic emission and natural BC.

4.2 Results

Our presentation of the results focuses primarily on the last three days of the simulation period (July 16 to 18, 1995) because the first two days are influenced to some extent by the initial conditions.

4.2.1 O₃

Both the spatial and temporal distribution of O₃ changed as a result of the changes in emissions and BC in the sensitivity simulation with biogenic influences removed. The response, in terms of absolute and relative changes in O₃, also varies as a function of time and location. We first analyze the response as a function of time. The response as a function of location will be discussed later.

Table 4-2 shows the response of O₃ to different emission and BC scenarios using two spatially aggregated metrics: domain maximum O₃ and domain average O₃. The first column presents the base case results. The second column presents the results of the emission reduction Case 2 shown in Figure 4-1. This case is equivalent to an anthropogenic emission case assuming that the BC are due to anthropogenic emissions outside the domain. Therefore, it represents an upper limit on the effects of anthropogenic emissions on O₃ and PM and a lower limit of the contribution of biogenic

Table 4-1. Boundary conditions used in the sensitivity simulations for the Nashville, TN domain.

Compound	Boundary condition in sensitivity simulation A	Boundary condition in sensitivity simulation B	Notes
O ₃	0.94 x O ₃ _{base,BC}	0.06 x O ₃ _{base,BC}	$O_3 _{sens,BC} = O_3 _{base,BC} \times \frac{O_3^a}{O_3^a + O_3^b}$ $O_3 _{sensB,BC} = O_3 _{base,BC} - O_3 _{sensA,BC}$ <p>O₃^a = O₃ due to anthropogenic emissions (see Figure 4-1) O₃^b = O₃ due to biogenic emissions (see Figure 4-1)</p>
PAR ALD2 OLE ETH FORM TOL XYL ISOP TERP	0.37 x PAR _{base,BC} 0.12 x ALD2 _{base,BC} 0.22 x OLE _{base,BC} ETH _{base,BC} FORM _{base,BC} TOL _{base,BC} XYL _{base,BC} 0.0 0.0	0.63 x PAR _{base,BC} 0.88 x ALD2 _{base,BC} 0.78 x OLE _{base,BC} 0.0 0.0 0.0 0.0 ISOP _{base,BC} TERP _{base,BC}	$VOC _{sens,BC} = VOC _{base,BC} \times \frac{VOC_{emis}^a}{VOC_{emis}^a + VOC_{emis}^b}$ $VOC _{sensB,BC} = VOC _{base,BC} - VOC _{sensA,BC}$ <p>VOC^a_{emis} = total anthropogenic VOC emissions VOC^b_{emis} = total biogenic VOC emissions</p>
NO _x	0.92 x NO _x _{base,BC}	0.08 x NO _x _{base,BC}	$NO_x _{sens,BC} = NO_x _{base,BC} \times \frac{NO_{xemis}^a}{NO_{xemis}^a + NO_{xemis}^b}$ $NO_x _{sensB,BC} = NO_x _{base,BC} - NO_x _{sensA,BC}$ <p>NO_x^a_{emis} = total anthropogenic NO_x emissions NO_x^b_{emis} = total biogenic NO_x emissions</p>

Table 4-1. Boundary conditions used in the sensitivity simulations for the Nashville, TN domain (continued).

Compound	Boundary condition in sensitivity simulation A	Boundary condition in sensitivity simulation B	Notes
CO	$CO _{base,BC} - 40 \text{ ppb}$	40 ppb	CO concentration at remote locations, 40 ppb (Seinfeld and Pandis, 1998), assumed to be the natural background.
NH ₃	$NH_3 _{base,BC} - 0.3 \text{ ppb}$	0.3 ppb	Background NH ₃ measurement at Oak Ridge TN (NAPAP, 1991).
SO ₂	$SO_2 _{base,BC} - 0.2 \text{ ppb}$	0.2 ppb	Globally averaged SO ₂ concentration of 0.167 ppb (Wayne, 1991) assumed to be the natural background.
PM sulfate	$sulfate _{base,BC} - 1 \mu\text{g m}^{-3}$	$1 \mu\text{g m}^{-3}$	Sulfate concentration at remote locations, $1 \mu\text{g m}^{-3}$ (Seinfeld and Pandis, 1998), assumed to be the natural background.
PM nitrate	$0.92 \times \text{nitrate} _{base,BC}$	$0.08 \times \text{nitrate} _{base,BC}$	Same treatment as NO _x BC.
PM ammonium	$0.85 \times \text{ammonium} _{base,BC}$	$0.15 \times \text{ammonium} _{base,BC}$	$NH_4^+ _{sens,BC} = NH_4^+ _{base,BC} \times \frac{NH_3 _{base,BC} - 0.3 \text{ ppb}}{NH_3 _{base,BC}}$ $NH_4^+ _{sensB,BC} = NH_4^+ _{base,BC} - NH_4^+ _{sensA,BC}$
PM EC	$EC _{base,BC} - 0.01 \mu\text{g m}^{-3}$	$0.01 \mu\text{g m}^{-3}$	EC concentration at remote locations, $0.01 \mu\text{g m}^{-3}$ (Seinfeld and Pandis, 1998), assumed to be the natural background.
PM OC	$OC _{base,BC} - 0.5 \mu\text{g m}^{-3}$	$0.5 \mu\text{g m}^{-3}$	OC concentration at remote locations, $0.5 \mu\text{g m}^{-3}$ (Seinfeld and Pandis, 1998), assumed to be the natural background.
Other PM	$\text{Other PM} _{base,BC} - 3 \mu\text{g m}^{-3}$	$3 \mu\text{g m}^{-3}$	Other PM at remote locations, $3 \mu\text{g m}^{-3}$ (Seinfeld and Pandis, 1998), assumed to be the natural background.

Table 4-2. O₃ results for Nashville sensitivity cases.

	Base case	Lower limit sensitivity case ^(a)	Best estimate sensitivity case A ^(b)	Best estimate sensitivity case B ^(c)
Maximum 1-hour average concentration on 16 July 1995 ^(e)	105 ppb	89 ppb	77 ppb	17 ppb
Location of 16 July maximum ^{(a) (d)}	74,29	76,28 or 77,27 or 81,24	77,25 or 77,21	10,59
Average surface O ₃ between noon and 7 p.m. on 16 July 1995	66.7 ppb	64.8 ppb	61.6 ppb	9.2 ppb
Average surface O ₃ between midnight and 7 a.m. on 17 July 1995	52.5 ppb	54.2 ppb	51.4 ppb	5.9 ppb
Average surface O ₃ from 16 July to 18 July 1995	60.3 ppb	59.8 ppb	56.6 ppb	8.2 ppb

(a) Anthropogenic emissions (no biogenic emission), base case BC

(b) Anthropogenic emissions, “anthropogenic” BC

(c) Biogenic emissions “natural” BC

(d) x,y where x is the grid cell number in the west-east direction and y is the grid cell number in the south-north direction from the south-west corner of the modeling domain

(e) day with observed maximum concentration.

emissions can be deduced by comparing the results of this case and those of the base case. This case is, therefore, referred to as the lower limit sensitivity case. Another sensitivity case with no biogenic emissions and zero BC, i.e., assuming BC are due to biogenic emissions, was considered to deduce a lower limit of the effects of anthropogenic emissions. However, this case was eliminated as irrelevant since the fraction of O₃ due to anthropogenic emissions was found to be quite high, as shown in Table 4-1. The third column is the sensitivity case with only anthropogenic emissions and “anthropogenic” BC. (We refer to the BC with no biogenic influence, estimated based on the procedure in Figure 4-1, as the “anthropogenic” BC.) The difference between the base case and sensitivity case A provides one estimate of the amount of O₃ and PM attributable to biogenic emissions. The last column is the sensitivity case with only biogenic emissions and “natural” BC; it provides an alternative estimate of O₃ attributed to biogenic emissions and is referred to as best estimate sensitivity case B.

On 16 July, when the episode maximum O₃ was observed, the relative change was 27% (28 ppb) for the maximum concentration with a small shift in the location (downwind of Nashville) from the base case to sensitivity case A. The maximum concentration responded to reductions in both emissions and BC. The maximum one-hour concentration decreased by 16 ppb with the elimination of biogenic emissions in the lower limit sensitivity case. It decreased by another 12 ppb with reduced BC in sensitivity case A (i.e., 28 ppb reduction). In the biogenic best estimate sensitivity case, a maximum of 17 ppb O₃ was produced on 16 July (the average concentration of O₃ at the boundary was 2.4 ppb for this simulation). The differences in the two best estimates of biogenic contributions are an indication of the non-linearities of O₃ chemistry.

The response of the domain average O₃ to the removal of biogenic emissions and influence at the boundary was smaller, both in absolute and relative terms, than that in the peak concentrations. The difference between the base case and best estimate sensitivity case A is 3.7 ppb, or 6% averaged over the entire domain on the last three days of the simulation. More interestingly, the lower limit sensitivity case with base case BC (Column 2 in Table 4-2) suggested that biogenic emissions may increase or decrease O₃ on (spatial and temporal) average. Removing biogenic emissions from the base case reduced O₃ by an average of 0.5 ppb (Columns 1 and 2 of Table 4-2). However, the

response of the spatial average O₃ concentrations differs at different times of the day. During the day, biogenic emissions had a small positive effect (i.e., production) on O₃ on average. During the night, however, the net effect of biogenic emissions was the removal of O₃. Reactive biogenic VOC (e.g., monoterpenes) are emitted during both day and night and have a scavenging effect on O₃. This nighttime scavenging may be enhanced by natural emissions of NO. When less background (BC) O₃ is present in sensitivity case B, biogenic emissions produce 8.2 ppb O₃, which is a larger net positive effect compared to that inferred by the difference between the base case and sensitivity case A. A smaller nighttime effect may indicate scavenging of O₃ produced during the day or deposition with no production. Wang and Jacob (1998) simulated O₃ concentrations of 10 to 15 ppb in the northern hemisphere before the industrial revolution. Our simulation of a biogenic-only environment predicted O₃ levels slightly lower but still consistent with that study.

Two distinct methods (sensitivity cases A and B) provide best estimates of biogenic contributions ranging from 4 to 8 ppb on a spatial average. Note that 40 ppb O₃ was assumed at the boundary in the base case simulation. O₃ seemed to be quite insensitive to biogenic emissions, even though the latter account for over 50% of the VOC emissions within the domain. We attribute this limited response to NO_x sensitivity within the Nashville, TN domain. When the production of O₃ is limited by the availability of NO_x, adding or removing a relatively large quantity of VOC and a small amount of NO_x has a small effect on the average O₃ concentrations over a large spatial domain. In fact, because of the reaction of O₃ with reactive biogenic VOC, some locations with significant biogenic VOC emissions are predicted to experience a slight increase in O₃ when biogenic emissions are removed.

Peak O₃ concentrations in the base case occurred downwind of major point sources and of the Nashville urban area. These locations are more abundant in anthropogenic NO_x emissions and are likely to exhibit higher VOC sensitivity. Therefore, greater responses of O₃ to the removal of biogenic emissions and biogenic influence at the boundaries were expected, and indeed predicted. On the other hand, in an environment with no anthropogenic emissions, the location of peak O₃ is determined by the interaction between biogenic emissions and meteorology.

It is informative to contrast the response in O₃ at urban vs. rural locations to the removal of biogenic emissions and/or changes in BC. Figure 4-2 presents the diurnal profiles of O₃ for the base case and sensitivity case A at three locations: (1) Nashville (NAS), (2) Youth, Inc. (YOU), which is located downwind of the Nashville urban area, and (3) Land Between Lakes (LBL), a rural location. The difference between these two concentrations is the estimate of biogenic contribution to O₃ based on perturbation of the base case. The O₃ concentrations in best estimate case B are also presented. This is the amount of O₃ produced in an environment with no anthropogenic influence.

The average NO_x concentrations in NAS, YOU, and LBL are 30 ppb, 3.3 ppb, and 0.73 ppb, respectively, in the base case. Therefore, NAS and YOU are likely to be more VOC-sensitive than LBL. As expected based on our discussion, the response of O₃, measured as the difference between the base case and sensitivity case A, was much stronger at the locations influenced by anthropogenic sources. The reductions in peak one-hour average O₃ at Nashville and Youth were 31.4 ppb (34%) and 28.5 ppb (28%), respectively on 16 July. The simulated maximum eight-hour average O₃ concentrations were reduced by 26.9 ppb (32%) and 23.9 ppb (26%) at these two sites on the same day. Three-day average O₃ concentrations were reduced by 12.1 ppb (26%) at Nashville and by 12.0 ppb (18%) at Youth between 16 and 18 July.

At the rural location, the response in sensitivity case A in the peak one-hour O₃ concentration on 18 July and maximum eight-hour average concentration on the same day were 7.4 ppb (9%) and 6.4 ppb (6%), respectively. The three-day average O₃ concentration decreased by 1.8 ppb (3%) in sensitivity case A at LBL. The response to the elimination of biogenic emissions and their influence on BC was smaller than that predicted at Nashville and Youth. The reduced O₃ response at LBL was consistent with increased NO_x sensitivity at the rural site.

As shown in Figure 4-2, the concentrations of O₃ in best estimate case B was fairly constant with time. The 3-day average O₃ concentration at LBL (10 ppb) is slightly higher than those at NAS and YOU (9 ppb) in this biogenic-only case. Compared to sensitivity case A, the biogenic contributions of 9-10 ppb O₃ estimated in case B are lower at urban sites but higher at the rural site. The peak one-hour O₃ concentration at LBL is 15.1 ppb (19% of base case value), whereas the peak concentrations at YOU and

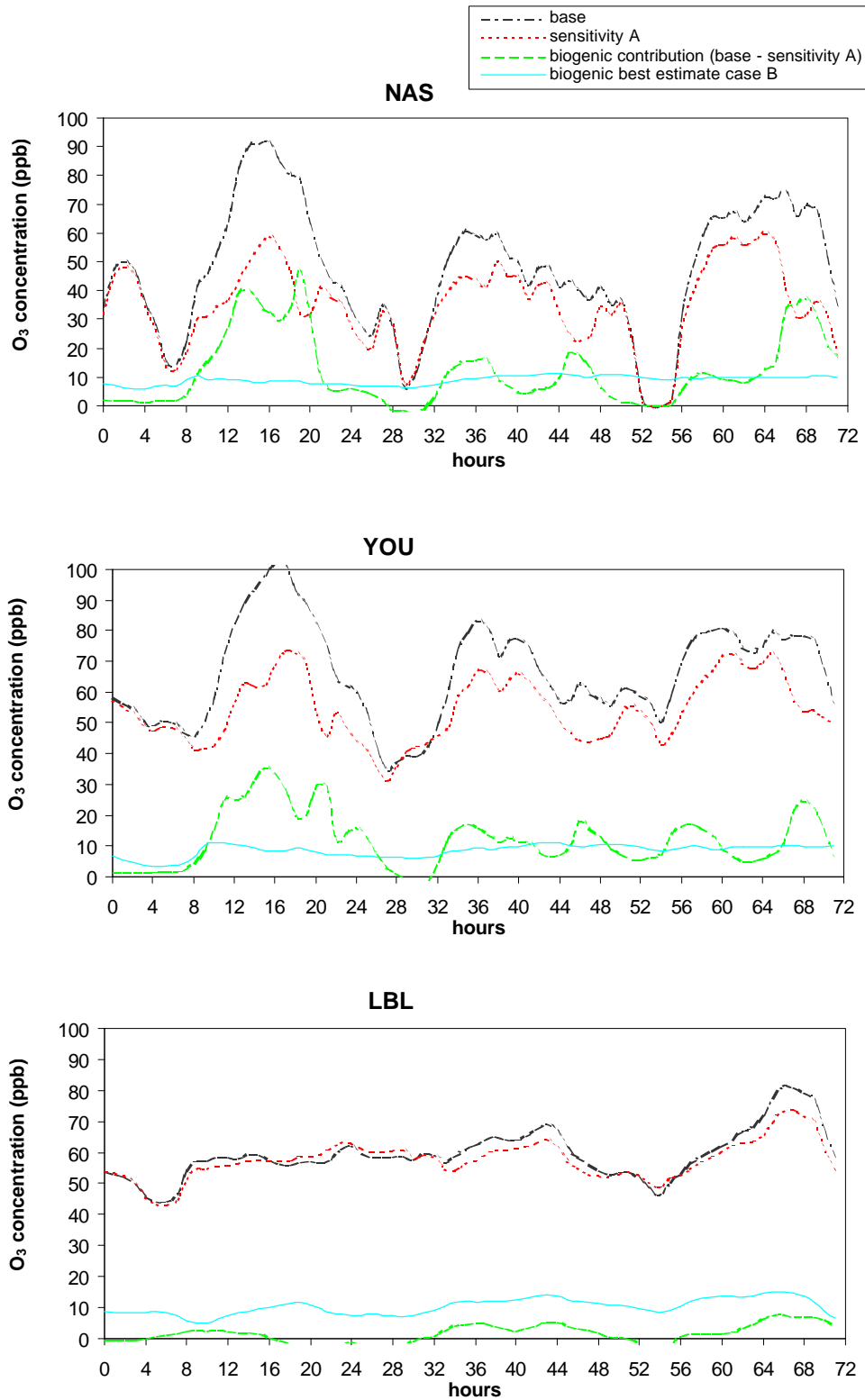


Figure 4-2. O₃ time series for the base case and best estimate sensitivity cases at (a) NAS, (b) YOU, and (c) LBL.

NAS are 11.1 ppb (11%) and 11.3 ppb (12%), respectively. The maximum eight-hour average O₃ concentrations were only slightly lower than the one-hour values due to the lack of significant temporal variations in case B. The maximum 8-hour concentrations at LBL, YOU and NAS are 14.2, 10.5, and 10.7 ppb, respectively, which represent 19, 11 and 13% of the base case maximum 8-hour concentrations.

In a NO_x-sensitive airshed like the base case of Nashville/Tennessee domain, the contribution of biogenic emissions to O₃ is most significant in areas with high anthropogenic NO_x emissions. We estimated under sensitivity case A the biogenic contribution at a representative urban location (Nashville) to be 31 ppb of O₃ (or 34%) for the maximum one-hour average concentration and 27 ppb of O₃ (or 32%) for the maximum eight-hour average concentration. At locations downwind of major urban areas (e.g., Youth, Inc.), the biogenic contributions were slightly smaller. Under sensitivity case B, the contributions were on the order of 10 ppb at all three locations. Biogenic contributions to O₃ production depend strongly on the availability of NO_x (emitted mostly from anthropogenic sources) and would likely decrease with further reductions of anthropogenic NO_x emissions (as NO_x availability would decrease). In an environment without anthropogenic emissions, the potential for O₃ production of biogenic emission is quite limited. Of the 3 locations studied, biogenic emissions produced a maximum of 15 ppb one-hour average O₃ and 14 ppb 8-hour average O₃ in the absence of anthropogenic NO_x. However, at present NO_x levels, biogenic contributions may affect the attainability of the one-hour and 8-hour NAAQS for O₃ since they may account for up to 1/3 of maximum O₃ concentrations in urban locations.

4.2.2 PM

The direct effect of the removal of biogenic emissions was the removal of all SOA formed from terpene precursors. The domain-averaged 24-hour average biogenic SOA concentrations were 0.26, 0.37, and 0.46 μg m⁻³ on July 16, 17, and 18, respectively, in the base case simulation.

The removal of biogenic (isoprene) emissions in case A also affected the simulated oxidant chemistry, such as O₃ and OH concentrations, and the formation of

other secondary PM components. Table 4-3 summarizes the predicted anthropogenic SOA concentrations in the base and sensitivity simulations. There was an increase in anthropogenic SOA throughout the simulation domain. The only locations where a decrease of anthropogenic SOA are predicted were locations downwind of major anthropogenic sources, where O₃ also decreased significantly as a result of the removal of biogenic emissions. An example is shown in Figure 4-3.

In sensitivity case A, the decrease in biogenic SOA more than offset the increase in anthropogenic SOA, resulting in a net decrease in SOA concentrations by 0.14 μg m⁻³, 0.22 μg m⁻³, and 0.31 μg m⁻³, respectively on 16, 17, and 18 July. The normalized changes were 19%, 24%, and 29% on these days. In the absence of anthropogenic emissions (i.e., case B), the ambient SOA produced from biogenic precursors was substantially less. The domain average was only 0.08, 0.14 and 0.18 μg/m³ on 16, 17 and 18 July. The ability of biogenic VOC to produce SOA depends on the availability of oxidants in the atmosphere. Therefore, the difference in biogenic SOA contribution implied by the two sensitivity cases is an indication of the non-linear chemistry responsible for their production.

In case A, since SOA represented a small fraction of total organic PM, e.g., decrease in biogenic SOA and increase in anthropogenic SOA did not affect the total OC content significantly. In Nashville, 0.35, 0.47, 0.44 μg m⁻³ of biogenic SOA were removed in the best estimate sensitivity case on these three days, representing 1.8%, 2.5%, and 1.9% of the predicted PM_{2.5}.

In case B, primary OC originates from BC only. With no emissions, primary OC concentrations within the domain were very low, averaging 0.11 μg m⁻³ on 16 July to 18 July. Therefore, SOA formed within the domain represent 44% to 62% of OC in the simulation with no anthropogenic influences.

Changes in the concentrations of the inorganic secondary PM were attributed to changes in both the oxidant levels and the “anthropogenic” BC of sensitivity case A. For example, over the last three days, an average increase of 0.1 μg m⁻³ was predicted for PM_{2.5} sulfate over the entire domain, while PM_{2.5} nitrate increased by 0.04 μg m⁻³. The increase in PM_{2.5} sulfate and nitrate was most likely a result of modified oxidant concentrations in the sensitivity case. Daytime OH concentrations increased by about 0.2

Table 4-3. Predictions of SOA in the base and best estimate sensitivity simulations.

	Domain-wide 24-hour average concentrations	Base case	Best estimate sensitivity case A	Best estimate sensitivity case B
Total SOA	July 16	0.63	0.49	0.08
	July 17	0.86	0.64	0.14
	July 18	1.08	0.75	0.18
Anthropogenic SOA	July 16	0.37	0.49	0
	July 17	0.49	0.64	0
	July 18	0.62	0.75	0
Biogenic SOA	July 16	0.26	0	0.08
	July 17	0.37	0	0.14
	July 18	0.46	0	0.18

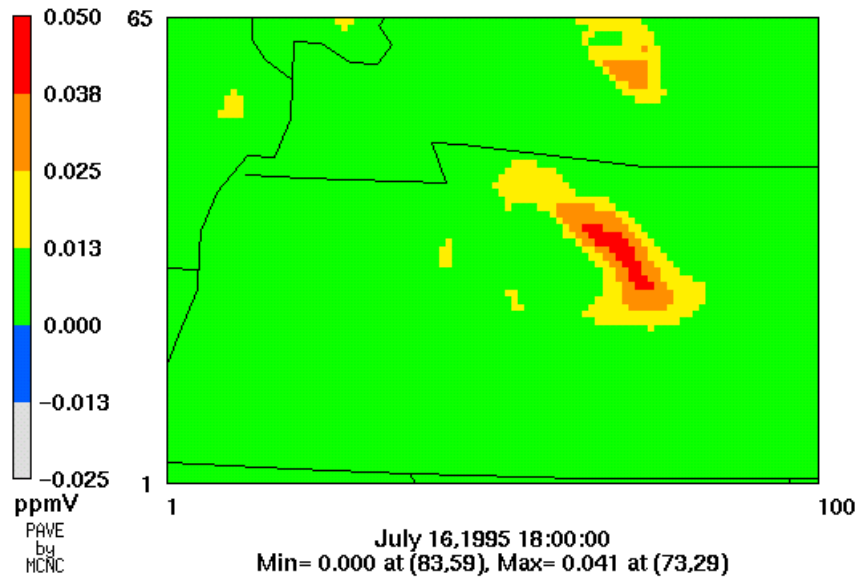
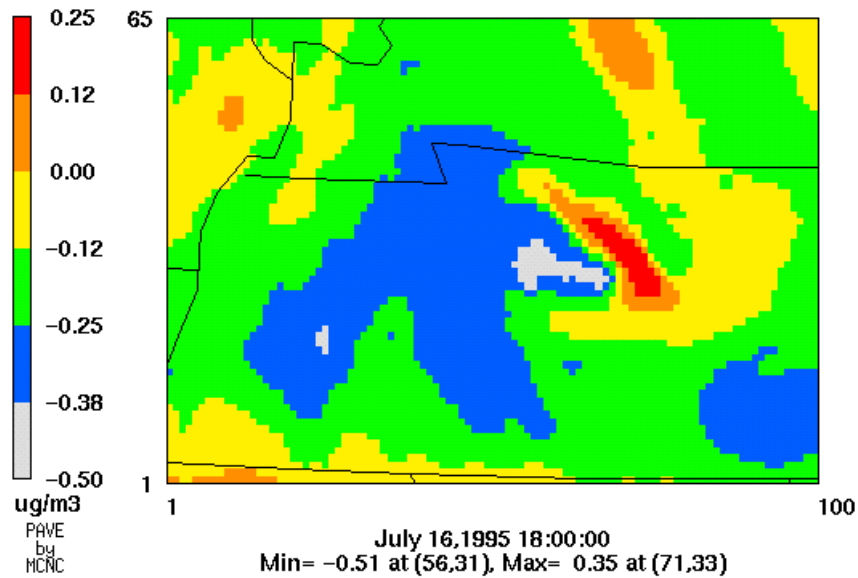


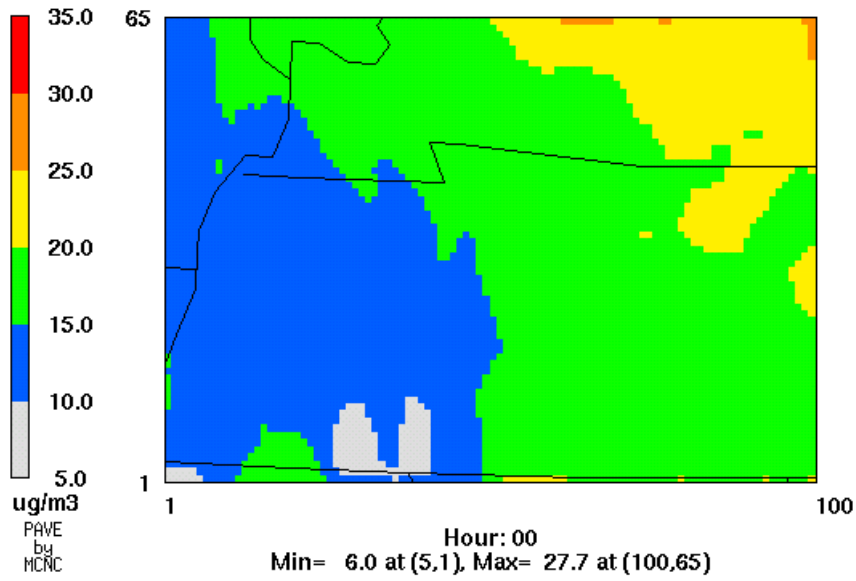
Figure 4-3. Differences in the concentrations of anthropogenic SOA (top) and O₃ (bottom) between the base case and best estimate sensitivity case A (i.e., contribution of biogenic precursors). Decreases in anthropogenic SOA concentrations in the sensitivity case is predicted at locations where O₃ concentrations also decrease.

ppt across much of the domain in sensitivity case A. In particular, PM_{2.5} sulfate increased by over 14 $\mu\text{g m}^{-3}$ within a power plant plume on the last day of the simulation, possibly due to the increase of hydroxyl radicals in rural areas in the sensitivity simulation. In a simulated atmosphere with natural BC and only biogenic emissions, PM_{2.5} concentrations within the modeling domain on the last 3 days of the simulation were 1.2, 1.3 and 1.4 $\mu\text{g/m}^3$ on a domain-wide basis. The amount of sulfate averaged 0.3 $\mu\text{g/m}^3$ over the entire domain while essentially no nitrate was observed, because of low concentrations of HNO₃ within the domain. Figure 4-4 presents the 24-hour average concentrations of PM_{2.5} in the base case and the best estimate sensitivity cases A and B on 16 July and 18 July. Overall, PM_{2.5} decreases of 19% and 17% were simulated on 16 and 18 July, respectively, in best estimate sensitivity case A. In addition to very low PM, the spatial distribution (Figure 4-4e and f) is also different in sensitivity case B. The gradient of PM_{2.5} from east to west, which is observed in the simulations with anthropogenic sources, is not as pronounced observed in the biogenic-only case on July 16 and not observed on July 18. Instead, relatively higher PM_{2.5} concentrations seem to originate from the boundaries.

We present in Table 4-4 the changes in 24-hour PM_{2.5} concentrations at Nashville between the base case and case A. At this urban location, PM_{2.5} concentrations decreased by roughly 10% over two 24-hour periods on 16 and 18 July, 1995, implying that the biogenic and natural contributions to PM_{2.5} were roughly 2 $\mu\text{g/m}^3$. The PM_{2.5} concentrations simulated in the biogenic-only case B were less than 2 $\mu\text{g/m}^3$ in Nashville.

From the base case to sensitivity case A, the purely primary PM components of anthropogenic origins, EC and other PM_{2.5}, decreased as a result of decreased BC. Sulfate, nitrate, and ammonium were all lower in the sensitivity case than in the base case, due to a combination of reduced BC and changes in chemistry. Although OC, the sum of primary and secondary OC, decreased in Nashville, the anthropogenic component of SOA actually increased, while primary OC and biogenic SOA were reduced in the sensitivity case. The former decreased due to reductions in its BC, and the latter was eliminated with the removal of biogenic emissions. The predictions of the biogenic-only sensitivity simulation (case B) were lower for most components than the expected effects based on the difference between the base case and sensitivity case A. The formation of

(a)



(b)

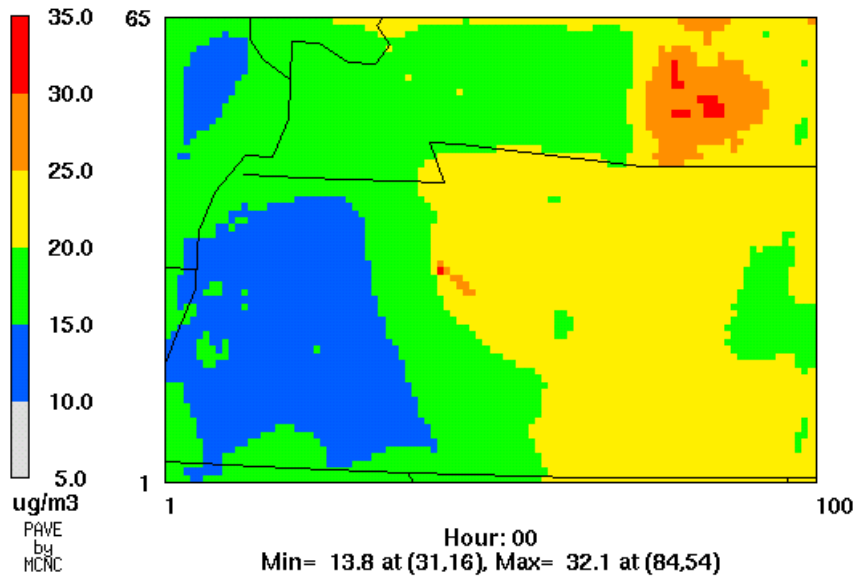
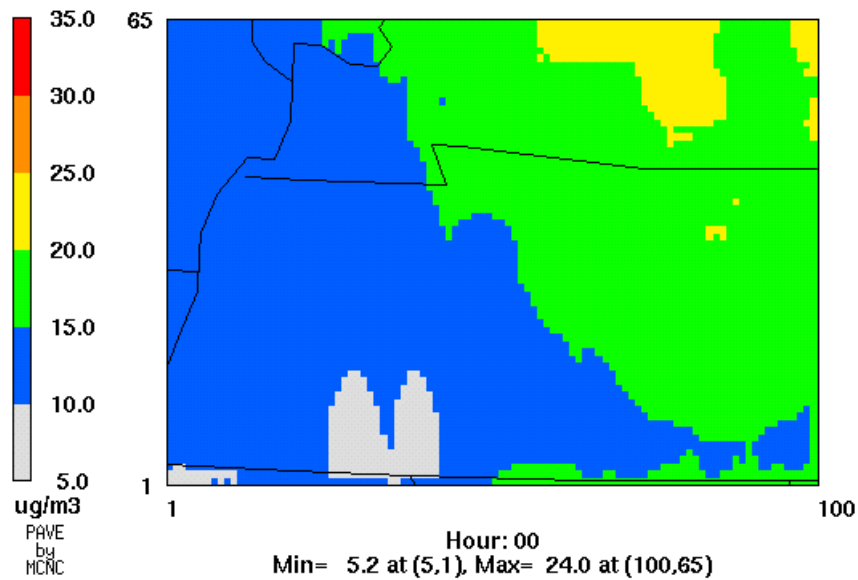


Figure 4-4. Spatial distribution of 24-hour average PM_{2.5}. (a) Base case on 16 July, (b) base case on 18 July, (c) best estimate sensitivity case A on 16 July, (d) best estimate sensitivity case A on 18 July, (e) best estimate sensitivity case B on 16 July, and (f) best estimate sensitivity case B on 18 July.

(c)



(d)

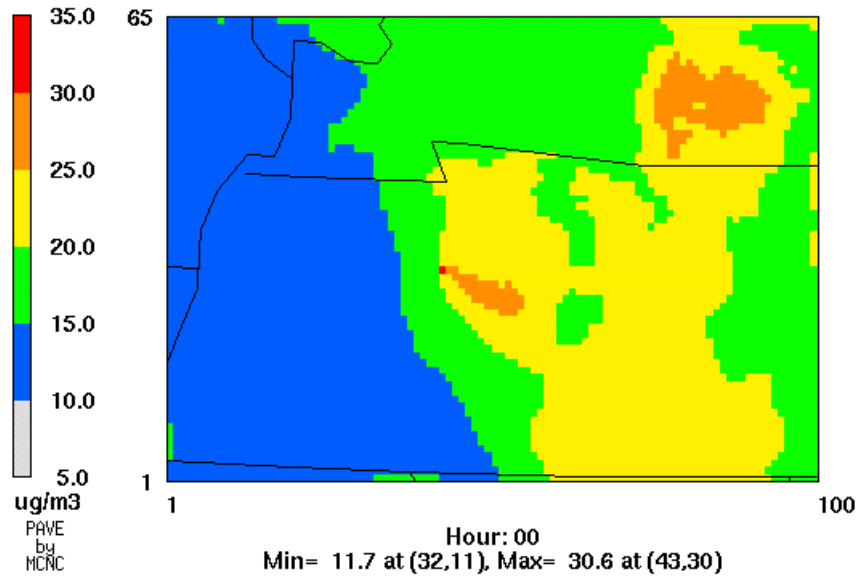
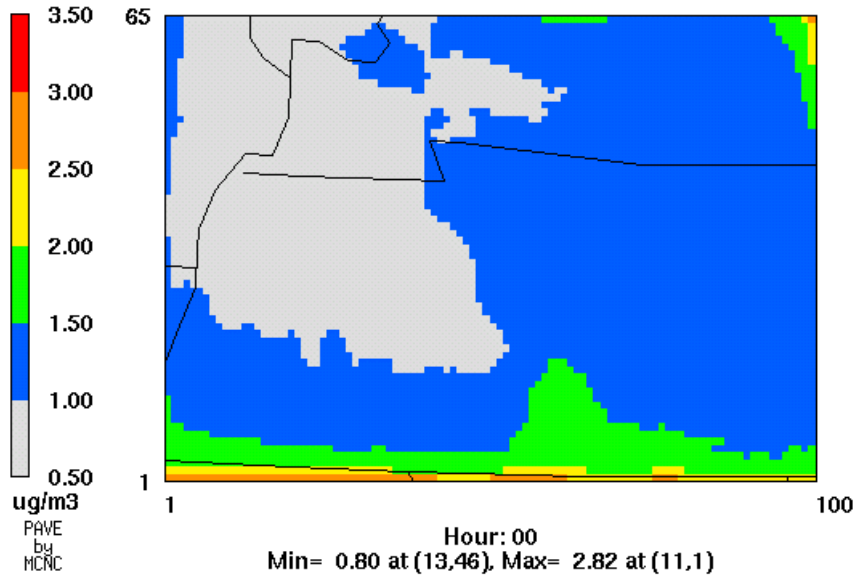


Figure 4-4. Spatial distribution of 24-hour average PM_{2.5}. (a) Base case on 16 July, (b) base case on 18 July, (c) best estimate sensitivity case A on 16 July, (d) best estimate sensitivity case A on 18 July, (e) best estimate sensitivity case B on 16 July, and (f) best estimate sensitivity case B on 18 July. (continued).

(e)



(f)

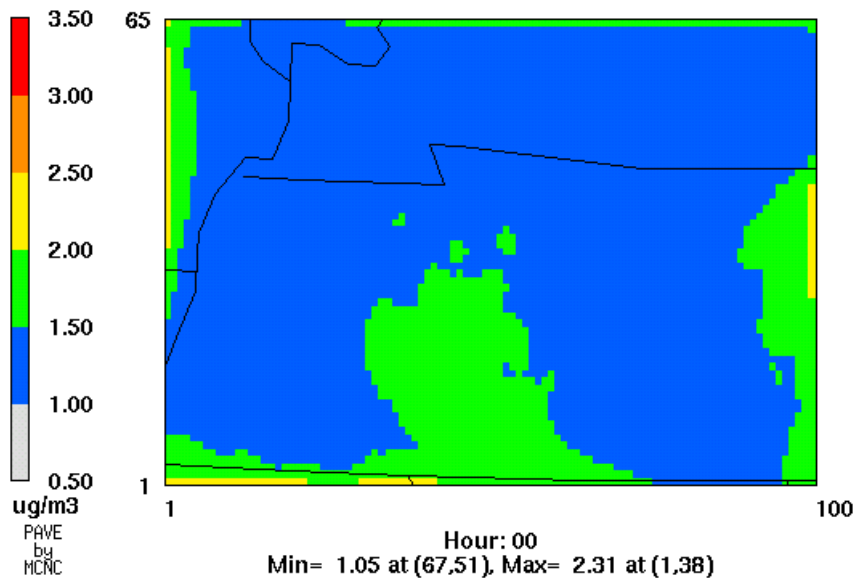


Figure 4-4. Spatial distribution of 24-hour average PM_{2.5}. (a) Base case on 16 July, (b) base case on 18 July, (c) best estimate sensitivity case A on 16 July, (d) best estimate sensitivity case A on 18 July, (e) best estimate sensitivity case B on 16 July, and (f) best estimate sensitivity case B on 18 July. (continued).

Table 4-4. PM_{2.5} on 16 July and 18 July in the base and best estimate sensitivity cases in Nashville.

	July 16			July 18		
	Base case ($\mu\text{g m}^{-3}$)	Best estimate sensitivity case A ($\mu\text{g m}^{-3}$)	Best estimate sensitivity case B ($\mu\text{g m}^{-3}$)	Base case ($\mu\text{g m}^{-3}$)	Best estimate sensitivity case A ($\mu\text{g m}^{-3}$)	Best estimate sensitivity case B ($\mu\text{g m}^{-3}$)
PM _{2.5}	19.3	16.9	1.1	23.0	21.4	1.3
PM _{2.5} sulfate	7.9	7.7	0.28	9.1	9.3	0.29
PM _{2.5} nitrate	1.4	1.1	0.00	1.5	1.3	0.00
PM _{2.5} ammonium	3.4	3.2	0.10	3.8	3.9	0.11
PM _{2.5} OC	3.4	2.5	0.21	3.0	2.0	0.30
- primary OC	2.3	2.1	0.09	1.7	1.5	0.10
- SOA (anthropogenic)	0.70	0.74	0.00	0.88	0.92	0.00
- SOA (biogenic)	0.35	0	0.12	0.44	0	0.20
PM _{2.5} EC	0.35	0.35	0.00	0.27	0.26	0.00
Other PM _{2.5}	2.9	1.7	0.52	5.3	4.2	0.61

secondary components seemed much decelerated in the clean case, due to reduced oxidants concentrations within the domain and reduced availability of precursors (e.g., SO₂, NO_x) from emissions and inflow from the boundaries. In addition, the deposition velocity is calculated as a function of the mode-mean diameter of the particles, which differs in cases with high and low PM_{2.5} concentrations.

The discussion illustrates that, like O₃, all secondary PM components, not just SOA, respond to changes in biogenic emissions and changes in BC. The elimination of biogenic emissions (primarily VOC and, to a smaller extent, NO_x) resulted in non-linear changes in oxidant concentrations, causing indirect effect on PM nitrate, sulfate, ammonium, and SOA derived from anthropogenic precursors.

5. SENSITIVITY OF MODELED PM CONTRIBUTION IN NASHVILLE TO TERPENE SPECIATION

BEIS2, the biogenic emissions inventory system that was used to generate the emission inventories used in the Nashville simulation, estimates the emission of one lumped terpene class. For the purpose of modeling the formation of biogenic SOA, a single lumped terpene class may not be adequate. As discussed in Sections 2 and 3, terpene speciation was needed for the simulation of SOA using the Odum/Griffin et al. methodology. Ambient data from Atlanta were used to speciate the terpene emissions into 12 individual compounds. Uncertainties in the speciation of terpenes may affect the predictions of SOA. To estimate uncertainties associated with the terpene speciation profile, we used an alternative speciation that represents a realistic case that differs significantly from that used in Section 3.

5.1 Alternative Terpene Speciation

The alternative terpene speciation profile is based on a mixed deciduous and coniferous forest in Wisconsin (Helmig et al., 1999). It is listed in Table 5-1. Compared to the base case profile of the Atlanta forest presented in Section 3, the alternative profile contains more α -pinene, β -pinene, 3-carene, and d-limonene and less terpinene, ocimene, and sesquiterpenes.

5.2 Results

Since the mechanistic representation of SOA formation from monoterpenes was treated in parallel to the original CBM-IV, changing the terpene speciation had no effect on the formation of gaseous pollutants, such as O₃ and anthropogenic SOA.

Significant changes in biogenic SOA concentrations were simulated when the alternative terpene speciation profile was applied to the BEIS2 terpene emissions. The most important result was that biogenic SOA production was halved due to the

Table 5-1. Alternative terpene speciation profile (mixed deciduous and coniferous forest in Wisconsin)

Compound	Mole %
α -pinene	23.8
Sabinene	0.0
β -pinene ⁽¹⁾	30.2
3-carene	4.1
Terpinene	4.0
d-limonene ⁽¹⁾	21.0
Ocimene	2.2
Terpinolene	2.4
Linalool ⁽²⁾	2.4
Terpinenol ⁽²⁾	2.4
Sesquiterpenes ⁽³⁾	0.4
Unreactives	7.1

(1) including other structurally similar compounds

(2) emission factors for linalool and terpinenol assign by analogy to terpinolene

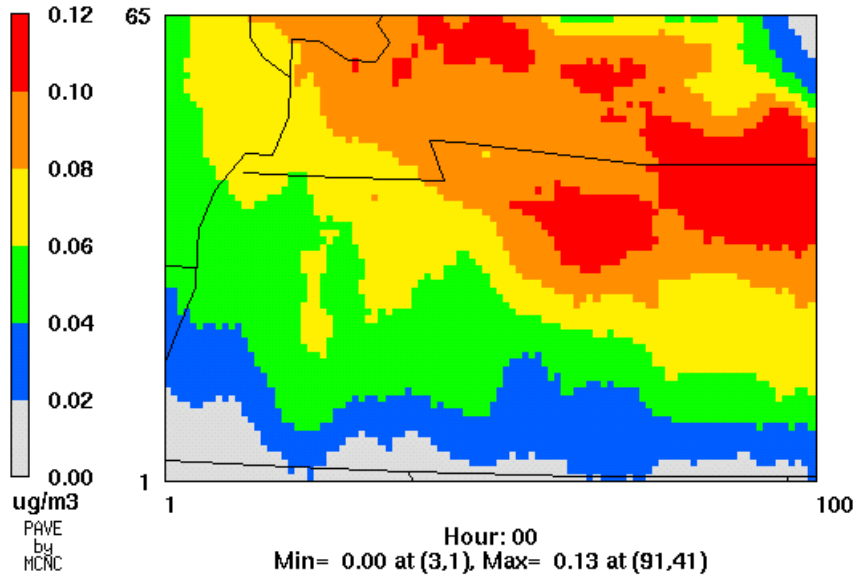
(3) humulene and caryophyllene

change in terpene speciation. The mean biogenic SOA concentration averaged over the entire domain decreased from $0.059 \mu\text{g m}^{-3}$ and $0.096 \mu\text{g m}^{-3}$ on 16 and 18 July to $0.030 \mu\text{g m}^{-3}$ and $0.046 \mu\text{g m}^{-3}$, respectively. Total SOA (i.e., biogenic + anthropogenic) averaged over the entire domain also decreased from $0.065 \mu\text{g m}^{-3}$ to $0.036 \mu\text{g m}^{-3}$ on 16 July (also see Figure 5-1). The corresponding change in SOA on 18 July was from $0.10 \mu\text{g m}^{-3}$ to $0.05 \mu\text{g m}^{-3}$. The simulated maximum 24-hour average SOA concentration also decreased by 50% to 55% on 16 and 18 July: the predicted maxima were $0.114 \mu\text{g m}^{-3}$ and $0.197 \mu\text{g m}^{-3}$ in the base case and $0.055 \mu\text{g m}^{-3}$ and $0.090 \mu\text{g m}^{-3}$ in the sensitivity case with new terpene speciation.

The key reason behind the decrease in the formation of biogenic SOA was the substitution of sesquiterpenes in the Georgia profile by less prolific SOA precursors in the Wisconsin profile. The domain average concentrations of SOA from humulene and caryophyllene, the two sesquiterpenes represented in the Odum/Griffin et al. SOA module, decreased by $0.044 \mu\text{g m}^{-3}$ and $0.071 \mu\text{g m}^{-3}$ on 16 and 18 July. The decrease of SOA from sesquiterpenes was offset by relatively smaller increases of SOA from monoterpene species that are more abundant in the Wisconsin profile, including α -pinene, β -pinene, 3-carene, and limonene. Of these compounds, α -pinene, β -pinene, and 3-carene react with multiple oxidants. In the present simulation, the reactions with O_3 were comparatively more efficient for the production of SOA than the reactions with OH for these monoterpenes. β -pinene also reacts with NO_3 , in addition to OH and O_3 . The contribution of the NO_3 reaction to SOA formation was higher than those of either the OH reaction or O_3 reaction.

An uncertainty of the order of 50% can be expected due to uncertain speciation of the monoterpene emissions. It is particularly important to resolve the emissions of sesquiterpenes, because these species are efficient SOA precursors. A BEIS3 type emissions inventory system, which models individual terpene emissions from vegetation species, will provide a much needed resolution for organic speciation. In addition, the NO_3 reaction appears to be an important SOA production mechanism. Therefore, a better understanding of the nitrate radical reaction will improve the prediction of SOA from biogenic compounds.

(a) Base case



(b) Sensitivity case with alternative terpene speciation

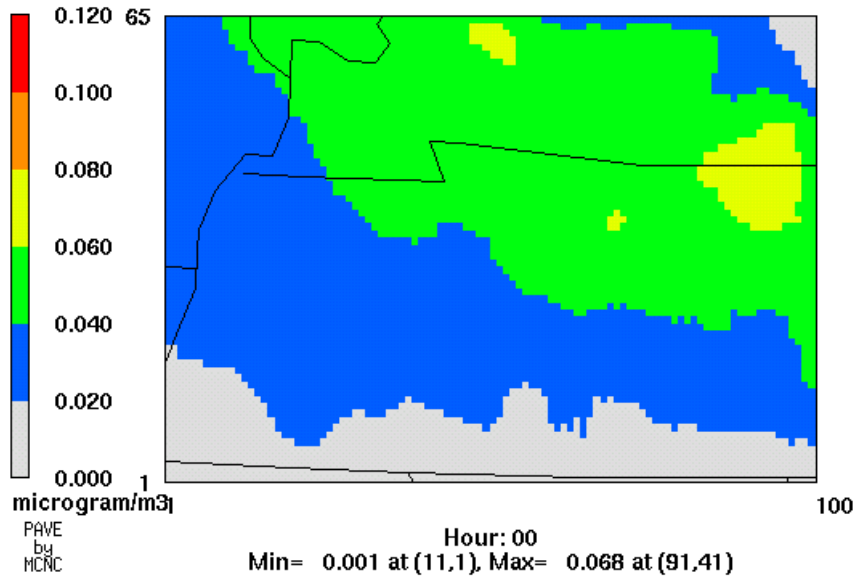


Figure 5-1. SOA distribution in the base case and sensitivity case with alternative terpene speciation on 16 July 1995.

6. BASE CASE SIMULATION IN THE NORTHEAST DOMAIN

An air quality simulation of the northeastern United States was conducted for O₃ and PM using Models-3/CMAQ. The PM simulation builds upon an O₃ base case simulation that was conducted for the NARSTO/Northeast domain under CRC Project A-24. In the simulations of the Nashville/Tennessee region, discussed in Sections 3 through 5, modifications were made to Models-3 to incorporate recent formulations for SOA formation: the Odum/Griffin et al. (Odum et al, 1997; Griffin et al., 1999), CMU/STI (Strader et al., 1998), and MADRID 2/AEC modules. Corresponding changes were made in the CBM-IV gas-phase chemical mechanism to simulate the formation of the condensable organic gases for the first two SOA modules. For MADRID 2, CACM was implemented. We selected the CRC-sponsored CMU/STI SOA module of Strader et al. (1998) for the NARSTO/Northeast simulation. CBM-IV is a widely used mechanism for O₃ formation. Based on the results of our Nashville simulations, the CMU/STI module provides higher SOA estimates than the Odum/Griffin et al. module. Furthermore, the Odum/Griffin et al. module requires speciated terpene inputs. Since BEIS2 provides terpene emissions without speciation, some default speciation of terpene compounds would need to be assigned based on limited experimental data. (BEIS3, when it becomes available, may provide emissions of individual terpene species.) Assumptions made in the chemical speciation of terpenes would introduce additional uncertainties into the modeling of biogenic aerosols, as shown in Section 5. The CMU/STI module uses only one surrogate terpene species, and its simple formulation is, therefore, compatible with BEIS2. We present in this section base case results of the Models-3 simulation conducted for the NARSTO/Northeast episode of 12-15 July 1995.

6.1 Technical Approach

6.1.1 Compilation of Models-3

The CBM-IV chemical mechanism was modified to include the production of condensable organic gases. The formation of SOA as an organic liquid solution was

represented with the CMU/STI module (see Section 2.2). Dry deposition of condensable organic compounds was modeled after higher aldehydes.

For the NARSTO/Northeast simulation, we also included cloud processes (i.e., RADM aqueous chemistry and wet deposition) in addition to aerosol processes. Due to significant cloud cover and some rainfall (as much as 3 cm per hour) observed during the July 12-15 episode, we believed it was important to simulate the effects of aqueous chemistry (e.g., cloud processing of sulfate) and wet deposition of PM.

6.1.2 Meteorological files

Meteorological inputs to Models-3/CMAQ were obtained from Environ, already processed from an MM5 simulation (with four-dimensional data assimilation) conducted at Pennsylvania State University by Nelson Seaman and co-workers (Seaman and Michelson, 1995) under another CRC-sponsored contract.

During this episode, there was a synoptic scale midtropospheric flow with a westerly component across the Appalachian Mountains. In the leeward side of the mountains, air sank and warmed, creating the mesoscale Appalachian lee trough. Winds ahead of the trough turned cyclonically and flowed in a south-southwesterly direction up the urban corridor. Having a marine origin, this air remained slightly cooler than the air to the west of the Appalachian Mountains. The result was a shallow boundary layer capped by hot midwestern air mass at middle levels. Nocturnal jets may have also played a role in long-range transport up the coast.

The MM5 simulation was performed between 1200 UTC 12 July to 0000 UTC 19 July 1995 on four nested domains (108 km, 36 km, 12 km, and 4 km). The highest resolution domain covered a region of 612 km x 444 km centered on the Mid-Atlantic states with 32 vertical layers. Forecast variables included the three wind components, temperature, water vapor, cloud water and ice, precipitation, and pressure. MM5 included surface fluxes of heat, moisture, and momentum, and a 1.5-order turbulent kinetic energy predictive planetary boundary layer scheme to represent turbulent processes. A column radiation parameterization was used to calculate temperature tendencies due to short and long wave radiative flux divergences. Subgrid-scale deep

conversion was applied in the three larger domains. Explicit microphysics was used with a simple ice scheme. FDDA was applied below 850 hPa to reduce growth error at the larger scales where allowing the 4-km solution to develop solely from dynamical and physical forcing.

6.1.3 Time-independent files

Time-independent files, such as land-use and elevation definitions, were obtained from Environ from the above-mentioned CRC-sponsored project. The domain used in the PM simulation contains 99 x 135 grid cells in 13 layers. This grid covers southwestern Massachusetts, Connecticut, New York, New Jersey, Pennsylvania, Maryland, Delaware, District of Columbia, and Virginia and corresponds to the 4-km-by-4-km inner grid of the NARSTO/Northeast domain.

6.1.4 Initial conditions and boundary conditions

Initial conditions (IC) and boundary conditions (BC) for gas-phase species were also obtained from the previous O₃ simulation of the Northeast region. Additional IC and BC were needed for PM and PM precursors, including terpenes, SO₂, and NH₃. The determination of IC and BC for the precursor gases, as well as for PM_{2.5}, PM₁₀, and PM composition (sulfate, nitrate, elemental carbon (EC), particulate organic carbon (OC), sea salt, dust, and other fine and coarse components) is discussed next.

The concentration of terpenes was in general small, with a domain average concentration of 0.2 ppb on the last two days of simulation in a simulation where a default value of 0.0 ppb was used for its IC and BC. Since terpenes are very reactive, we do not expect the effects of terpene IC and BC on SOA formation to propagate beyond the spin-up day or far within the domain. (Note that the effects of terpenes on O₃ are simulated in the original CBM-IV mechanism using OLE, PAR, and ALD2 groups.) Without any experimental measurements as a basis to select non-zero IC and BC, the default IC and BC of 0 ppb were used in our simulation. Therefore, the results for biogenic SOA represented the SOA formed from emissions within the domain.

For SO₂, limited measurements were available from the IMPROVE network. The measured values were 0.5 and 1.4 ppb during the July episode at Shenandoah National Park, to the southwest of the modeling domain. Therefore, a value of 0.95 ppb was chosen to represent the regional background and used to set the IC and BC of SO₂. For NH₃, we used a constant value of 2 ppb for both the IC and BC, based on our Nashville simulation work. To obtain the vertical distribution of boundary and initial concentrations, we assumed that the mixing ratio of the gaseous species was constant with height (see discussion of vertical profiles below).

Some data were available from the IMPROVE networks for PM₁₀, PM_{2.5}, and some PM_{2.5} components, i.e., sulfate, nitrate, EC, and OC. The monitoring schedule of the IMPROVE network was twice a week on Wednesdays and Saturdays. Since the simulation covered the period from 12 July 1995 (Wednesday) to 15 July 1995 (Saturday), the two 24-hour measurements were averaged to determine the BC. Two sites are located to the southwest of the modeling domain: Shenandoah National Park and Dolly Sods Wilderness Area. The measurements at these two sites were quite similar on 12 July and 15 July. We defined the southern BC using data from Shenandoah National Park and the western BC using data from Dolly Sods Wilderness Area. The closest IMPROVE site to the northern boundary was Lye Brook Wilderness Area. No PM data were available from Lye Brook Wilderness Area on 15 July and measurements on 12 July were low for several fine PM components, especially sulfate and ammonium. An alternative data source was taken into consideration to define the northern boundary. Under NESCAUM sponsorship, a five-site monitoring network was operated in the states of Massachusetts and New York in 1995 (Cass et al., 1999). One of these sites was Quabbin Reservoir in rural Massachusetts, just north of the modeling domain. Samples were collected every 6th day at this site, and the site was in operation on 14 July 1995. The measured sulfate, ammonium, OC, and EC concentrations from this data set seemed consistent with data from the IMPROVE sites other than Lye Brook Wilderness Area. However, the concentration of nitrate was negligible at Quabbin Reservoir and the nitrate concentration at Lye Brook Wilderness Area on 12 July was used instead at the northern boundary. For the coarse components and the unspecified anthropogenic component of PM_{2.5}, measurements at Quabbin Reservoir were significantly higher (factor of 2 to 10)

than those observed at the national park sites, while measurements at Lye Brook Wilderness Area were about 30 to 60% of the measurements at the other sites on the same day. Since there was no obvious reason to select one set of data over another for these PM components, an average of the two was used to define the BC. BC derived from the IMPROVE and NESCAUM networks were applied over the ocean, which comprised a part of the eastern and southern boundaries.

The distribution of PM and PM components as a function of height was based on the vertical profile of the inert species carbon monoxide (CO) calculated in the O₃ simulation for the 12-km domain. This vertical profile corresponds to a nearly constant mixing ratio, indicating strong vertical mixing during this episode. The default PM vertical profiles used in the Models-3 IC and BC (EPA, 1999) was not suitable for this simulation because they represent an environment with very limited mixing compared to that indicated by the distribution of gases in the 12-km NARSTO/Northeast simulation. The IC for the PM components were determined as the average of the BC over land. Table 6-1 presents the BC of the PM components at the surface.

6.1.5 Emissions

Emissions files were prepared for PM_{2.5}, PM₁₀, SO₂, NH₃, and terpenes. County-level emissions of NH₃, SO₂, PM_{2.5}, and PM₁₀ were obtained from EPA's National Emission Trends (NET) database, grouped by source category codes (SCC). The generation of three-dimensional, season-specific, temporally-resolved gridded emission fields involved different processing for area source and point source emissions. An Access data base program was used to temporally resolve area source emissions based on temporal profiles provided by EPA (T. Braverman, personal communication). Spatial allocation of area sources was accomplished using a Unix pre-processor developed at AER to produce gridded emissions from county emissions. Point sources were processed with the emissions model SMOKE, which calculated plume rise based on the meteorology input files used in the air quality simulation. For further details, please refer to Section 3.1.

Table 6-1. Boundary conditions for PM components at the surface for the Northeast simulation ($\mu\text{g}/\text{m}^3$).

Boundary	North ⁽¹⁾	South	West
Site(s)	Quabbin (Q) or Lye Brook (LB) ⁽²⁾	Shenandoah	Dolly Sods
Sulfate ⁽³⁾	18 (Q)	16.93	16.37
Ammonium ⁽³⁾	6.8 (Q)	6.43	6.21
Nitrate ⁽³⁾	0.18 (LB)	0.26	0.24
Organic compounds ⁽³⁾	5 (Q)	7.47	3.33
Elemental carbon ⁽³⁾	0.7 (Q)	0.74	1.23
Unspecified PM _{2.5} ⁽³⁾	10.37	6.01	10.04
Unspecified coarse PM ⁽⁴⁾	6.58	1.03	0.53
Sea salt ⁽⁵⁾	1.74	0.80	0.57
Soil ⁽⁵⁾	5.61	8.52	4.17

- (1) The northern boundary conditions were also assigned to the eastern boundary.
- (2) The northern boundary conditions were defined by measurements at Quabbin (Q), measurements at Lye Brook Wilderness (LB), or an average of the two.
- (3) PM_{2.5} composition, assigned to the accumulation mode.
- (4) At IMPROVE sites, unspecified coarse PM is assumed to be 10% of the difference between PM₁₀ and PM_{2.5} (PM_{coarse}) (Jacobson, 1997). At NESCAUM sites, OC and EC in coarse PM are assigned to the unspecified coarse PM category.
- (5) At IMPROVE sites, sea salt and soil are assumed to make up 90% of all PM_{coarse} (PM_{coarse} = PM₁₀ – PM_{2.5}) (Jacobson, 1997); relative contribution of each is calculated from the ratio of sea salt to soil in PM_{2.5} measurements. At NESCAUM sites, dust is assigned to the soil category, inorganic species (sulfate, chloride, nitrate, ammonium) in PM_{coarse} are assigned to the sea salt category.

6.2 Modeling Results

6.2.1 Simulation time

The simulation time for the NARSTO/Northeast inner domain was about 1.2 CPU hour per hour modeled on a Sun Ultra 60 workstation. The episode from 12 July (00:00 local time) to 15 July 1995 (19:00 local time) was completed in 105.5 hours with the CMU/STI SOA module. Note that this simulation requires more CPU resources compared to the Nashville simulation because (1) the domain contains 78% more grid cells (Northeast: 99 x 135 x 13; Nashville: 100 x 65 x 15) and (2) simulating cloud processes adds about 15% CPU time to that required by the PM simulation.

6.2.2 Gas-phase concentrations

O₃ concentrations were high during the 12-15 July 1995 episode. Model performance statistics are summarized in Table 6-2 for one-hour average O₃ concentrations. The domain-wide maximum one-hour average O₃ concentration of 183 ppb was predicted at 3 p.m. near New York City, NY on 15 July 1995. (The observed domain-wide maximum O₃ concentration was 184 ppb on 15 July 1995 (<http://air31.air.dec.state.ny.us>) during this episode.) However, O₃ levels exceeding the one-hour average NAAQS of 120 ppb were observed on 13-14 July as well. Figure 6-1 shows the temporal profiles of surface O₃ concentrations at two IMPROVE sites, Edwin B. Forsythe National Wildlife Refuge, N.J. and Washington D.C. High O₃ resulted at least in part from the carryover from one day to the next, since O₃ concentrations remained high at night (e.g., surface O₃ concentrations at the Edwin Forsythe site). Spatial plots at the time of maximum O₃ concentrations on 14 and 15 July 1995 are presented in Figure 6-2. O₃ tended to be highest along the entire eastern seaboard stretching from Annapolis, MD to New Haven, CT. Regional buildup of O₃ was also observed on 14 July throughout Pennsylvania and parts of New Jersey. On 15 July, widespread exceedances of the NAAQS were observed in Maryland, Delaware, Pennsylvania, and New Jersey, and extending to New York City and Connecticut. Low

Table 6-2. Model performance statistics of one-hour average O₃ concentrations for the Models-3/CMAQ simulation of the Northeast domain, 13-15 July 1995 (source: Karamchandani et al., 2001)

Paired peak error ⁽¹⁾	-22%
Gross error	31%
Fractional gross error	0.31
Bias	7%
Fractional Bias	-0.01

(1) Paired in both space and time

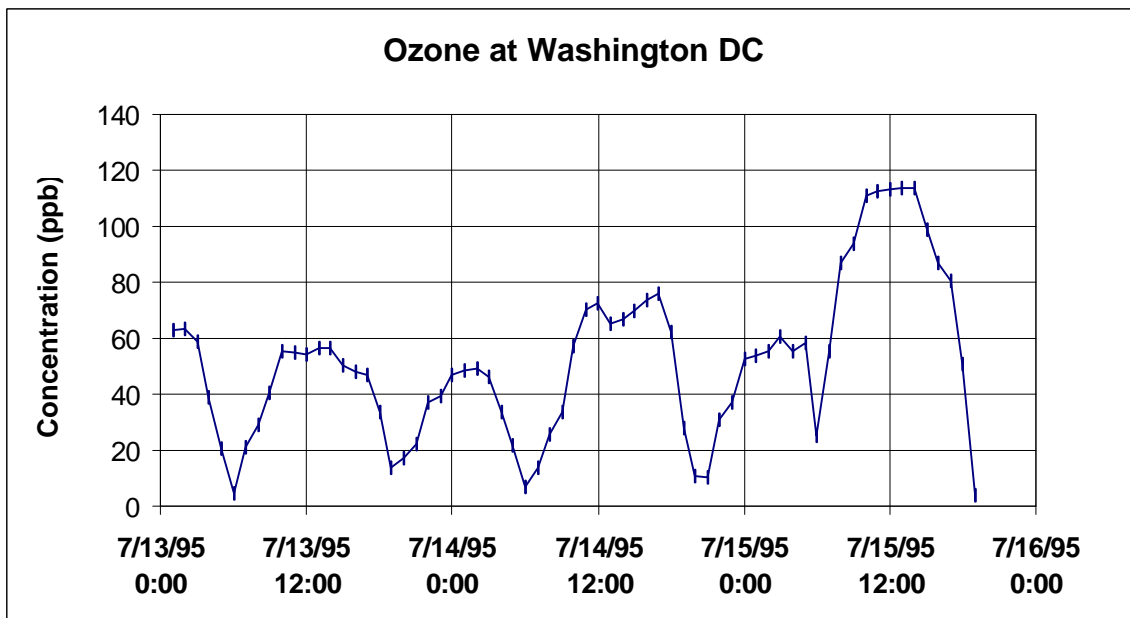
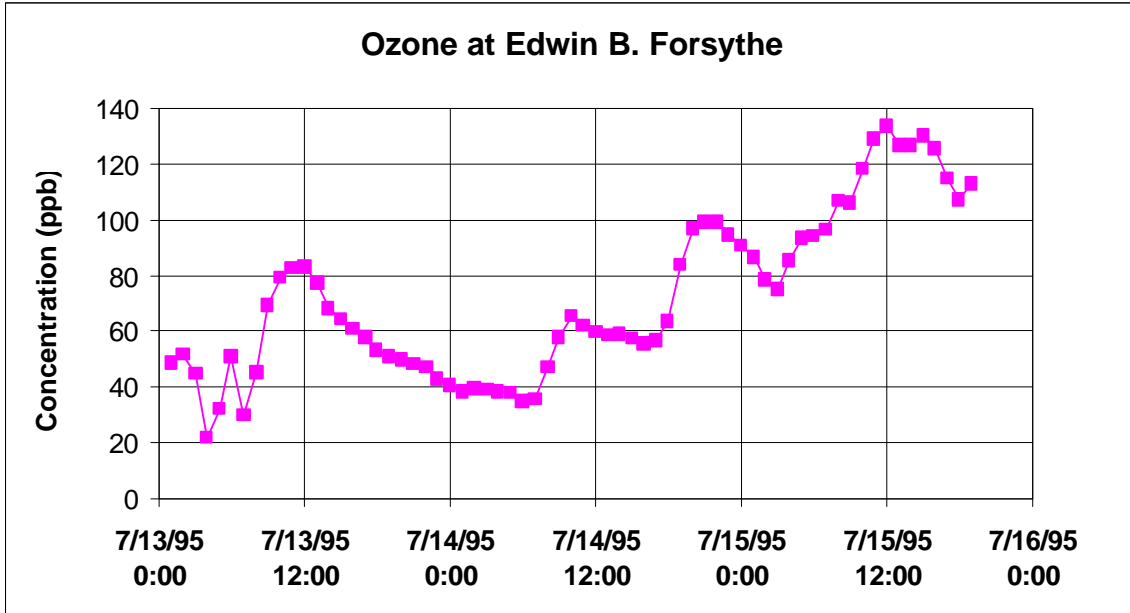


Figure 6-1. Temporal O₃ profiles at two IMPROVE sites from 13 July 1995 to 15 July 1995.

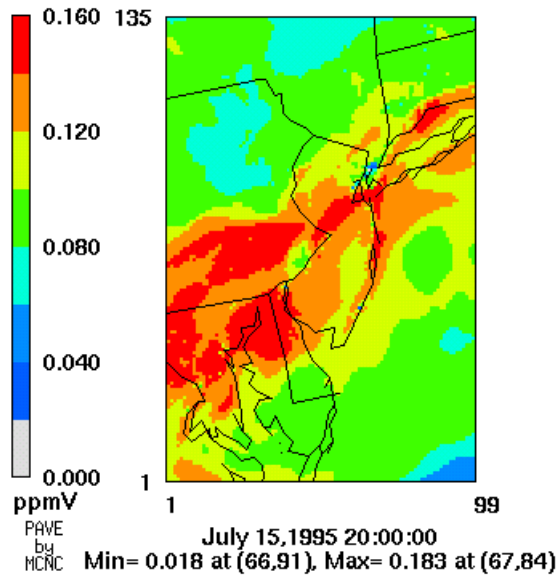
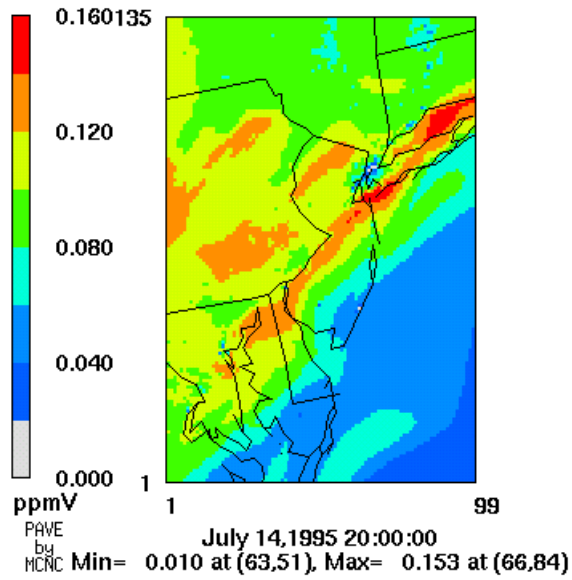


Figure 6-2. Spatial distribution of O₃ at 3 p.m. EST on 14 July 1995 and 15 July 1995.

O₃ concentrations occurred over the Atlantic ocean in the southeastern part of the domain.

Biogenic precursors of SOA (i.e., terpenes) were emitted most abundantly from forest-covered areas. Terpene emissions increase with temperature, therefore, emissions were highest during the day. However, simulated concentrations tended to be higher at night. Low day-time concentrations may be due to dilution and efficient chemical removal.

Figure 6-3 shows the temporal profiles of biogenic and anthropogenic condensable organic compounds predicted by the CMU/STI SOA module at the Edwin Forsythe and Washington, D.C. sites. The concentrations of gas-phase condensable compounds were generally quite small. While anthropogenic compounds were more abundant compared to biogenic compounds at these sites, their concentration only ranged from about 20 ppt in rural areas to about 30 to 40 ppt in Washington, D.C. The concentrations of the biogenic condensables are lower by a factor of 50 than the anthropogenic condensables in Washington, D.C., and by a factor of 20 at the Edwin Forsythe site. The distribution of anthropogenic and biogenic condensables seemed consistent with the VOC mixture of precursors at the two sites. The reason for the low concentrations of biogenic condensables in the gas phase is that the condensables have partitioned heavily into the particulate phase (see Section 3.3). Both biogenic and anthropogenic compounds display strong diurnal trends. Biogenic secondary compounds are abundant at night, when precursor concentrations were also high. High concentrations of anthropogenic compounds were predicted during the day, possibly driven by day-time emissions of anthropogenic VOC sources.

6.2.3 PM Results

Figure 6-4 shows the spatial distribution of the 24-hour average PM_{2.5} concentrations on 14 July and 15 July 1995. PM_{2.5} concentrations were typically regionally distributed. A notable exception was in the vicinity of New York City, where very high concentrations can be attributed to more abundant local area sources. There were also locations where local removal process (e.g., wet deposition) affected the

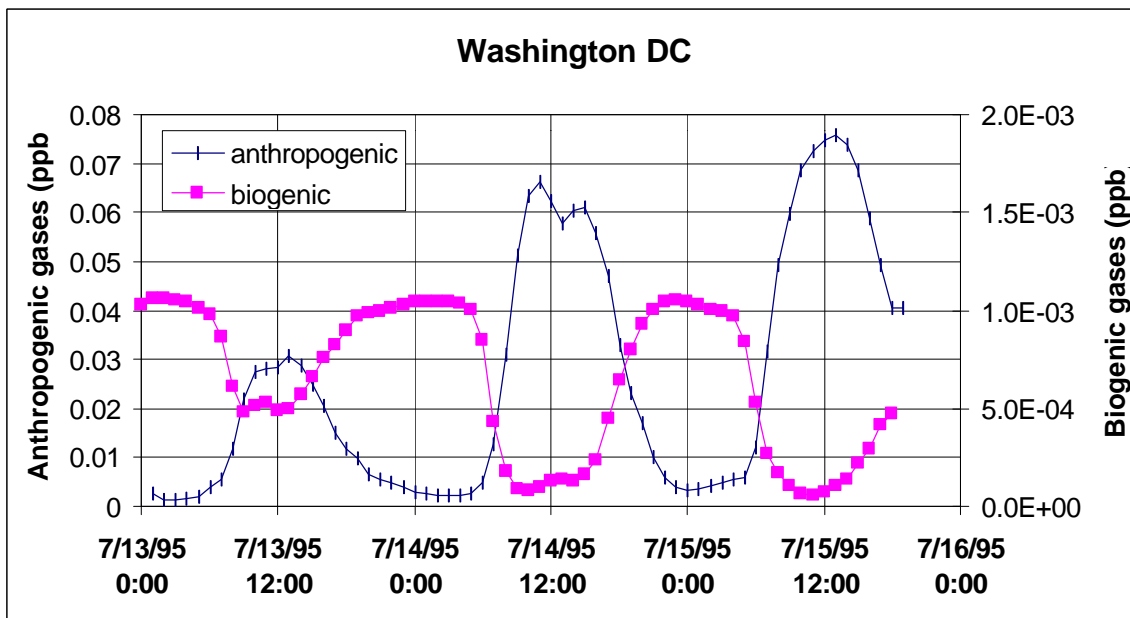
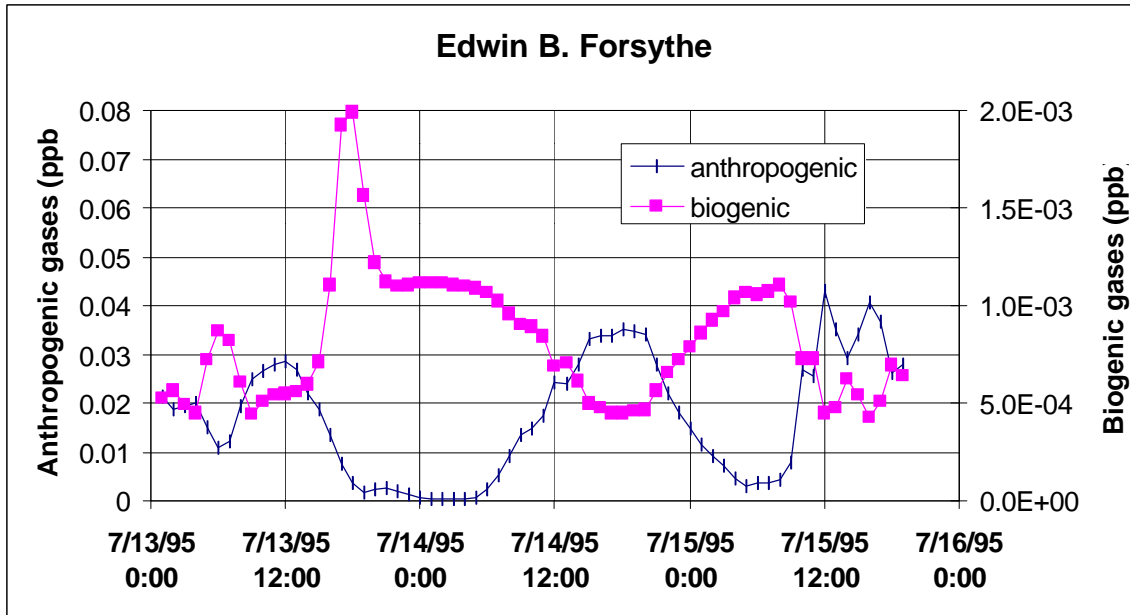


Figure 6-3. Temporal profiles of anthropogenic and biogenic condensable gases at two IMPROVE sites, 13-15 July 1995

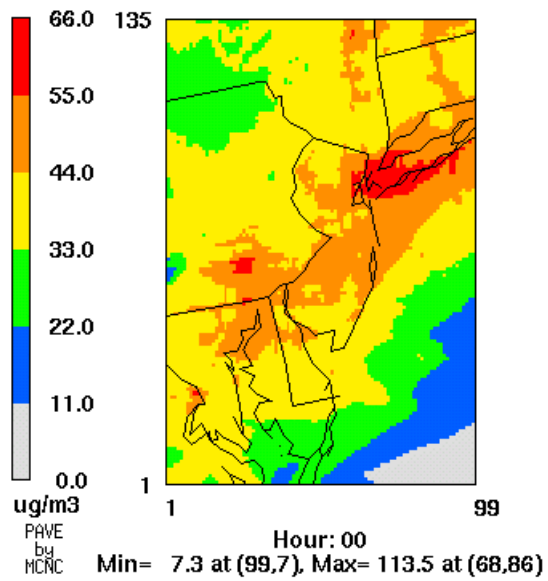
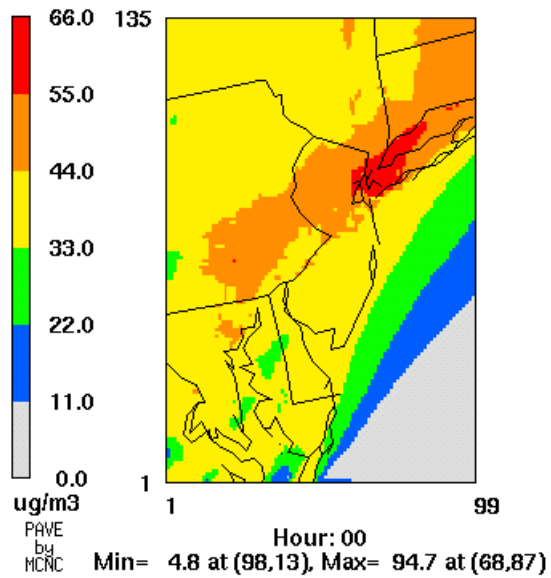


Figure 6-4. Spatial distribution of 24-hour average $PM_{2.5}$ on 14 July and 19-hour average $PM_{2.5}$ on 15 July 1995.

concentration of fine PM at least temporarily. Low concentrations of PM_{2.5} were predicted over the ocean, especially in the southeastern corner of the domain. Figures 6-5 and 6-6 show the temporal profiles of PM_{2.5} and various PM components. PM_{2.5} tended to accumulate at night, but showed no strong diurnal profile at the Edwin Forsythe National Wildlife Refuge and Washington, D.C. sites. In general, higher PM_{2.5} concentrations were predicted at Washington, D.C. than at Edwin Forsythe, which may be a result of PM emissions in urban areas. The temporal profiles of PM_{2.5} components (sulfate, EC, primary OC, and SOA) do not correlate well with each other at the Edwin Forsythe site (Figure 6-6).

The Washington, D.C. site and the Edwin B. Forsythe National Wildlife Refuge site are two IMPROVE monitoring stations located within the modeling domain that were operational on 15 July, the last day of the simulation. A comparison of 24-hour average PM_{2.5} and major PM_{2.5} components is presented in Table 6-3 (19-hour average for modeled values). For these two sites, PM_{2.5} concentrations were underpredicted by 20 to 30%. Sulfate, a key component of PM_{2.5}, was underpredicted by 9 to 30%. Ammonium predictions were closer, but were associated with non-negligible nitrate concentrations (1 to 4 $\mu\text{g m}^{-3}$) that were not typically observed on the East coast (see Tables 6-1 and 6-3). EC was underpredicted at the Washington, D.C. site but seemed reasonable at the Edwin Forsythe site. Particulate OC was underpredicted by a larger percentage than other PM_{2.5} components. Unspecified/other components were underpredicted by roughly the same proportion as PM₁₀ and PM_{2.5}. On a composition basis, sulfate, ammonium, and other PM_{2.5} components were predicted in proper proportions. EC was overpredicted at the Edwin Forsythe site, and underpredicted in Washington, D.C. Nitrate was overpredicted and OC was underpredicted at both sites.

Three factors contributed to a general underprediction of PM mass in this simulation. First, there were large uncertainties in the boundary conditions assumed for particulate matter, due to a paucity of data. The surface boundary conditions were interpolated from very limited data from the IMPROVE and NESCAUM networks. The vertical profiles applied to PM boundary and IC were also highly uncertain, since there were no experimental data of aloft PM for evaluation. The relatively long atmospheric residence time of fine particles implies that the boundary conditions have a strong effect

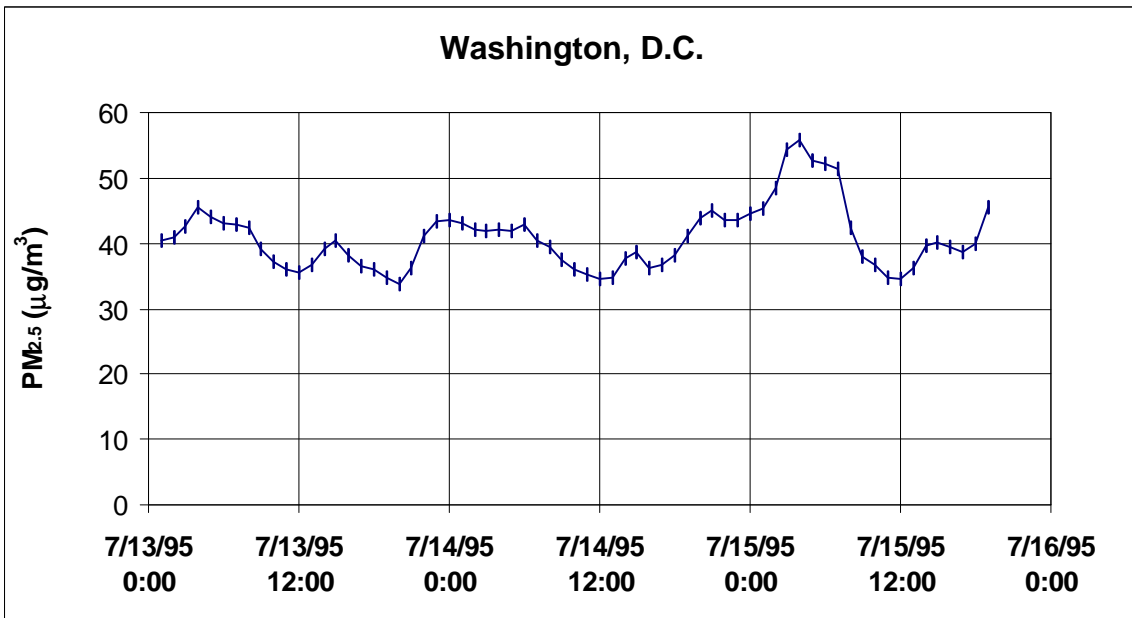
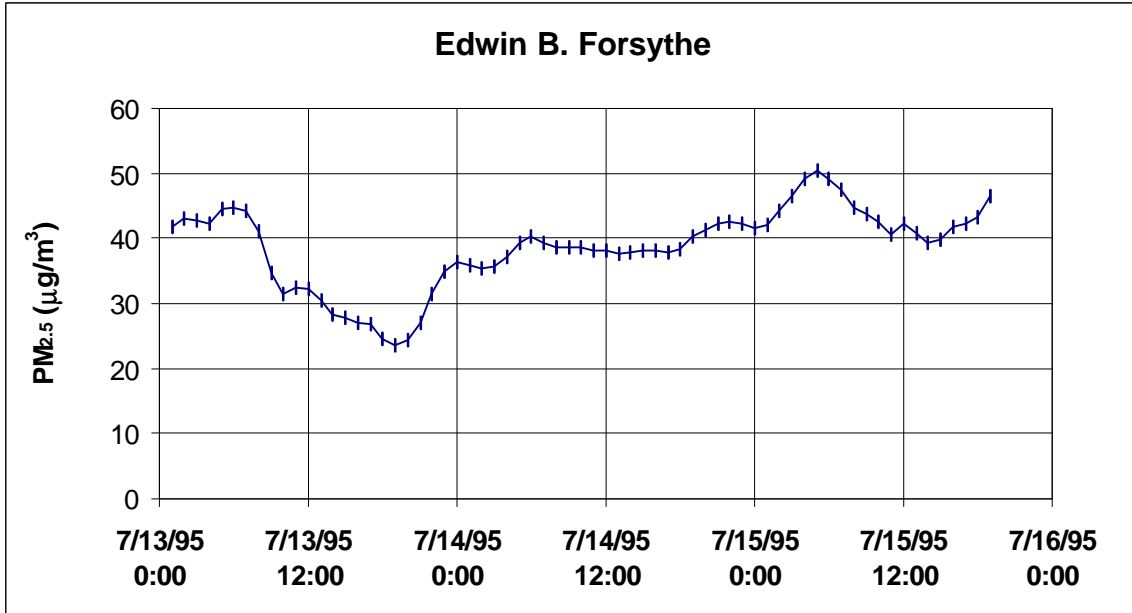


Figure 6-5. Temporal profiles of PM_{2.5} at two IMPROVE sites, 13 – 15 July 1995.

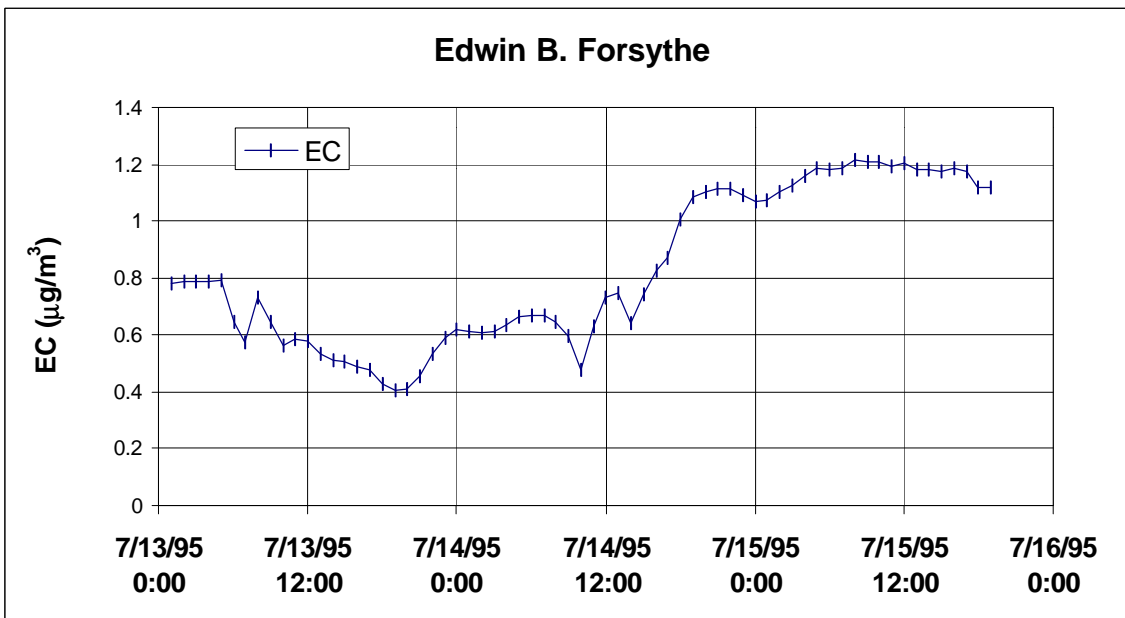
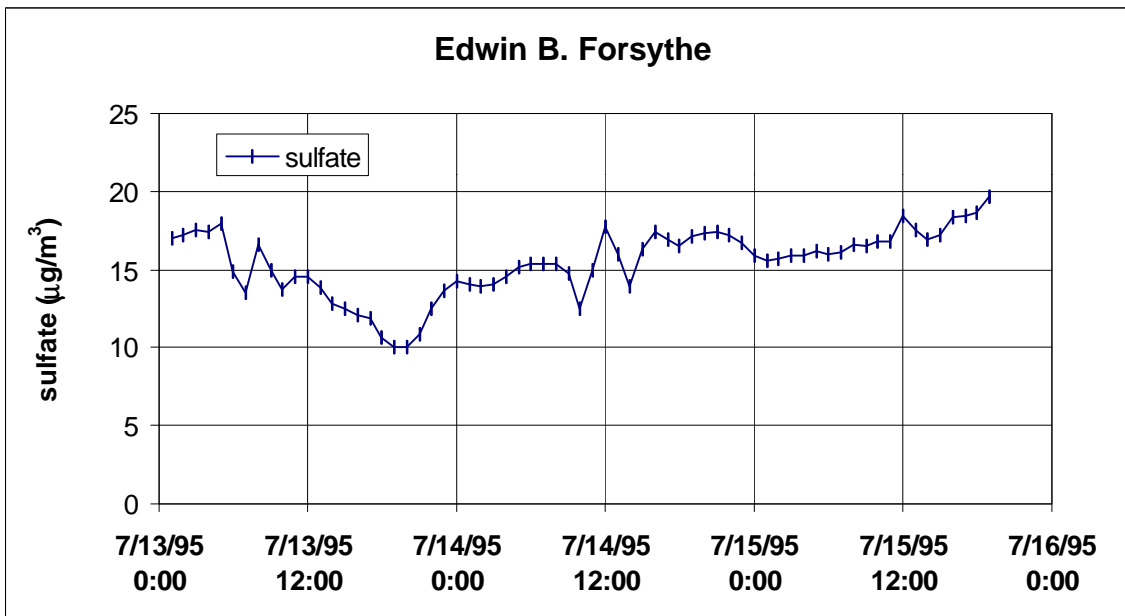


Figure 6-6. Temporal profiles of PM_{2.5} components at the Edwin B. Forsythe NWR site, 13 – 15 July 1995: (a) sulfate, (b) elemental carbon (EC), (c) primary organic carbon (POC), (d) SOA (CMU/STI module).

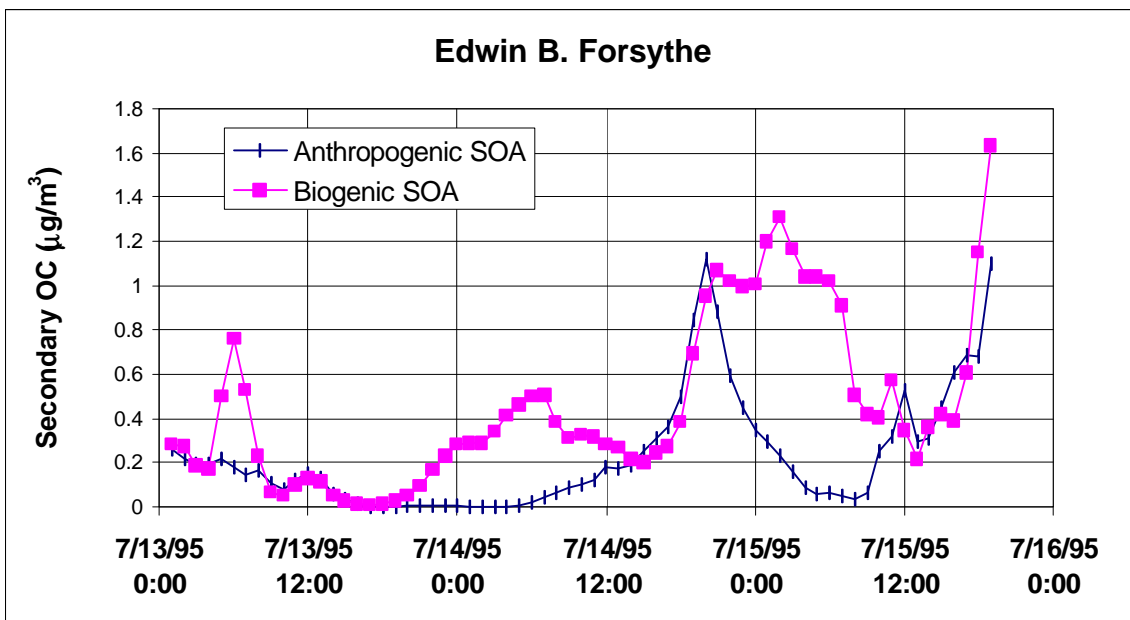
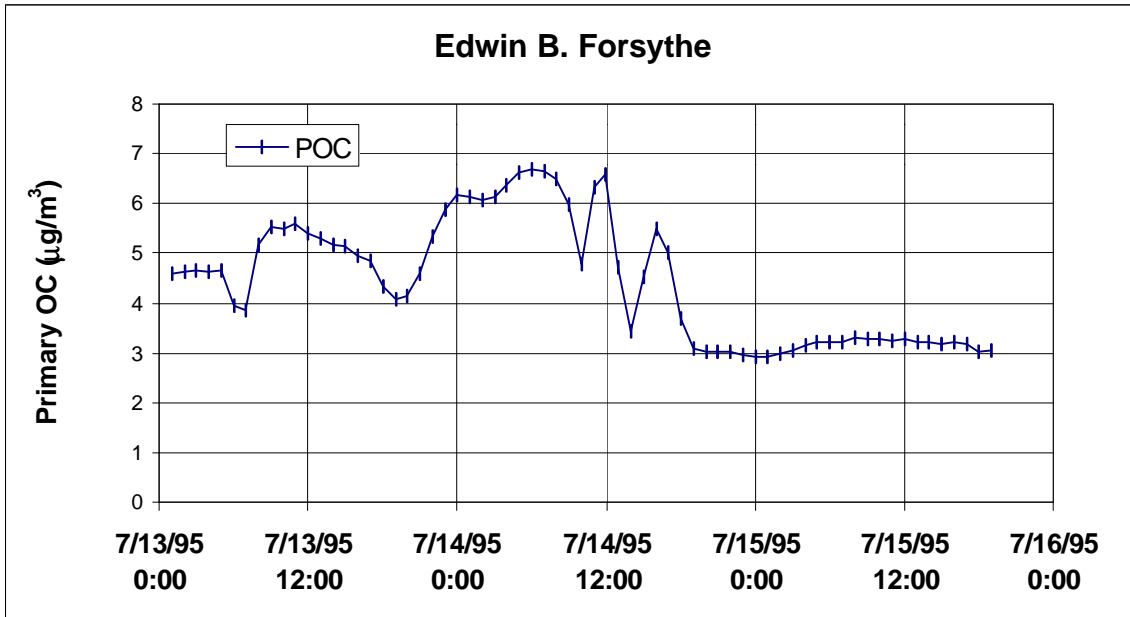


Figure 6-6. Temporal profiles of PM_{2.5} components at the Edwin B. Forsythe NWR site, 13 – 15 July 1995: (a) sulfate, (b) elemental carbon (EC), (c) primary organic carbon (POC), (d) SOA (CMU/STI module) (continued).

Table 6-3. Measured vs. predicted PM_{2.5} and PM_{2.5} components, 15 July 1995 (µg/m³).

	PM_{2.5}	Sulfate	Nitrate	Ammonium	EC	OC	Other PM_{2.5} components
Edwin Forsythe, N.J							
Observed	60.6	24.1	0.50	9.2	1.1	9.2	16.5
% of observed fine PM	--	40	1	15	2	15	27
Predicted	43.9	17.0	3.4	7.4	1.2	4.3	10.6
% of predicted fine PM	--	39	8	17	3	10	24
Washington D.C.							
Observed	54.6	18.1	0.48	6.9	1.9	13.0	14.3
% of observed fine PM	--	33	1	13	4	24	26
Predicted	44.7	16.9	3.7	7.3	1.1	4.2	11.5
% of predicted fine PM	--	38	8	16	3	9	26

on the fine particle concentrations within the modeling domain. If a regional build-up of PM occurred during the simulation period (and there were some indication of this from the IMPROVE data from July 12 and July 15, with PM on July 15 about 50% to 75% higher than on July 12), greater upwind concentrations of fine particles, at the surface and aloft, would increase predicted PM concentrations. Second, an underestimation of PM emissions within the domain could explain some of the underpredictions of PM_{2.5}, EC, OC, and the unspecified/other component. Third, deposition of particles was a very significant removal process over the ocean and the northwestern corner of the domain on the last simulation day. For several hours, the deposition fluxes (for sulfate) were of the order of 0.01 kg/hectare/hr, which could deplete 20 µg m⁻³ PM sulfate in 2 hours if the surface layer was 100 m thick. These deposition fluxes cannot be evaluated because of the lack of pertinent data.

The effect of clouds on PM was small overall. However, for soluble species like sulfate, significant concentration fluctuations were observed with the passage of clouds and rain. Increased sulfate production was associated with non-raining clouds. At specific locations, more than 30 µg m⁻³ sulfate could be attributed to aqueous-phase oxidation of sulfate in clouds. However, events of rain were associated with significant removal of soluble PM species. These effects were generally localized and short-lived, and contributed only to a 0.33 µg m⁻³ net decrease in sulfate on the last day of the simulation, averaged over the entire domain. Note that an underprediction of sulfate increases the partition of nitrate into the particle phase. The cause of nitrate overprediction may also be related to the dynamics of gas-phase production of nitric acid, as nitrate seemed also to be associated with urban plumes that are rich in nitrogen oxides (Figure 6-7). At present, these processes cannot be evaluated independently due to the lack of simultaneous measurements of PM and condensable gases.

In addition to uncertainties in the boundary conditions and PM emissions, other factors may also contribute to the discrepancy between the predicted and observed concentrations of EC and OC. First, a default speciation factor was applied within Models-3 to allocate EC and OC emissions from input PM_{2.5} emissions. These factors, 1% of PM_{2.5} for EC and 2% of PM_{2.5} for OC, may not be applicable everywhere in the domain. Second, the measurements of EC and OC may suffer from artifacts. Third, since

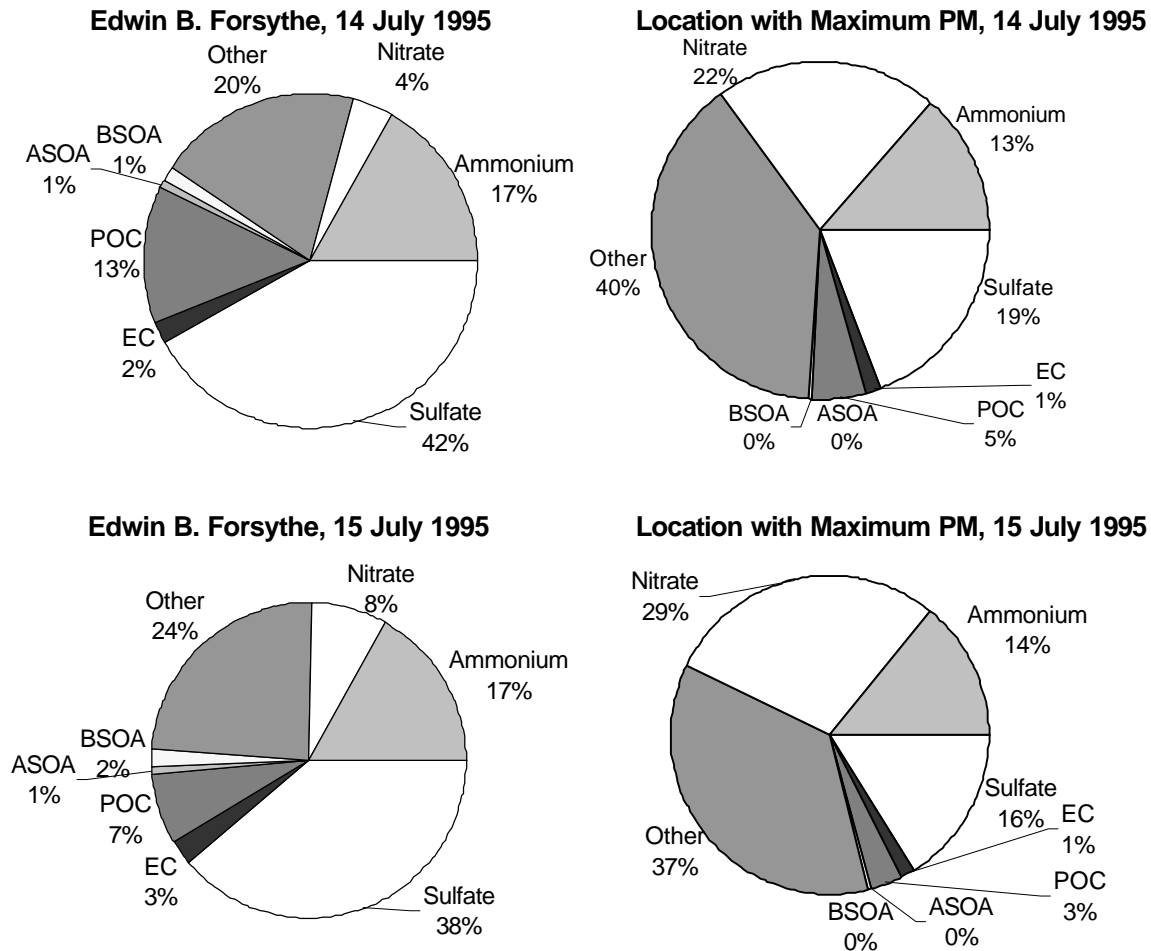


Figure 6-7. Average predicted composition of PM_{2.5} components at the Edwin B. Forsythe site and the location of maximum simulated PM_{2.5} (near New York City) on 14 July 1995 (24-hour average) and 15 July 1995 (19-hour average). POC is primary organic carbon, EC is elemental carbon, ASOA is anthropogenic SOA and BSOA is biogenic SOA predicted by the CMU/STI module.

SOA is a component of OC, uncertainties in the predictions of SOA (e.g., in the Nashville simulation, three distinct SOA modules gave quite different results) add to uncertainties in predicted OC. SOA tend to account for a small fraction of PM_{2.5}, about 3% at the Edwin B. Forsythe National Wildlife Refuge site, and negligible in areas of high PM concentrations driven by high emissions, such as New York City. On a domainwide basis including locations over water, biogenic SOA averaged a little more than 0.3 $\mu\text{g m}^{-3}$ on each of the last two days of the simulation, while anthropogenic SOA account for about 0.3 $\mu\text{g m}^{-3}$. The maximum one-hour average concentration of anthropogenic SOA was 12 $\mu\text{g m}^{-3}$ observed in New Haven, CT, downwind of New York City. The yield of SOA may be limited by the emission of SOA precursors and formation of condensable compounds. The emission density of terpenes and the average concentrations of biogenic SOA in the land-locked part of the domain were similar to the earlier Nashville simulation. However, there were areas in New Jersey and Maryland with high terpene emissions where SOA concentrations as high as 2 $\mu\text{g m}^{-3}$ were observed. There are large uncertainties associated with biogenic VOC emissions inventories, as shown in Section 5. These uncertainties may translate into uncertain biogenic SOA predictions.

In the Northeast, the average concentrations of condensable organic gases were less than 1 ppt ($\sim 5 \text{ ng m}^{-3}$) for biogenic condensables and 0.017 ppb ($\sim 0.1 \mu\text{g m}^{-3}$) for anthropogenic condensables over the entire domain. Therefore, much of the condensable compounds formed in the gas phase partitioned into the particle phase, with biogenic compounds being the less volatile of the two classes, which explains why biogenic SOA were predicted in slightly greater concentrations than anthropogenic SOA.

7. CONTRIBUTION OF BIOGENIC EMISSIONS TO O₃ AND PM_{2.5} IN THE NORTHEAST DOMAIN

7.1 Description of the Sensitivity Studies

The approach used to design sensitivity case studies to address the influence of biogenic species on O₃ and PM_{2.5} was explained in Section 4.1. The same approach was used for the Northeast domain. Biogenic and anthropogenic influences on the BC are presented in Table 7-1 for this domain. Anthropogenic sources accounted for almost all NO_x emissions in this domain. For VOC, biogenic compounds accounted for over 50% of PAR emissions, but for smaller percentages of ALD2 and OLE. The contributions of biogenic emissions to PAR, ALD2 and, OLE are noticeably smaller in the Northeast domain than in the Nashville domain (Table 4-1). The O₃ BC for the sensitivity cases were determined from the relative influence of biogenic and anthropogenic emissions (see Figure 4-1). In this domain, O₃ concentrations were quite high at the boundaries. Anthropogenic influence dominated over biogenic influence, although the predicted relative contribution of anthropogenic emissions to O₃ is smaller than that in the Nashville domain (81% vs. 94%). As a result, BC of sensitivity simulation B that represents only natural and biogenic conditions were high compared to the corresponding BC of the Nashville simulation. For example, the O₃ western BC approached 20 ppb on the last day of the simulation. Such a value, however, is not unrealistic for an O₃ episode since Wang and Jacob (1998) simulated average O₃ concentrations up to 15 ppb with a global model.

7.2 Results

7.2.1 O₃

Table 7-2 compares the key domain-wide O₃ results in the Northeast simulations. Simulated O₃ generally decreased in the Northeast as a result of reduced emissions and influx from the boundaries. The removal of biogenic emissions with no change in BC

Table 7-1. Boundary conditions used in the sensitivity simulations for the Northeast domain.

Compound	Boundary condition in sensitivity simulation A	Boundary condition in sensitivity simulation B	Notes
O ₃	0.81 x O ₃ _{base,BC}	0.19 x O ₃ _{base,BC}	$O_3 _{sensA,BC} = O_3 _{base,BC} \times \frac{O_3^a}{O_3^a + O_3^b}$ $O_3 _{sensB,BC} = O_3 _{base,BC} - O_3 _{sensA,BC}$ <p>O₃^a = O₃ due to anthropogenic emissions (see Figure 4-1) O₃^b = O₃ due to biogenic emissions (see Figure 4-1)</p>
PAR ALD2 OLE ETH FORM TOL XYL ISOP TERP	0.68 x PAR _{base,BC} 0.30 x ALD2 _{base,BC} 0.45 x OLE _{base,BC} ETH _{base,BC} FORM _{base,BC} TOL _{base,BC} XYL _{base,BC} 0.0 0.0	0.32 x PAR _{base,BC} 0.70 x ALD2 _{base,BC} 0.55 x OLE _{base,BC} 0.0 0.0 0.0 0.0 ISOP _{base,BC} TERP _{base,BC}	$VOC _{sensA,BC} = VOC _{base,BC} \times \frac{VOC_{emis}^a}{VOC_{emis}^a + VOC_{emis}^b}$ $VOC _{sensB,BC} = VOC _{base,BC} - VOC _{sensA,BC}$ <p>VOC^a_{emis} = total anthropogenic VOC emissions VOC^b_{emis} = total biogenic VOC emissions</p>
NO _x	0.97 x NO _x _{base,BC}	0.03 x NO _x _{base,BC}	$NO_x _{sensA,BC} = NO_x _{base,BC} \times \frac{NO_{xemis}^a}{NO_{xemis}^a + NO_{xemis}^b}$ $NO_x _{sensB,BC} = NO_x _{base,BC} - NO_x _{sensA,BC}$ <p>NO_x^a_{emis} = total anthropogenic NO_x emissions NO_x^b_{emis} = total biogenic NO_x emissions</p>

Table 7-1. Boundary conditions used in the sensitivity simulations for the Northeast domain (continued).

Compound	Boundary condition in sensitivity simulation A	Boundary condition in sensitivity simulation B	Notes
CO	$CO _{base,BC} - 40 \text{ ppb}$	40 ppb	CO concentration at remote locations, 40 ppb (Seinfeld and Pandis, 1998), assumed to be the natural background.
NH ₃	$NH_3 _{base,BC} - 0.3 \text{ ppb}$	0.3 ppb	Background NH ₃ measurement in MA, average of summer measurements at two sites (NAPAP, 1991).
SO ₂	$SO_2 _{base,BC} - 0.2 \text{ ppb}$	0.2 ppb	Globally averaged SO ₂ concentration of 0.167 ppb (Wayne, 1991) assumed to be the natural background.
PM sulfate	$sulfate _{base,BC} - 1 \mu\text{g m}^{-3}$	$1 \mu\text{g m}^{-3}$	Sulfate concentration at remote locations, $1 \mu\text{g m}^{-3}$ (Seinfeld and Pandis, 1998), assumed to be the natural background.
PM nitrate	$0.97 \times \text{nitrate} _{base,BC}$	$0.03 \times \text{nitrate} _{base,BC}$	Same treatment as NO _x BC.
PM ammonium	$0.85 \times \text{ammonium} _{base,BC}$	$0.15 \times \text{ammonium} _{base,BC}$	$NH_4^+ _{sensA,BC} = NH_4^+ _{base,BC} \times \frac{NH_3 _{base,BC} - 0.3 \text{ ppb}}{NH_3 _{base,BC}}$ $NH_4^+ _{sensB,BC} = NH_4^+ _{base,BC} - NH_4^+ _{sensA,BC}$
PM EC	$EC _{base,BC} - 0.01 \mu\text{g m}^{-3}$	$0.01 \mu\text{g m}^{-3}$	EC concentration at remote locations, $0.01 \mu\text{g m}^{-3}$ (Seinfeld and Pandis, 1998), assumed to be the natural background.
PM OC	$OC _{base,BC} - 0.5 \mu\text{g m}^{-3}$	$0.5 \mu\text{g m}^{-3}$	OC concentration at remote locations, $0.5 \mu\text{g m}^{-3}$ (Seinfeld and Pandis, 1998), assumed to be the natural background.
Other PM	$\text{Other PM} _{base,BC} - 3 \mu\text{g m}^{-3}$	$3 \mu\text{g m}^{-3}$	Other PM at remote locations, $3 \mu\text{g m}^{-3}$ (Seinfeld and Pandis, 1998), assumed to be the natural background.

Table 7-2. O₃ results for Northeast simulations.

	Base case	Low limit sensitivity case ^(a)	Best estimate sensitivity case A ^(b)	Best estimate sensitivity case B ^(c)
Episode 1-hour average maximum (on 15 July 1995)	183 ppb	169 ppb	153 ppb	34 ppb
Location of episode maximum ^(d)	67,84	81,104	81,104	36,67
Average surface O ₃ between noon and 7 p.m. on 15 July 1995	102.3 ppb	100.1 ppb	86.4 ppb	19.5 ppb
Average surface O ₃ between midnight and 7 a.m. on 15 July 1995	85.8 ppb	86.1 ppb	70.2 ppb	17.0 ppb
Average surface O ₃ between 13 July and 16 July 1995 (7 p.m. local)	74.8 ppb	73.4 ppb	62.5 ppb	17.4 ppb

(a) Anthropogenic emissions (no biogenic emission), base case BC

(b) Anthropogenic emissions, “anthropogenic” BC

(c) Biogenic emissions, natural BC

(d) x, y where x is the grid cell number in the west-east direction and y is the grid cell number in the south-north direction from the south-east corner of the modeling domain.

(i.e., lower limit sensitivity case) caused a 1.4 ppb decrease in domain-wide O₃ concentrations and a 14 ppb decrease in the domain peak O₃. This case represented the lower limit of biogenic contributions to O₃. A 30 ppb decrease in the domain-wide maximum one-hour average O₃ concentration was simulated in best estimate sensitivity case A (i.e., with modified “anthropogenic” BC), which predicted significant exceedances of the NAAQS within the domain. Note that the location of the maximum shifted towards the Northeast with the removal of biogenic emissions. In best estimate sensitivity case A, the largest decrease at an individual location was 66 ppb (cell 62, 82, in New Jersey, near New York City). The mean decrease was 12.3 ppb throughout the domain, 16% of the base case domain average O₃ concentration on 13 – 15 July. Although best estimate sensitivity case A showed a smaller decrease in the spatially averaged O₃ concentration (12.3 ppb) than in the domain peak concentration (30 ppb) from the base case, the percentage change was consistently 16% in both domain-wide metrics. The spatial average O₃ concentrations over two eight-hour periods are listed in Table 7-2. In an afternoon and an evening period, the average O₃ decreased by 15.9 and 15.6 ppb, respectively. Although O₃ decreased from the base case to sensitivity case A during both time periods, nighttime increases in O₃ were simulated in the lower limit sensitivity case where emissions were reduced but boundary conditions were unchanged. Daytime O₃ decreased in both cases. One possible explanation is that nighttime infusion of O₃ at the boundary is significant in this domain. The removal of O₃ at night by reactive biogenic alkene emissions or anthropogenic NO_x emissions may be a key chemical process contributing to the overall predicted O₃ concentrations.

Whereas removing biogenic emissions and their influences on the BC caused small differences in the domain-averaged O₃ concentrations, sensitivity case B with only biogenic emissions and natural BC showed higher biogenic contribution to O₃ with a domain-averaged concentration of 17 ppb averaged over the three-day period between 13 and 15 July 1995. This average concentration is slightly higher than the pre-industrial O₃ levels simulated by Wang and Jacob (1998). Higher levels of O₃ may be attributable to the extreme meteorological conditions associated with the O₃ episode, as evident in the relatively high levels of O₃ present in the BC. (The episode average O₃ BC for sensitivity case B was 11 ppb in the Northeast, as opposed to 2.4 ppb in the Nashville biogenic

simulation.) The peak O₃ concentration of 34 ppb was simulated on 15 July over the southern part of Pennsylvania. (A longer “spin up period was needed for this sensitivity simulation because the effect of the relatively high initial condition persisted into the morning hours of the second day). As shown in Table 7-2, biogenic contributions to O₃ was higher during the day (20 ppb) than at night (17 ppb). The lower concentrations at night are consistent with O₃ scavenging by terpenes.

Figure 7-1 illustrates the temporal profiles of O₃ at Edwin B. Forsythe and Washington, D.C. in the base and best estimate sensitivity cases. The concentrations of O₃ in sensitivity case A were always lower than in the base case, with a maximum difference of 28 ppb in Washington, D.C. attributed to the contribution of biogenics. The maximum one-hour simulated O₃ was below the NAAQS in the base case (114 ppb) in Washington, D.C. It decreased to 89 ppb, which is a 22% decrease. The maximum 8-hour average O₃ decreased from 105 ppb (exceeding the proposed NAAQS of 80 ppb) to 81 ppb (23%). The response of O₃ to reduced emissions and boundary influx was very similar between Washington, D.C. and Edwin B. Forsythe, despite their different land use/land cover characteristics. At the latter site, O₃ was also lower in concentration at all hours in the sensitivity case than in the base case except early on 13 July 1995. The maximum difference in O₃ between the base and sensitivity cases at this site is 33 ppb. At Edwin B. Forsythe, the maximum one-hour average O₃ concentration decreased by 21% from 134 ppb to 106 ppb. The maximum 8-hour average simulated O₃ concentration was 100 ppb in the sensitivity case, a 20% decrease from the base case value of 126 ppb.

With natural BC and biogenic emissions only, O₃ concentrations in sensitivity case B showed less pronounced diurnal fluctuations. The maximum one-hour O₃ concentrations reached only 24 ppb in Washington, D.C. At Edwin B. Forsythe, the highest concentration was observed early in the morning of 13 July, presumably due to undue influence of the boundary conditions. On July 15, the maximum one-hour O₃ concentration was predicted to be 25 ppb. The maximum 8-hour average O₃ at these sites were 21 ppb and 24 ppb (neglecting high concentrations during the morning hours of 13 July) in sensitivity case B. These concentrations represent very similar biogenic contributions as those deduced from the concentration deviations of sensitivity case A.

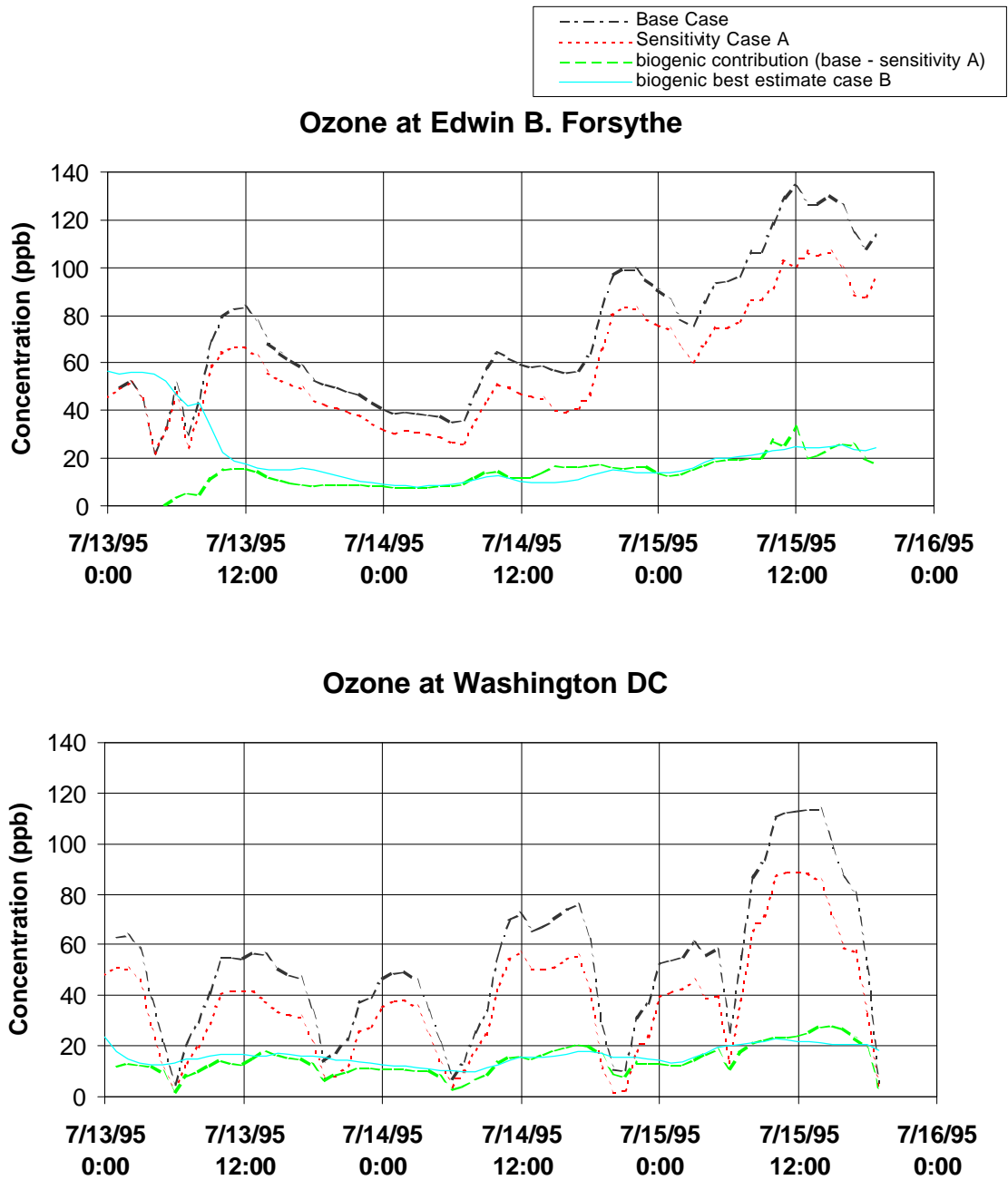


Figure 7-1. O₃ temporal profiles at Edwin B. Forsythe and Washington, D.C. in the base and best estimate sensitivity cases.

We contrast the findings in the Northeast domain, where biogenic contributions estimated from two sensitivity cases were similar, to those in Nashville, where removing biogenic emissions from the base case have a more significant effect on O₃ production than the contribution obtained in a biogenic-only environment. The difference in these two cases may be an indication that the Northeast is the less NO_x sensitive of the two domains.

The results of sensitivity cases indicate that on a domain-wide basis, biogenic contributions to average O₃ concentrations ranged from 12 to 17 ppb (16 – 23% of the base case concentration). Exceedances of the one-hour and 8-hour O₃ NAAQS were probably caused by anthropogenic emissions in the Northeast and/or transported O₃ and precursors of anthropogenic origins. Biogenic emissions within the domain and its influence on O₃ and precursors at the boundary further deteriorated the air quality during the simulated episode.

7.2.2 PM

With the elimination of biogenic emissions and biogenic influences from the boundary conditions, no SOA of biogenic origins were predicted in sensitivity simulation A. This amounted to a removal of 0.3 μg m⁻³ SOA, averaged over the entire domain from 13 to 15 July 1995. On individual days, the 24-hour average (17-hour average on 15 July 1995) concentrations of biogenic SOA were 0.25 μg m⁻³, 0.35 μg m⁻³, and 0.32 μg m⁻³ averaged over the entire domain.

The decrease in biogenic SOA was partially offset by an increase of SOA from anthropogenic precursors. The domainwide anthropogenic SOA increased from 0.27 μg m⁻³ in the base case to 0.29 μg m⁻³ in best estimate sensitivity case A. The difference in the formation of anthropogenic SOA was spatially non-uniform. In the area centered around New York City and Long Island, less anthropogenic SOA were produced in the sensitivity case. However, in areas farther removed from metropolitan New York but affected by the city plume, more anthropogenic SOA were formed in sensitivity case A compared to the base case.

No SOA entered the domain through the boundary; therefore, changes in the SOA from anthropogenic VOC precursors must have resulted from changes in the oxidant

chemistry. The domainwide increase predicted for anthropogenic SOA was possibly related to an overall increase in some oxidant levels. OH concentrations generally increased in sensitivity case A. Locations where the production of anthropogenic SOA was curbed coincided with locations with less daytime OH along the corridor linking the major cities in the Northeast.

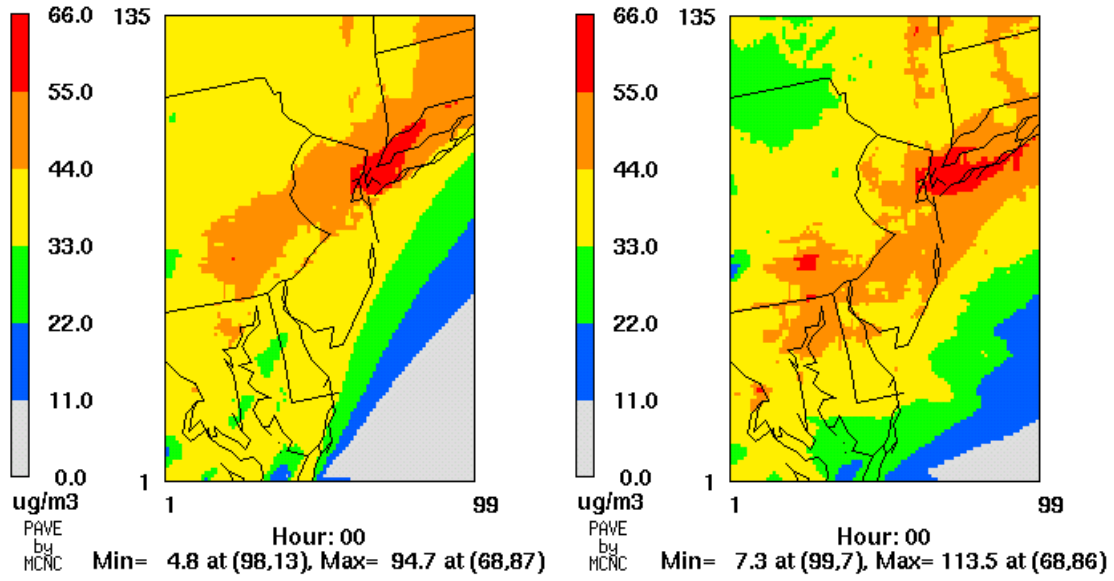
Formation of biogenic SOA in sensitivity case B is reduced from the base case of $0.3 \mu\text{g m}^{-3}$ to $0.05 \mu\text{g m}^{-3}$, due mostly to reduced oxidant concentrations in this simulation. Higher SOA concentrations tended to occur in the southeastern part of the domain and over New Jersey, although high biogenic SOA were also simulated at other locations over land.

Overall, sensitivity case A shows a $\text{PM}_{2.5}$ decrease of about $4 \mu\text{g m}^{-3}$ from the base case, which is larger than can be accounted for by the net change in SOA. The reasons behind the simulated $\text{PM}_{2.5}$ reductions were reductions in both primary and other key secondary $\text{PM}_{2.5}$ components. Primary components, such as EC, primary OC, and other $\text{PM}_{2.5}$ species, decreased due to reductions in the BC. The total reduction of primary these $\text{PM}_{2.5}$ components averaged $2.3 \mu\text{g m}^{-3}$ over the three-day period between 13 and 15 July 1995. On a domainwide basis, fine particulate sulfate decreased by $0.48 \mu\text{g m}^{-3}$ and nitrate by $0.53 \mu\text{g m}^{-3}$ over the last three days. These decreases resulted from a combination of reduced influx from the boundaries and changes in chemical production within the domain; the latter led to both increases or decreases in concentrations depending on the location. Because oxidants generally increased in non-urban areas, the simulated decreases in sulfate and nitrate over much of the domain were probably attributable to reduced transport from the BC.

On the other hand, an average $\text{PM}_{2.5}$ concentration of $1.8 \mu\text{g m}^{-3}$ was predicted in sensitivity case B. Because the PM inventory represented only anthropogenic sources within the Northeast domain, natural BC alone contributed to the components of PM that were not chemically produced. Chemical production of PM was quite limited as well, due to reduced emissions of precursors.

Spatial distributions of the 24-hour average $\text{PM}_{2.5}$ concentrations on 14 and 15 July are shown in Figure 7-2 for the base case and the sensitivity cases. The effects of decreased boundary influx of $\text{PM}_{2.5}$ in sensitivity case A can be inferred from the general

(a) Base case



(b) Sensitivity case A

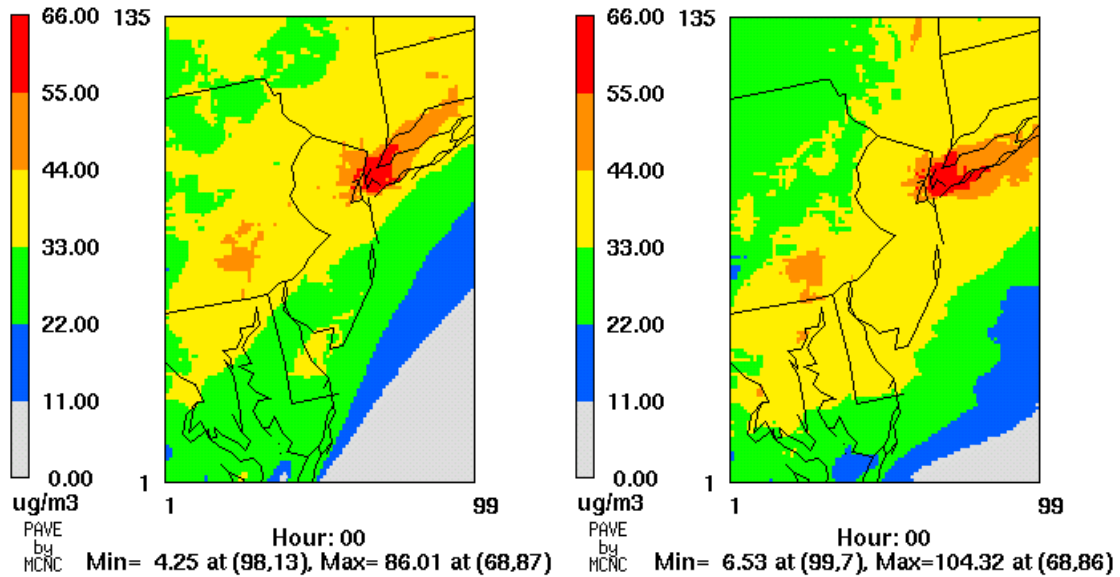


Figure 7-2. Spatial distribution of 24-hour average $PM_{2.5}$ on 14 (left) and 15 (right) July 1995 in the base (top), best estimate sensitivity case A (middle), and best estimate sensitivity case B (bottom).

(c) Sensitivity case B

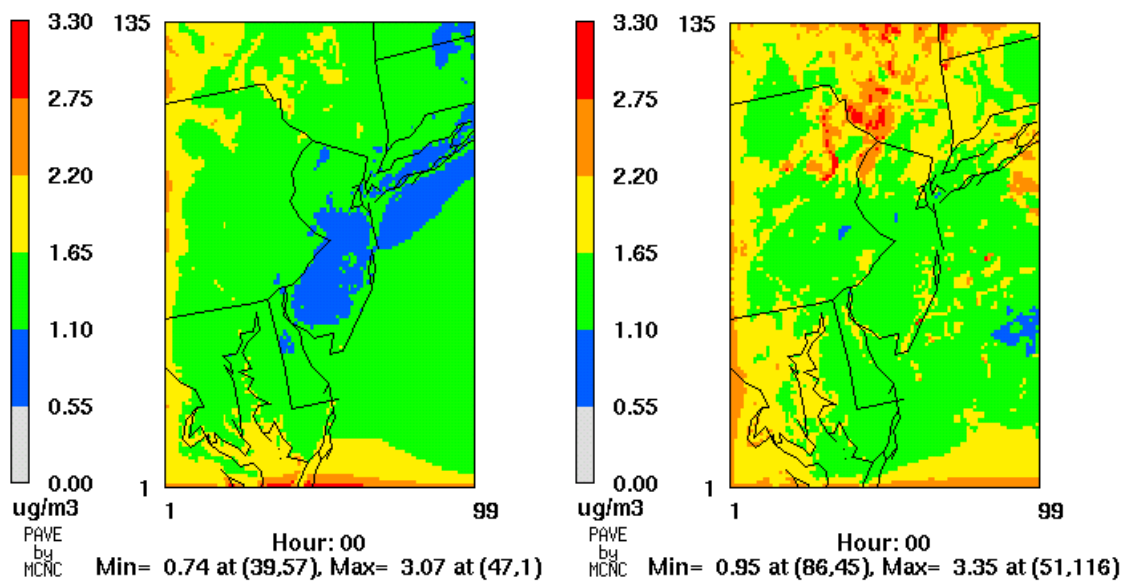


Figure 7-2. Spatial distribution of 24-hour average PM_{2.5} on 14 (left) and 15 (right) July 1995 in the base (top), best estimate sensitivity case A (middle), and best estimate sensitivity case B (bottom) (continued).

decrease of PM concentrations in the non-urban areas. For example, over the water in the southeast corner of the domain, where there are no significant sources, the reduction of the domain minimum 24-hour average PM_{2.5} concentrations from 4.7 µg m⁻³ to 4.2 µg m⁻³ can be attributed entirely to changes in the boundary conditions. Over land, the spatial distributions of PM_{2.5} were quite similar in the base case and sensitivity simulation A. The spatial distribution of PM_{2.5} in sensitivity case B shows the influence of the BC in a simulation with no direct PM emissions. Some higher PM concentrations were predicted over land in the northern part of the domain presumably due to the production of secondary PM.

In Washington, D.C, the average concentrations of PM_{2.5} on 14 July and 15 July were reduced by 4.7 µg m⁻³ and 5.8 µg m⁻³, respectively, in sensitivity case A compared to the base case. At Edwin B. Forsythe, the PM_{2.5} reduction ranged from 5.2 µg m⁻³ to 6.2 µg m⁻³. The contribution of biogenic and natural PM estimated in sensitivity case B was smaller at both locations. At Edwin B. Forsythe, the episode average PM concentration was only 2.4 µg m⁻³ and the concentration at Washington, D.C. was 1.9 µg m⁻³. Sensitivity case A provided the relatively higher estimate of biogenic and natural contribution to PM. The respective relative changes were 14% and 12%-13% at Edwin B. Forsythe and Washington, D.C. in this case. Since these locations did not violate the 24-hour NAAQS for PM_{2.5}, biogenic and natural PM did not affect the predicted attainment of the PM_{2.5} standard.

Table 7-3 shows the concentration changes of PM_{2.5} and individual components in Washington, D.C. on July 14 and July 15 (19 hour average). On both days, a 14% decrease in PM_{2.5} concentrations was predicted when biogenic emissions and their influence at the boundary were eliminated (sensitivity case A). All major components decreased in concentrations. Primary PM, such as EC, primary OC, and other PM_{2.5}, decreased due to reduced influx at the boundary. The secondary inorganic components of sulfate, nitrate, and ammonium decreased due to retarded secondary production and the reduction in BC. In contrast, a slight increase in the formation of anthropogenic SOA was predicted on July 14, while a 1% decrease was simulated on July 15. The response in anthropogenic SOA was due to changes in the oxidant chemistry, because SOA was not transported into the domain from the boundary.

Table 7-3. PM_{2.5} on 14 July and 15 July in the base and best estimate sensitivity cases in Washington, D.C.

	July 14			July 15		
	Base case ($\mu\text{g m}^{-3}$)	Best estimate sensitivity case A ($\mu\text{g m}^{-3}$)	Best estimate sensitivity case B ($\mu\text{g m}^{-3}$)	Base case ($\mu\text{g m}^{-3}$)	Best estimate sensitivity case A ($\mu\text{g m}^{-3}$)	Best estimate sensitivity case B ($\mu\text{g m}^{-3}$)
PM _{2.5}	39.5	34.2	1.7	44.7	38.9	2.2
PM _{2.5} sulfate	15.6	14.8	0.3	16.9	16.2	0.4
PM _{2.5} nitrate	1.5	1.0	0.0	3.7	2.8	0.2
PM _{2.5} ammonium	6.3	5.8	0.1	7.3	6.7	0.2
PM _{2.5} OC	4.6	3.8	0.2	4.2	3.4	0.2
- primary OC	3.9	3.5	0.2	3.2	2.7	0.2
- SOA (anthropogenic)	0.27	0.29	0	0.73	0.73	0
- SOA (biogenic)	0.4	0	0.1	0.28	0	0.1
PM _{2.5} EC	1.0	1.0	0.0	1.2	1.2	0.0
Other PM _{2.5}	10.4	7.7	1.0	11.5	8.7	1.2

The composition of $PM_{2.5}$ changed only slightly as a result of changes in precursor emissions and BC in best estimate sensitivity case A. Due to a smaller decrease in sulfate compared to total $PM_{2.5}$, the relative contribution of sulfate increased in sensitivity case A. The percentage of nitrate decreased slightly, while ammonium either stayed roughly constant or increased slightly. The contribution of EC and OC (primary plus secondary) also stayed fairly constant. The contribution of the “other” category decreased. Changes in composition between the base case and sensitivity case A tended to be less apparent at locations dominated by primary emissions, e.g., around New York City.

In sensitivity case B, PM concentrations were much lower than those in the base case and sensitivity case A. Because within-domain emissions of PM were absent in this case and concentrations of these components were also reduced at the boundary, primary PM components were low in concentration. Secondary PM was also not produced in abundance due to reduced oxidant levels and reduced emissions of precursor gases. Therefore, the composition of $PM_{2.5}$ changed dramatically between the base case and sensitivity case B. The contributions of sulfate, nitrate, and ammonium to $PM_{2.5}$ combined to be only 28% in Washington, D.C. Due to the lack of emissions and low concentrations at the boundary, the contribution of EC was negligible. The contribution of biogenic SOA accounted for 3% of $PM_{2.5}$. Primary OC originated only from the boundary and accounted for ~10% of $PM_{2.5}$, bringing the total contribution of organic compounds to 13%. The “other” component, also originating from BC, dominated $PM_{2.5}$ concentrations when anthropogenic influences were eliminated.

8. CONCLUSIONS

We have applied state-of-the-science 3-D O₃ and PM models to Nashville, TN and the Northeast to study the contribution of biogenic emissions to the concentrations of O₃ and PM. Several key conclusions can be drawn from these modeling studies.

- Limited model evaluation using ambient isoprene data indicates that the BEIS2-generated inventory is accurate to a factor of 2 for isoprene.
- Despite large contributions of biogenic compounds to the VOC emissions inventories (over 50%), the contributions of biogenic VOC to the overall production of O₃ were relatively small in both domains. The domain-average biogenic contribution to surface O₃ was estimated to be 6% to 14% in the Nashville/Tennessee domain and 16% to 23% in the Northeast domain. We postulated that large areas of each domain were sensitive to the availability of NO_x. Therefore, O₃ was not very sensitive to biogenic emissions, consisting mainly of VOC.
- Using a full perturbation approach to remove biogenic emissions from the base case simulations, the contributions of biogenic emissions to peak one-hour and 8-hour O₃ concentrations at urban locations were higher than the domain average contributions. In Nashville, biogenic emissions were estimated to account for 34% and 32%, respectively, of the peak one-hour and 8-hour O₃ concentrations. The corresponding fractions were 22% and 23% in Washington, D.C. In urban areas, anthropogenic NO_x were quite abundant and O₃ production tended to be more sensitive to biogenic VOC.
- Alternative estimates of biogenic contributions to O₃ were provided in simulations representing natural conditions with no anthropogenic emissions. In Nashville, the estimated contributions to O₃ were smaller than the above estimates (on the order of 10 ppb) because of the low NO_x concentrations associated with such a scenario. However, in the Northeast, this simulation predicted higher biogenic contributions of 24 ppb and 21 ppb to the maximum one-hour and 8-hour average O₃ concentrations, respectively. These estimates

are in better agreement with the full perturbation approach and may indicate increased VOC sensitivity relative to the Nashville simulation.

- The effects of biogenic emissions (of mostly VOC and a small amount of NO_x) on O₃ manifested in the simulations via their interaction with anthropogenic emissions of NO_x. Biogenic emissions may contribute to non-attainment of the one-hour and 8-hour NAAQS in some urban areas (e.g., Nashville), while contributing to the non-attainment of the eight-hour standard in others (e.g., Washington, D.C.).
- Due to small contributions of SOA of biogenic origins to the total simulated PM_{2.5}, the contribution of biogenic emissions to the production of SOA within the domain was typically small. However, widespread emissions of reactive biogenic VOC in many parts of the domains affected the production of secondary inorganic PM (e.g., nitrate, sulfate, ammonium) and anthropogenic SOA in the sensitivity simulations. In addition, reductions of PM at the boundary had a significant effect on the simulated PM concentrations within the domain owing to the long atmospheric lifetimes of fine PM. Very little PM was predicted in sensitivity simulations with natural conditions. The estimated PM_{2.5} contributions from biogenic and natural sources ranged from 1.3 to 1.5 μg m⁻³ in the Nashville, Tennessee domain, and from 1.8 to 4.0 μg m⁻³ in the Northeast domain.

Several important lessons were learned in terms of regional PM modeling. In the Nashville simulations, the predicted PM_{2.5} and sulfate concentrations were found to be commensurate with available data. However, the upwind boundary concentrations of fine particles may be a significant source of uncertainty for the predicted fine particle concentrations. In the Northeast, PM tends to be underpredicted. Upwind boundary concentrations of fine particles, especially aloft and at offshore locations, are a significant source of uncertainty for the predicted fine particle concentrations in the Northeast domain as well. Improvements to the PM emission inventory are much needed, including the speciation of fine and coarse PM. The default PM composition profiles used in Models-3/CMAQ may not be applicable everywhere.

Significant uncertainties in the modeling of SOA are highlighted in this work. The predictions of three different SOA modules differed by as much as a factor of 40. For example, the domain average SOA concentrations on 16 July predicted by Odum/Griffin et al., CMU/STI, and MADRID 2 were 0.065, 0.63, and 2.39 $\mu\text{g}/\text{m}^3$, respectively. There are significant discrepancies in (a) the SOA precursors considered, (b) the reactions forming condensable products, (c) the amount of condensable products formed, (d) the theories of gas/particle partition represented, and (e) the parameters used in the absorption partition modules. These areas are elaborated upon as follows:

- Different terpene speciation profiles can cause a 50% change in the predicted amount of SOA in the Odum/Griffin et al. mechanism, which considers explicit terpene species. Therefore, a BEIS3 type emissions model with explicit terpene representation is desirable.
- The NO_3 reaction appeared to be an important mechanism for SOA formation. Further research should help elucidate the reaction mechanisms and the identities of the condensable products.
- A lumped acid was an abundant water soluble SOA precursor in the MADRID 2/CACM formulation. This condensable product may be formed from anthropogenic and biogenic precursors, including secondary products of isoprene, which is traditionally not regarded as an SOA precursor. The formation of water soluble condensable compounds and water soluble SOA is another major knowledge gap pertaining to SOA.
- SOA may be formed via absorption, adsorption, aqueous dissolution, and saturation. Current modules fail to represent more than one or two of these pathways, and, except for MADRID 2, do not address the simultaneous partition due to several processes.
- Further experimental work is needed to define the identities of the partitioning compounds as well as the parameters for the gas/particle partition of SOA. Current modules differ significantly in both areas. For example, the Odum/Giffin et al. module predicted higher formation of biogenic SOA than anthropogenic SOA, while the reverse was true in the CMU/STI module. The

partition parameters used in the CMU/STI and AEC modules favored partitioning into the particulate phase over the gas phase, but the opposite result was obtained in the Odum/Griffin et al. approach. Temperature dependence may be an important factor, since experimental smog chamber data (e.g., used in Odum/Griffin et al.) are typically obtained at high temperatures that may not be favorable to the condensation of SOA.

9. REFERENCES

- Cass, G.R., L.G. Salmon, D.U. Pedersen, J.L. Durant, R. Bigg, A. Lunts, M. Utell, 1999. Determination of Fine Particle and Coarse Particle Concentrations and Chemical Composition in the Northeastern United States, 1995, Northeast States for Coordinated Air Use Management, Boston, MA.
- EPA, 1999. Science algorithms of the EPA Models-3 Community Multiscale Air Quality (CMAQ) Modeling System. EPA/600/R-99/030, U.S. Environmental Protection Agency, Research Triangle Park, NC.
- EPRI, 1999. Organic Aerosol Partition Module Documentation, TR-113095, EPRI, Palo Alto, CA.
- Gery, M.W., G.Z. Whitten, J.P. Killus, 1988. Development and Testing of the CBM-IV for Urban and Regional Modeling. EPA Report No. EPA/600/3-88/012. U.S. EPA, Research Triangle Park, NC 27711.
- Griffin, R.J., D.R. Cocker III, R.C. Flagan and J.H. Seinfeld, 1999. Organic aerosol formation from the oxidation of biogenic hydrocarbons, *J. Geophys. Res.*, **104**, 3555-3567.
- Helmig, D., J. Greenberg, A. Guenther, P. Zimmerman, C. Geron, 1998. Volatile organic compounds and isoprene oxidation products at a temperate deciduous forest site, *J. Geophys. Res.*, **103**, 22397 – 22414.
- Helmig, D., L. Klinger, A. Guenther, L. Vierling, P. Zimmerman and C. Geron, 1999. Biogenic volatile organic compound emissions (BVOCs) I. Identifications from three continental sites in the U.S., *Chemosphere*, **38**, 2163-2187.
- Hsu, H.H., Y. Nishioka, G.A. Allen, P. Koutrakis, and R.M. Burton, 1997. The

- Metropolitan Acid Aerosol Characterization Study: Results from the summer 1994 Washington, D.C. field study, *Environ. Health Perspectives*, **105**, 826-834.
- Jacobson, M.Z., 1997. Development and application of a new air pollution modeling system. Part III: Aerosol-phase simulations, *Atmos. Environ.*, **31**, 587-608.
- Karamchandani, P, K. Vijayaraghavan, S-Y. Wu, C. Seigneur, 2000. Development and Evaluation of a State-of-the-Science Plume-in-Grid Air Quality Model, Draft EPRI report, EPRI, Palo Alto, CA.
- Karamchandani, P.K., C. Seigneur, K. Vijayaraghavan, S.-Y. Wu, L. Santos, I. Sykes, 2001. Further development and evaluation of Models-3/APT. AER Document No. CP080-01-1, Report to EPRI, Palo Alto, CA.
- Lamb, B., D. Grosjean, B. Pun and C. Seigneur, 1999. Review of the Emissions, Atmospheric Chemistry, and Gas/Particle Partition of Biogenic Volatile Organic Compounds and Reaction Products, Final Report, Coordinating Research Council, Atlanta, GA.
- Lyman W.J., W.F. Reehl, D.H. Rosenblatt, 1990. Handbook of Chemical Property Estimation Methods, American Chemical Society, Washington, D.C.
- McMurry, P.H. and S.K. Friedlander, , 1979. New particle formation in the presence of an aerosol, *Atmos. Environ.*, **13**, 1635-1651.
- Meng, Z., D. Dabdub, J.H. Seinfeld, 1998. Size-resolved and chemically resolved model of atmospheric aerosol dynamics, *J. Geophys. Res.*, **103**, 3419-3435.
- NAPAP, 1991. Acidic Deposition: State of Science and Technology. The U.S. National Acid Precipitation Assessment Program, Washington, D.C.

- Nenes, A., S. Pandis, C. Pilinis, 1999. Continuous development and testing of a new thermodynamic aerosol module for urban and regional air quality models, *Atmos. Environ.*, **33**, 1553-1560.
- Odum, J.R., T.P.W. Jungkamp, R.J. Griffin, H.J.L. Forstner, R.C. Flagan and J.H. Seinfeld, 1997. Aromatics, reformulated gasoline, and atmospheric organic aerosol formation, *Environ. Sci. Technol.*, **31**, 1890-1897.
- Pankow, J.F., 1994. An absorption model of the gas/aerosol partition involved in the formation of secondary organic aerosol, *Atmos. Environ.*, **28**, 189-193.
- Pun, B.K., R. Griffin, C. Seigneur, J.H. Seinfeld, 2000. Application of a new organic aerosol partition module, AAAR Conference, St. Louis, MO, November 6-10, 2000.
- Pun, B.K., C. Seigneur, M. Leidner, P. Karamchandani, S. Roe, R. Strait, K. Thesing, J. Wilson, M. Mullen, 2001a. Scoping Study for Regional Haze in the Upper Midwest, AER Document No. CP089-01-1, Report to LADCO, Des Plaines, IL. www.ladco.org.
- Pun, B.K., Y. Zhang, K. Vijayaraghavan, S.-Y. Wu, C. Seigneur, J.H. Seinfeld, 2001b. Development of New Aerosol Modules and Incorporation into MODELS-3/CMAQ, AER Document No. CP083-00-1a, Report to EPRI, Palo Alto, CA.
- Seaman, N.L., and S.A. Michelson, 1995. Mesoscale meteorological structure of a high-ozone episode during the 1995 NARSTO-Northeast study, *J. Appl. Meteor.*, **39**, 384-398.
- Seinfeld, J.H., 1986. Atmospheric Chemistry and Physics of Air Pollution, Wiley, New York, NY.

- Seinfeld, J.H. and S.N. Pandis 1998. *Atmospheric Chemistry and Physics*, Wiley, New York, NY.
- Starn T.K., P.B. Shepson, S.B. Bertman, J.S. White, B.G. Splawn, D.D. Riemer, R.G. Zika, K. Olszyna, 1998. Observations of isoprene chemistry and its role in ozone production at a semirural site during the 1995 Southern Oxidant Study, *J. Geophys. Res.*, **103**, 22425 – 22435.
- Strader, R., C. Gurciullo, S. Pandis, N. Kumar and F.W. Lurmann, 1998. Development of Gas-Phase Chemistry, Secondary Organic Aerosol, and Aqueous-Phase Chemistry Modules for PM Modeling, 1998, Final Report STI-997510-1822-FR, Coordinating Research Council, Atlanta, GA.
- Strader, R., F. Lurmann, S.N. Pandis, 1999. Evaluation of secondary organic aerosol formation in winter, *Atmos. Environ.*, **33**, 4849-4863.
- Venkatram, A. and J. Pleim, 1999. The electrical analogy does not apply to modeling dry deposition of particles, *Atmos. Environ.*, **33**, 3075-3076.
- Wang, Y. and D.J. Jacob, 1998. Anthropogenic forcing on tropospheric ozone and OH since preindustrial times, *J. Geophys. Res.*, **103**, 31123-31135.
- Wayne, R.P., 1991. *Chemistry of the Atmospheres*, 2nd edition, Clarendon Press, Oxford, UK.
- Zhang, Y. K. Vijayaraghavan, B. Pun, C. Seigneur, J.H. Seinfeld, N. Kumar, 2000. Comparison of two aerosol modules in Models-3/CMAQ: simulation of PM_{2.5} formation in the Los Angeles Basin, EPRI, Air Quality II: Conference on Mercury, Trace Elements, and Particulate matter, September 19-21, 2000, McLean, Virginia.